

Water Quality and its Spatial Variability in Lake Cuitzeo, Mexico

Marcela Galindo De Obarrio
March, 2005

Water Quality and its Spatial Variability in Lake Cuitzeo, Mexico

by

Marcela Galindo De Obarrio

Thesis submitted to the International Institute for Geo-information Science and Earth Observation in partial fulfilment of the requirements for the degree of Master of Science in Geo-Information Science and Earth Observation, Specialisation: Environmental Systems Analysis and Management.

Thesis Assessment Board

Chairman	Dr. Ir. C. M.M. Mannaerts
External Examiner	Dr. E.O. Seyhan - Free University Amsterdam
Primary Supervisor	Dr. Z. Vekerdy
Second Supervisor	Dr. R.O. Strobl



**INTERNATIONAL INSTITUTE FOR GEO-INFORMATION SCIENCE AND EARTH OBSERVATION
ENSCHEDA, THE NETHERLANDS**

Disclaimer

This document describes work undertaken as part of a programme of study at the International Institute for Geo-information Science and Earth Observation. All views and opinions expressed therein remain the sole responsibility of the author, and do not necessarily represent those of the institute.

Abstract

Lake Cuitzeo is Mexico's second largest fresh water lake with an area of 400 km². Its economic importance, its complex behaviour and biodiversity, justify its proclamation as a Wetland of International Importance by the Ramsar Convention. The government of the province of Michoacán has expressed interest in developing a management plan to promote the conservation of the wetland; and since water quality is considered part of the basic performance indicators when designing a wetland management plan, its analysis is necessary. This study aims to understand the water quality status in different parts of the lake, and the spatial variability of some water quality components; also to uncover the relationship between water quality, eutrophic levels and wetlands vegetation, and finally to determine if there is a relationship between information provided by optical multi-spectral sensors and water quality. Different analysis methods, such as statistical analysis, and graphical analysis, were used for the interpretation of water quality; Ordinary Kriging and Trend Surface Fitting were used to determine the spatial variability of the water quality parameters; and Principal Component Analysis was used in a correlation analysis with obtained water quality values, and was also used for CoKriging of transparency values. Results indicate diversities in water quality for the different parts of the lake, also how currents are the influencing factor in the spatial distribution of some water quality parameters, while dilution affects others more, and finally how the high correlation between Principal Component 1 and transparency proved useful in the CoKriging attempt, and how with further study the correlation could also prove useful for monitoring changes in the lake over time, as well as identifying specific sampling locations, becoming a time and money saving tool for those in charge of monitoring the water body.

Acknowledgements

The first person I'd like to express my gratitude to is Mr. Ricardo Anguizola. Without his help I would not have come to ITC in the first place; the opportunity he gave me is invaluable, I thank you!

I am eternally grateful to Dr. Zoltán Vekerdy, my dear supervisor, for his time, effort, ideas, help, discussions, jokes, and overall support during this period, we've had fun; to Dr. Robert Strobl, my second supervisor, for his valuable knowledge of chemistry, and related ideas, all applied in this thesis; and to Dr. David Rossiter for his present and long distance guidance with geostatistics; to me you are my third supervisor. Thanks to Drs. Daniel Jager for all his help in preparing for fieldwork and to Drs. Boudewijn de Smeth for his help in the lab after the fieldwork. Also to all the WREM, and other ITC staff who have shared their knowledge and expertise with us throughout this year and a half.

Special thanks to the evaluating committee, Dr. Ir. C. M.M. Mannaerts, Dr. E.O. Seyhan, et al., for taking the time to read and evaluate my work. And to the ISIS programme (copyright CNES) for the SPOT data provided, and used for the last chapters of this thesis.

Thank you to my classmates; we've shared so many good experiences together, from our first days in the orienting exercise up to our graduation day. Joseph, Parth and Kitsiri (the ones I've shared the most laughs with), you will always have a special place in my heart!

My deepest gratitude goes to all the people in Mexico who worked so hard to make our lives easier; especially to Dr. José Luis Palacio and Dr. Alejandro Velasquez for putting everything together with Zoltán, and to Dr. Manuel Mendoza (& family) for making it happen. Many thanks to Dr. Silke Cram for her interest in my work, and for her wonderful guidance during fieldwork. To Dr. Lucy Mora for her incredible help and countless hours of lab work. To Ulfrano for being my sampling partner, and for being so patient and taking us to every corner of the lake we asked him to; also to his family for welcoming us into their home every afternoon. Thanks to Lupita and Don Jorge for their kind manners and their always "willing to help" spirit; and to my fieldwork companions Nega and Rodrigo for putting up with me for one month, under extremely stressful and tiresome, but very rewarding conditions.

My appreciation goes to my mother, father, brother, sister (in law) and the rest of my family for supporting me, praying for me, and caring for my work (even though they're not very familiar with it). Also, many thanks to all my friends in ITC, Panama, and in other parts of the world, from whom I've received only words of encouragement.

There are no words to thank Maurizio; you are my friend, my helping hand, my strength, support and guidance. Thank you for your unconditional love and confidence in me.

Finally I want to thank God. I've always put my faith in him, and he's never let me down!

Table of contents

Abstract	I
Acknowledgements	II
List of figures	V
List of tables	VII
1. Introduction	1
1.1. Problem statement.....	1
1.2. Objectives	1
1.3. Specific research questions.....	2
1.4. Research methods	2
1.5. Outline of the thesis	4
2. Description of the study area.....	5
2.1. Lake Cuitzeo basin.....	5
2.2. Geology.....	6
2.3. Climate.....	6
2.4. Hydrology	8
2.5. Soils	10
2.6. Vegetation.....	11
2.7. Socio-economic values	11
3. Water quality assessment	13
3.1. Hydrological variables.....	13
3.1.1. Results of streamflow measurements and discharge calculations.....	14
3.1.2. Comparison of obtained discharge to historical values.....	15
3.2. Lake cuitzeo water quality issues	15
3.3. Sampling Lake Cuitzeo.....	16
3.3.1. Zonation of the lake.....	16
3.3.2. Sampling sites.....	17
3.4. Water quality survey	18
3.4.1. Chemical analysis of the water samples.....	18
3.4.2. Reliability check.....	19
3.4.2.1. Duplicate comparison	19

3.4.2.2.	Anion-cation balance	20
3.4.3.	Interpretation of the samples	21
3.4.3.1.	General lake chemistry analysis	21
3.4.3.2.	Statistical data analysis	22
3.4.3.3.	Water types	25
3.4.3.4.	Graphical analysis.....	27
3.5.	Location of thermal springs in the lake	29
3.6.	Eutrophic state of the lake	30
3.7.	Suitable areas for wetland vegetation.....	33
4.	Spatial variability of water quality	35
4.1.	Geostatistical analysis of the parameters.....	35
4.1.1.	Non-spatial analysis of variables.....	35
4.1.2.	Variograms and models used for the analysis	37
4.1.3.	Kriging predictions.....	38
4.1.4.	Other interpolation methods and results.....	41
5.	Remote sensing and water quality	45
5.1.	Principal component analysis of remotely sensed data	45
5.2.	Correlation analysis of remotely sensed data and water quality	49
5.3.	Remote Sensing applied to CoKriging of water quality parameters	51
5.4.	Remote sensing applied to water quality monitoring in Lake Cuitzeo.....	55
6.	Conclusions and recommendations	57
6.1.	Conclusions.....	57
6.2.	Recommendations and future research.....	59
	References	67
	Appendix A: Hydrological analysis	69
	Appendix B: Chemical analysis	74
	Appendix C: Geostatistical analysis	79
	Appendix D: Water quality and remote sensing	82
	Appendix E: Wetlands management plan	84

List of figures

Figure 1-1: Flow chart of research methods	4
Figure 2-1: Study Area: Mexico - Lake Cuitzeo Basin.....	5
Figure 2-2: Average monthly temperatures over 15 years	7
Figure 2-3: Average monthly rainfall over 20 years	7
Figure 2-4: Rainfall oscillations per year over 20 years	8
Figure 2-5: Main rivers flowing into Lake Cuitzeo	8
Figure 2-6: Location of gauging stations in the basin.....	9
Figure 2-7: Average monthly precipitation and Pan Evapotranspiration over 20 years	10
Figure 3-1: Streamflow measurement sites in the Cuitzeo basin	13
Figure 3-2: Historical discharge values.....	15
Figure 3-3: Zonation of Lake Cuitzeo.....	17
Figure 3-4: Sampling sites for Lake Cuitzeo	18
Figure 3-5: Ion balance in typical lakes vs. ion balance in Lake Cuitzeo.....	22
Figure 3-6: Five-number summary comparison for pH in the different parts of the lake.....	23
Figure 3-7: Five-number summary comparison for EC in the different parts of the lake.....	23
Figure 3-8: Five-number summary comparison for Na in the different parts of the lake	23
Figure 3-9: Five-number summary comparison for Ca in the different parts of the lake	23
Figure 3-10: Five-number summary comparison for Mg in the different parts of the lake	23
Figure 3-11: Five-number summary comparison for Cl in the different parts of the lake.....	23
Figure 3-12: Five-number summary comparison for HCO ₃ in the different parts of the lake	24
Figure 3-13: Five-number summary comparison for SO ₄ in the different parts of the lake.....	24
Figure 3-14: Comparison of standard deviation values (pH).....	24
Figure 3-15: Comparison of standard deviation values (Ca and Mg).....	24
Figure 3-16: Comparison of standard deviation values (EC, Na, Cl, HCO ₃ and SO ₄)	24
Figure 3-17: Water types in the Central part of the lake.....	25
Figure 3-18: Water types in the Eastern part of the lake	25
Figure 3-19: Water types in the Passageway between C and E parts of the lake	26
Figure 3-20: Water types in the Western part of the lake	26
Figure 3-21: Thiessen polygons representing water types in the lake.	27
Figure 3-22: Piper plot for the Central part of the lake.....	27
Figure 3-23: Piper plot for the Eastern part of the lake	27
Figure 3-24: Piper plot for the Western part of the lake	28
Figure 3-25: Piper plot for the Passageway between the C and E parts of the lake.....	28
Figure 3-26: Main ions represented on the Stiff diagrams.....	28

Figure 3-27: Stiff diagrams for the western and central part of the lake.....	29
Figure 3-28: Stiff diagrams for the passageway and eastern parts of the lake.....	29
Figure 3-29: Location of potential thermal waters inside the lake	30
Figure 3-30: Remote sensing applied to eutrophication detection in the Central part of the lake.....	32
Figure 3-31: Remote sensing applied to eutrophication detection in the Eastern part of the lake	32
Figure 4-1: Histogram of Hardness.....	36
Figure 4-2: Box plot for the log of EC.....	36
Figure 4-3: Box plot for HCO ₃	36
Figure 4-4: Histogram of the log of Cl.....	36
Figure 4-5: Histogram of the log of pH.....	36
Figure 4-6: Box plot for the log of Alkalinity.....	36
Figure 4-7: Variogram model for log of EC.....	37
Figure 4-8: Variogram model for log of Cl.....	37
Figure 4-9: Variogram model for Hardness	38
Figure 4-10: Variogram model for log of Bicarbonate	38
Figure 4-11: Ordinary kriging results for the log of EC	39
Figure 4-12: Ordinary kriging results for the log of Cl.....	39
Figure 4-13: Current observed in band 1 of SPOT image.....	39
Figure 4-14: Current revealed in interpolation result.....	39
Figure 4-15: Ordinary kriging results for Hardness	40
Figure 4-16: Ordinary kriging results for log ₁₀ of Bicarbonate	40
Figure 4-17: Experimental variogram for pH.....	42
Figure 4-18: Interpolation results for pH values	43
Figure 4-19: Interpolation results for Na	43
Figure 4-20: Interpolation results for Mg.....	43
Figure 4-21: Interpolation results for Transparency	43
Figure 4-22: Interpolation result for depth.....	43
Figure 4-23: Interpolation result for Ca	43
Figure 5-1: Differences in the water captured by PCA-PC1	47
Figure 5-2: Differences in the water captured by PCA-PC2.....	47
Figure 5-3: Differences in the water captured by PCA-PC3.....	48
Figure 5-4: Differences in the water captured by PCA-PC4.....	48
Figure 5-5: Cross-variogram for Transparency and PC1	53
Figure 5-6: Transparency predictions using Ordinary Kriging.....	54
Figure 5-7: Transparency predictions using Universal Kriging.....	54
Figure 5-8: Transparency prediction variances for Ordinary Kriging	54

Figure 5-9: Transparency prediction variances for CoKriging	54
Figure 5-10: Difference between CoKriging and Ordinary Kriging predictions	54
Figure 5-11: Relationship between Transparency and Sodium	56
Figure 5-12: Relationship between Transparency and Bicarbonate	56
Figure 5-13: Relationship between Transparency and Chloride.....	56

List of tables

Figure 1-1: Flow chart of research methods	4
Figure 2-1: Study Area: Mexico - Lake Cuitzeo Basin.....	5
Figure 2-2: Average monthly temperatures over 15 years	7
Figure 2-3: Average monthly rainfall over 20 years	7
Figure 2-4: Rainfall oscillations per year over 20 years	8
Figure 2-5: Main rivers flowing into Lake Cuitzeo	8
Figure 2-6: Location of gauging stations in the basin.....	9
Figure 2-7: Average monthly precipitation and Pan Evapotranspiration over 20 years	10
Figure 3-1: Streamflow measurement sites in the Cuitzeo basin	13
Figure 3-2: Historical discharge values.....	15
Figure 3-3: Zonation of Lake Cuitzeo.....	17
Figure 3-4: Sampling sites for Lake Cuitzeo	18
Figure 3-5: Ion balance in typical lakes vs. ion balance in Lake Cuitzeo.....	22
Figure 3-6: Five-number summary comparison for pH in the different parts of the lake.....	23
Figure 3-7: Five-number summary comparison for EC in the different parts of the lake.....	23
Figure 3-8: Five-number summary comparison for Na in the different parts of the lake	23
Figure 3-9: Five-number summary comparison for Ca in the different parts of the lake	23
Figure 3-10: Five-number summary comparison for Mg in the different parts of the lake	23
Figure 3-11: Five-number summary comparison for Cl in the different parts of the lake.....	23
Figure 3-12: Five-number summary comparison for HCO ₃ in the different parts of the lake	24
Figure 3-13: Five-number summary comparison for SO ₄ in the different parts of the lake.....	24
Figure 3-14: Comparison of standard deviation values (pH).....	24
Figure 3-15: Comparison of standard deviation values (Ca and Mg).....	24
Figure 3-16: Comparison of standard deviation values (EC, Na, Cl, HCO ₃ and SO ₄)	24
Figure 3-17: Water types in the Central part of the lake.....	25
Figure 3-18: Water types in the Eastern part of the lake	25
Figure 3-19: Water types in the Passageway between C and E parts of the lake	26
Figure 3-20: Water types in the Western part of the lake	26
Figure 3-21: Thiessen polygons representing water types in the lake.	27
Figure 3-22: Piper plot for the Central part of the lake.....	27
Figure 3-23: Piper plot for the Eastern part of the lake	27
Figure 3-24: Piper plot for the Western part of the lake	28
Figure 3-25: Piper plot for the Passageway between the C and E parts of the lake.....	28
Figure 3-26: Main ions represented on the Stiff diagrams.....	28

Figure 3-27: Stiff diagrams for the western and central part of the lake.....	29
Figure 3-28: Stiff diagrams for the passageway and eastern parts of the lake.....	29
Figure 3-29: Location of potential thermal waters inside the lake	30
Figure 3-30: Remote sensing applied to eutrophication detection in the Central part of the lake.....	32
Figure 3-31: Remote sensing applied to eutrophication detection in the Eastern part of the lake	32
Figure 4-1: Histogram of Hardness.....	36
Figure 4-2: Box plot for the log of EC.....	36
Figure 4-3: Box plot for HCO ₃	36
Figure 4-4: Histogram of the log of Cl.....	36
Figure 4-5: Histogram of the log of pH.....	36
Figure 4-6: Box plot for the log of Alkalinity.....	36
Figure 4-7: Variogram model for log of EC.....	37
Figure 4-8: Variogram model for log of Cl.....	37
Figure 4-9: Variogram model for Hardness	38
Figure 4-10: Variogram model for log of Bicarbonate	38
Figure 4-11: Ordinary kriging results for the log of EC	39
Figure 4-12: Ordinary kriging results for the log of Cl.....	39
Figure 4-13: Current observed in band 1 of SPOT image.....	39
Figure 4-14: Current revealed in interpolation result.....	39
Figure 4-15: Ordinary kriging results for Hardness	40
Figure 4-16: Ordinary kriging results for log ₁₀ of Bicarbonate	40
Figure 4-17: Experimental variogram for pH.....	42
Figure 4-18: Interpolation results for pH values	43
Figure 4-19: Interpolation results for Na	43
Figure 4-20: Interpolation results for Mg.....	43
Figure 4-21: Interpolation results for Transparency	43
Figure 4-22: Interpolation result for depth.....	43
Figure 4-23: Interpolation result for Ca	43
Figure 5-1: Differences in the water captured by PCA-PC1	47
Figure 5-2: Differences in the water captured by PCA-PC2.....	47
Figure 5-3: Differences in the water captured by PCA-PC3.....	48
Figure 5-4: Differences in the water captured by PCA-PC4.....	48
Figure 5-5: Cross-variogram for Transparency and PC1	53
Figure 5-6: Transparency predictions using Ordinary Kriging.....	54
Figure 5-7: Transparency predictions using Universal Kriging.....	54
Figure 5-8: Transparency prediction variances for Ordinary Kriging	54

Figure 5-9: Transparency prediction variances for CoKriging	54
Figure 5-10: Difference between CoKriging and Ordinary Kriging predictions	54
Figure 5-11: Relationship between Transparency and Sodium	56
Figure 5-12: Relationship between Transparency and Bicarbonate	56
Figure 5-13: Relationship between Transparency and Chloride.....	56

1. Introduction

Wetlands provide countless benefits; they are a source of food, protection and other vital habitat factors for a variety of fish and wildlife species, in many cases including endangered and threatened species. They also have economic value associated with recreational, commercial, and sustainable use of fish and wildlife resources (USEPA 2004).

Lake Cuitzeo is located in the Mexican Neo-Volcanic belt, at the lowest part of a 4026-km² basin, it is Mexico's second largest fresh water lake (Alfaro, Martinez et al. 2001). Its economic importance for the province of Michoacán, its complex behaviour and biodiversity, justify its possible proclamation as a Wetland of International Importance by the Ramsar Convention¹.

1.1. Problem statement

The mission statement for the Ramsar Convention is the conservation and wise use of all wetlands through local, regional and national actions and international cooperation, as a contribution towards achieving sustainable development throughout the world (Ramsar 2002). The local government has expressed interest in implementing a management plan to promote Lake Cuitzeos conservation; however the development of an appropriate management plan will be made difficult by diverse factors that affect the dynamics of the wetland.

For example, little inflow to the lake during dry periods affects the water cover in the northern and western parts of the lake, to the point where they become dry areas; while the eastern and central parts of the lake bed remain covered with water. Regardless of dry or wet periods, during the last ten years, there has been an increase in the vegetation cover of the lake, suggesting that the quality of the inflowing water might be one of the factors triggering vegetation growth.

Finally, its shape and the uneven distribution of inflow difficult the homogeneous mixing of the water throughout the entire body of the lake; consequently each part of the lake seems to have different water quality conditions. These differences have to be taken into consideration in the water management plans.

1.2. Objectives

The main objective is to perform a first-time water quality analysis of Lake Cuitzeo, and to determine the spatial variability of these water quality parameters in the highest sampled part of the lake at the end of the rainy season of 2004.

¹ The Convention on Wetlands, signed in Ramsar, Iran, in 1971, is an intergovernmental treaty which provides the framework for national action and international cooperation for the conservation and wise use of wetlands and their resources.

Specific objectives for this study are:

- To determine the water quality status at representative sample points, located throughout Lake Cuitzeo, at the end of the rainy season of 2004.
- To map the spatial variability of the water quality parameters, by means of the samples obtained at the end of the rainy season of 2004.
- To identify the areas with highest growth of aquatic vegetation.
- To determine if there is a relationship between the reflectance values of optical multi-spectral sensors and selected water quality parameters.

1.3. Specific research questions

Answers for the following questions are sought:

1. What is the state of the water quality at representative sample points distributed throughout the different parts of Lake Cuitzeo?
2. What is the relationship between water quality, eutrophic levels and wetland vegetation? Which areas of the lake are suitable for development of wetland vegetation?
3. What is the spatial distribution of the water quality parameters in the central part of the lake? How precisely can they be modelled?
4. What is the relationship, if any, between reflectance values of optical multi-spectral sensors and water quality?

1.4. Research methods

Literature review

A number of documents were studied; they contain the latest information on Limnology, wetlands management, analysis and interpretation of water quality data, statistics, techniques for spatial analysis, geostatistics applied to the environment, and other topics.

Collection and analysis of existing data

Some data was collected from Mexican sources, it consisted of Landsat ETM and SPOT and MSS satellite images, also contour maps, a map of the geology of the basin, a soils map, a map with hydrological properties of surface water and groundwater of the basin, location of gauging stations, location of meteorological stations and some precipitation and temperature data. In order to get familiarized with the area the data mentioned was studied, but also analyses of the spectral properties of satellite images were done to establish possible areas where homogeneities or heterogeneities exist in the lake.

Fieldwork preparation

First, the decision is taken on which water quality parameters to measure. Then, a stratified random sampling strategy is developed focusing on areas which seem to have higher variability, and need higher sampling density.

Fieldwork

Following the sampling strategy, several water samples were taken and in situ measurements were done. After a preliminary interpolation of some of the first results, the strategy was modified to focus on areas which suggested higher variability.

Besides the collection of samples from the lake itself, also streamflow measurements, and discharge calculations were done for the canals flowing into the lake.

Finally, water samples were collected from the main canals, pumping stations and one of the thermal springs on the coast of the west side of the lake.

Further precipitation and temperature data was collected from the Mexican authorities and UNAM², as well as topographic maps.

Data analysis and interpretation

First, the hydrological behaviour of the catchment was studied through the analysis of streamflow measurements and discharge calculations. This was compared to past year behaviours to assess how the current situation is related to long term averages and trends.

The water quality samples were subjected to analysis in the field and in the laboratory of UNAM. As part of the reliability check the anion-cation balance was calculated for each sample and a comparative analysis was performed on some duplicate samples in the ITC laboratory. For the interpretation of the samples, statistical, water type and graphical analyses were carried out. Also, through correlation analysis, possible locations for thermal springs inside the lake are identified. Finally water quality, eutrophication and wetlands vegetation are linked.

For the spatial variability analysis of the water quality, a zonation of the lake was defined in order to capture the water quality differences in the diverse parts of the lake. Through Ordinary Kriging and Trend Surface Fitting the spatial variability of the water quality parameters was mapped.

To determine whether there was a relationship between the pattern observed in the central part of the lake, and any of the analyzed water quality parameter, a principal component analysis was performed on the lake water, and the values of the Principal Components at the sampling points were correlated to the results from the water quality analysis.

Final Assessment:

The final assessment exposed the diversities in water quality in the different parts of the lake; it also shed some light on the relationship between vegetation growth and decay, generation of nutrients, water quality and eutrophication. It showed how the spatial distribution of some water quality variables are affected by the generation of currents in the lake, while others are affected more by dilution. And finally, having found a statistical relationship between some principal components and some water quality variables, it encouraged a temporal experiment that could help in better understanding the dynamics of the lake.

² Universidad Nacional Autónoma de México.

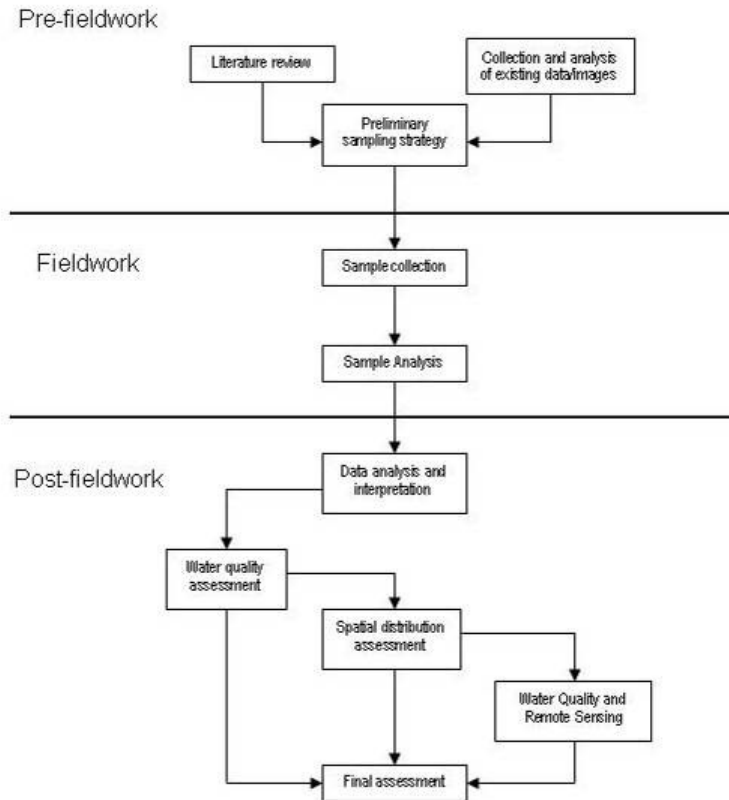


Figure 1-1: Flow chart of research methods

1.5. Outline of the thesis

- **Chapter 1:** General introduction of the area, problem statement, general and specific objectives, research questions, and research methods.
- **Chapter 2:** A description of the study area that focused on physical characteristics, geology, and hydrological behaviour of the catchment, vegetation and socio-economical values.
- **Chapter 3:** Describes the water quality data assessment in terms of hydrological variables, water quality issues of the area, analysis of the parameters, reliability check, interpretation of the data, and relationship between water quality, eutrophication and wetlands vegetation.
- **Chapter 4:** Explains the spatial variability of the water quality by means of zonation of the lake, and different types of geostatistical analysis of the parameters.
- **Chapter 5:** Depicts the correlation between patterns in the water, observed through satellite images, and water quality parameters.
- **Chapter 6:** Presents the conclusions found in the study, offered recommendations, as well as future research possibilities for the area.

2. Description of the study area

Mexico is the world's most populous Spanish speaking country with 101,457,200 inhabitants, and it is located between 19° 43'N and 99° 14'W. Its mostly mountainous landscape is dominated by ranges of the Sierra Madre, and their numerous volcanoes. However, other landscape types include the desert conditions in the far-northwest, the basically flat Yucatan Peninsula, and the tropical rain forests of the far-southeast. Its land area is 1,908,690 km², which is divided into 31 states and 1 federal district.

2.1. Lake Cuitzeo basin

The Lake Cuitzeo basin is a hydrological unit with an area of 4026 km², which was calculated upon the definition of the catchment's water divide. It is located in Mexico's Transversal Volcanic System, between 19°30'–20°05' N and 100°35'–101°30' W. Figure 2-1 shows the study area for this project, it is located mostly in the province of Michoacán; however the Northern part of the basin is located in the state of Guanajuato, in the central part of Mexico. Figure 2-1 depicts the location of the basin in the central part of Mexico, as well as the location of the lake in the basin.

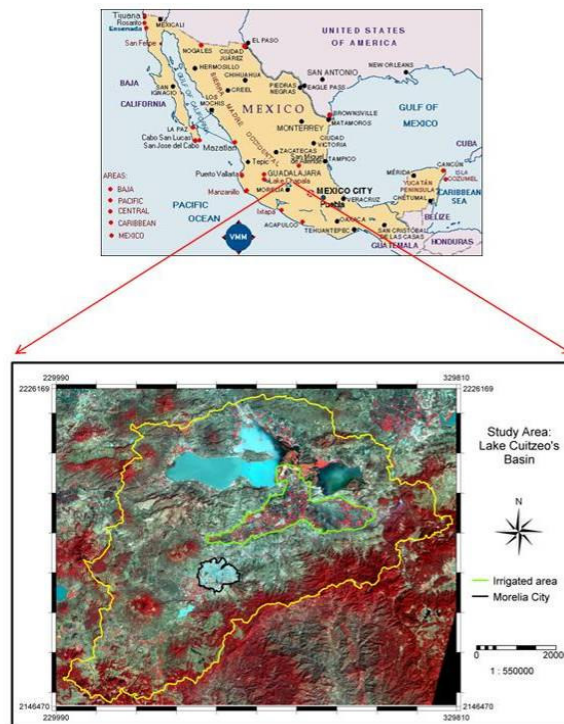


Figure 2-1: Study Area: Mexico - Lake Cuitzeo Basin

Both the city of Morelia and an agriculture field are located upstream of the lake. The main inflows to the lake pass through the agriculture field as irrigation canals, and enter the lake in the mid portion between the center, northern and eastern parts of the lake.

2.2. Geology

The basin forms part of the Cuitzeo-Chapala lagoon depression. All the structural elements have faults in the NE-SW and E-W directions. The lake is tectonically delimited by semi-grabens³ mainly made up from volcanic rocks and Quaternary deposits.

According to the hydrological map provided by UNAM before fieldwork, out of the 4026 km² basin, 72% is formed by consolidated material with low possibilities for groundwater storage, 12% is non consolidated material with low possibilities for groundwater storage, 8% is covered by water bodies, 7% is non consolidated material with high possibilities of groundwater storage, and 1% is non consolidated material with medium possibilities for groundwater storage.

The basin has been exposed to recent volcanism. In 1943 the areas inhabitants experienced the Paricutin volcano's worst activity. Reports state that the lava reached 15 m below the crater's rim, which stands at more than 2000 meters a.m.s.l. Paricutin forms part of an 1120 kilometer line of volcanoes called the Transversal Volcanic Axis that extends across Mexico in the East-West direction.

Post-volcanic activities play an important role in the alteration of water quality in the lake; it is a fact that thermal springs have developed all around the lake, located mostly around the eastern and western ends of the lake, but also some are suspected to have developed inside the lake as well.

2.3. Climate

Meteorological data for the basin has been recorded over 43 rainfall stations since 1923, but in an interrupted manner; lack of data either from a certain year or from a certain station makes it hard to calculate accurate temperature, rainfall or evapotranspiration values for the entire basin.

It is know though that the basin experiences a raise in humidity and a decrease in temperature, corresponding to the increase of altitude from the Northern part of the catchment at 1830 meters a.m.s.l. to the Southern part of the catchment at 2440 meters a.m.s.l.

The mean temperature in the basin is approximately 15°C. Figure 2-2 shows monthly average temperature readings from 1970 until 1995 in station #16-091: Planta de bombeo Zinzimeo, located between 19°52'00.34" N and 100°58'09.64" W, just south of the lake in the irrigated area. Notice the lowest temperatures between 13.8 and 14.1°C in January and December, and the highest of 21°C in June.

³ A classic set of parallel fault-bounded valleys.

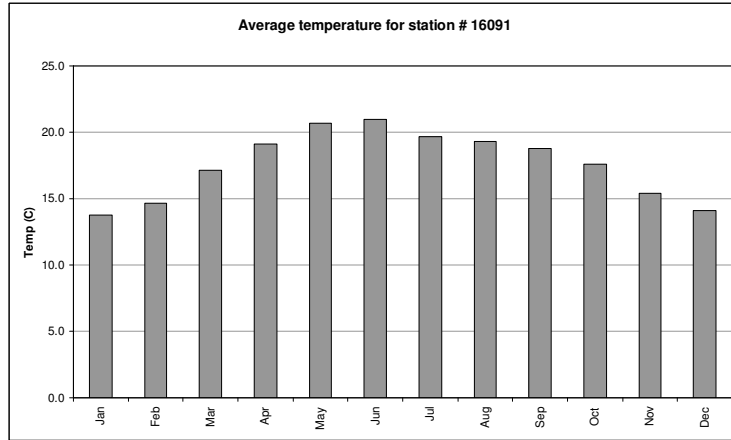


Figure 2-2: Average monthly temperatures over 15 years

The dominant climate in the basin is temperate with summer rains from May to October. Figure 2-3 shows the monthly average rainfall from 1980-2000 measured in the same station as for temperature, Planta de bombeo Zinzimeo; it clearly illustrates which are the high and low rainfall months during the year.

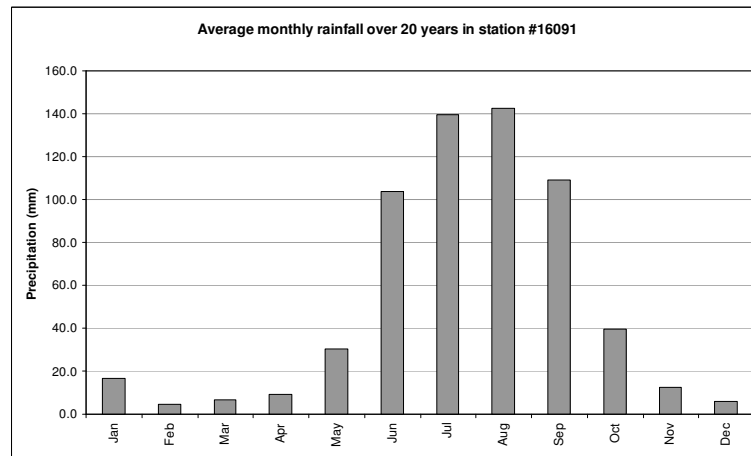


Figure 2-3: Average monthly rainfall over 20 years

The average annual precipitation ranges between 600 to 1000 mm, however every five to ten years they experience higher rainfalls ranging from 1000 to 1500 mm. As an example of the rainfall oscillation, figure 2-4 shows the rainfall measured from 1980 until 2000 in station #16-120: Santiago Undameo, located between 19°36'03.91" N and 101°16'26.61" W further south from the lake, in the water reserve for the city of Morelia; notice the highs in 1982, 1987, 1991 and 1998, and lows in 1984, 1989, 1994 and 2000.

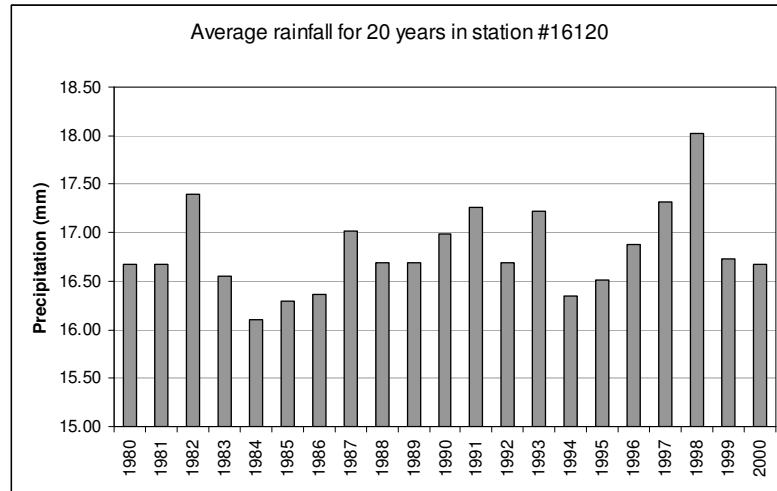


Figure 2-4: Rainfall oscillations per year over 20 years

2.4. Hydrology

The main inflows to the lake are the Viejo de Morelia, Grande de Morelia and Querendaro Rivers. The Viejo de Morelia and Grande de Morelia Rivers drain from SW–NE and the Querendaro drains from E-W. They are borne in high mountainous areas, and keep their course until they reach the agricultural area to the south of the lake, where they each split into several irrigation canals, and then reach the lake between the central and eastern parts. Figure 2-5 shows the main courses of the three mentioned rivers as they flow into the lake.

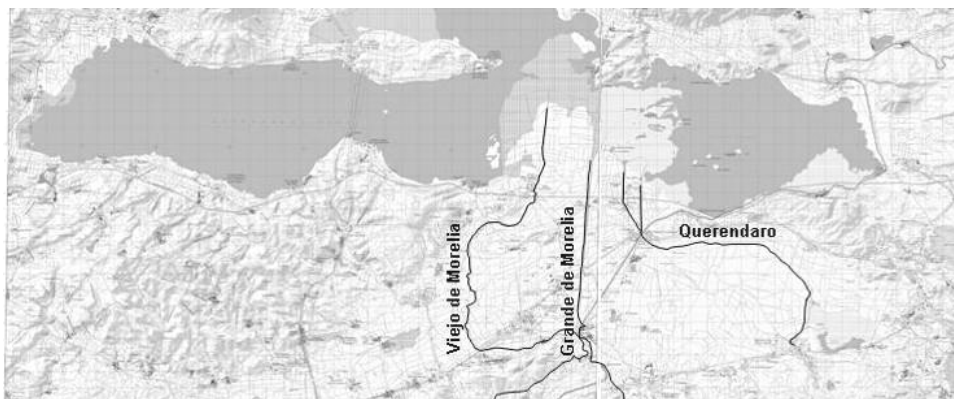


Figure 2-5: Main rivers flowing into Lake Cuitzeo

Table 2-1 describes the distribution of the drainage coefficients in the basin. The first column shows the percentage of the land in the basin and the second column describes the drainage coefficient in that percentage of land.

Table 2-1: Distribution of drainage coefficients in the basin

Basin percentage	Drainage coefficient
1%	20-30%
76%	10-20%
12%	5-10%
2%	0-5%
8%	Water bodies

Discharge has been gauged in 17 stations in the basin, however not all of these are not functioning anymore. There have been eight different stations in the main inflow, Rio Grande de Morelia; five stations in different canals, one station in Rio Querendaro, one station in Guadalupe Creek, and one station in the drinking water take. Figure 2-6 shows the location of the gauging stations in the basin.

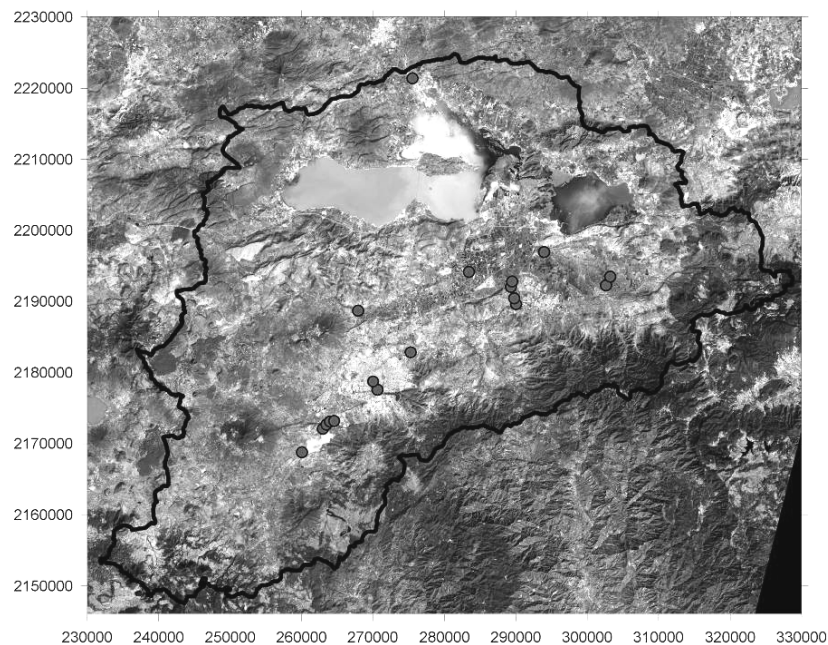


Figure 2-6: Location of gauging stations in the basin

The lake has only one superficial outlet in the northern part; it is a canal that only extracts water from the lake whenever this part is full, about every five to ten years. There might be some leakage through volcanic faults in the lake, however taking into account the basins low possibilities for groundwater storage, it is hypothesised that most of the drying out of the lake happens due to low rainfall periods and Evapotranspiration. In the gauging stations the Evapotranspiration is measured through the Pan method, since this method tends to overestimate the Evapotranspiration values, the measurements are multiplied by a coefficient of 0.7 to obtain more realistic values. Figure 2-7 shows average monthly precipitation, Evapotranspiration and temperature, over 20 years from 1980-2000 in station #16-091: Planta de bombeo Zinzimeo. Notice Evapotranspiration values increase as temperature increases, also as rainy season begins both temperature and Evapotranspiration values decrease.

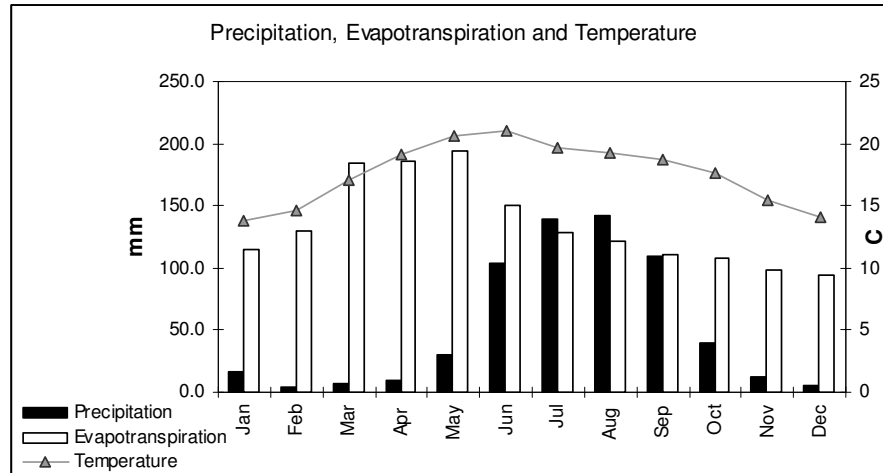


Figure 2-7: Average monthly precipitation and Pan Evapotranspiration over 20 years

2.5. Soils

The soils in the Cuitzeo basin have been classified according to the categorization dictated by the Food and Agriculture Organization of the United Nations (FAO). Table 2-2 shows the soil types present in the Cuitzeo basin, and identifies the most dominant ones.

Table 2-2: Soil types in the Cuitzeo basin

Soil type	Area %
Acrisols	11.3
Andosols	11.6
Cambisols	2.2
Gleysols	0.6
Leptosols	6.6
Luisols	24.8
Phaeozems	18.5
Planosols	4.1
Regosols	1.3
Solonchaks	0.6
Vertisols	18.5

Luisols are the main soil type in the basin. They are soils having an *argic* horizon, or subsurface horizon which has distinctly higher clay content than the overlying horizon. These soils often have a specific set of morphological, physico-chemical and mineralogical properties other than a mere clay increase.

Vertisols and Phaeozems are the second most dominant soil types in the basin. Vertisols are soils with a *vertic* horizon; which are characterised by a heavy texture (more than 30% of clay) and the presence of polished, shiny ped surfaces (slickensides). Phaeozems are soils with a *mollic* horizon; they have a base saturation of 50 percent or more and a calcium carbonate-free soil matrix.

Andosols and Acrisols are the third most dominant soil types. Andosols are soils having a *vitric* or *andic* horizon. The *vitric* horizon is a surface or subsurface horizon dominated by volcanic glass and other primary minerals derived from volcanic ejecta; and the *andic* horizon is a horizon resulting from moderate weathering of mainly pyroclastic deposits. Acrisols also have an *argic* horizon, like the one described for the Livisols.

Out of the main five soil types three have very high clay content. Soils dominated by clay have low infiltration rates due to their smaller sized pore spaces, and this consequently generates runoff. This runoff carries sediments and fertilizers used in the agriculture fields, onto the lowest part of the basin, where the lake is, and most of it gets deposited there.

2.6. Vegetation

Around 40% of the basin is covered by crops or agriculture land, 20% is covered by natural Pine and Encino trees, 15% is covered by subtropical bushes, and 15% is covered by meadows. The main agricultural crops are corn (which is the staple food or base of the traditional diet), coffee and cotton.

In the lake, all types of wetland macrophytes exist. Most of the surface-floating macrophytes or ephydates correspond to the Water Hyacinth type (*Eichhornia crassipes*); the emergent macrophytes or hyperhydates, in local terms is known as Tule (*Scirpus ssp* and *Typha Domingensis*); and the submersed macrophytes or hyphydates are Coture (*Potamogeton Pectinatus*) (Rojas and Novelo 1995), (O'Sullivan and Reynolds 2003).

2.7. Socio-economic values

The basin is composed of 26 municipalities, 20 of those are in the state of Michoacán, and the city of Morelia is the biggest city in the basin, and the capital of the state. The population was 387, 775 by 1995. Some of the main localities around the lake are San Agustín del Pulque, Santa Ana Maya, Estación Querendaro, and Cuitzeo del Porvenir; their main economic activities are fishing, agriculture, and cattle raising.

There has been a strong migration movement in the state of Michoacán developing since the 1940's. The principal destinations are the United States of America, the state of Jalisco, and Mexico's Federal District. This migration has caused the abandonment of a lot of the agriculture lands, and in return corn production has been affected on a national level because, as mentioned before, corn is the staple food or the base of the traditional diet in the country.

The denomination of Lake Cuitzeo as a Wetland of International Importance is seen as an opportunity that will help impel the regions economy, as the localities surrounding the lake will have an increase in tourists, and "eco-tourism" related activities. The three basic challenges generally faced in this area relate to biodiversity conservation, promotion of community development, and management of eco-tourism as a viable alternative. In the process of overcoming these three challenges employment will be developed, especially in those communities that have more access to the lake. This new

employment boom might attract new people, or keep the people there from leaving, as new opportunities arise.

3. Water quality assessment

In this chapter, we seek to answer the first two groups of research questions:

- What is the state of the water quality at representative sample points distributed throughout the different parts of Lake Cuitzeo?, and
- What is the relationship between water quality, eutrophic levels and wetlands vegetation? Which areas of the lake are suitable for development of wetland vegetation?

The research methods used to answer the first question include hydrological variable analysis, sample recollection, statistical and chemical analysis, and interpretation of the different analyses results. Also, an identification of possible thermal water springs inside the lake was made. For the second question, a comparison of the samples to eutrophication values was done, as well as an assessment of the most suitable areas for vegetation development was carried out, through an evaluation of the current vegetation in the lake.

3.1. Hydrological variables

Variations in hydrological conditions have important effects on water quality, that is why hydrological measurements are essential for the interpretation of water quality data and for water resource management (Kuusisto 1996). For the purpose of understanding these hydrological conditions, streamflow measurements and discharge calculations were performed on the main inflows to the lake. Figure 3-2 shows the sites where the measurements were done in the Cuitzeo basin during fieldwork.

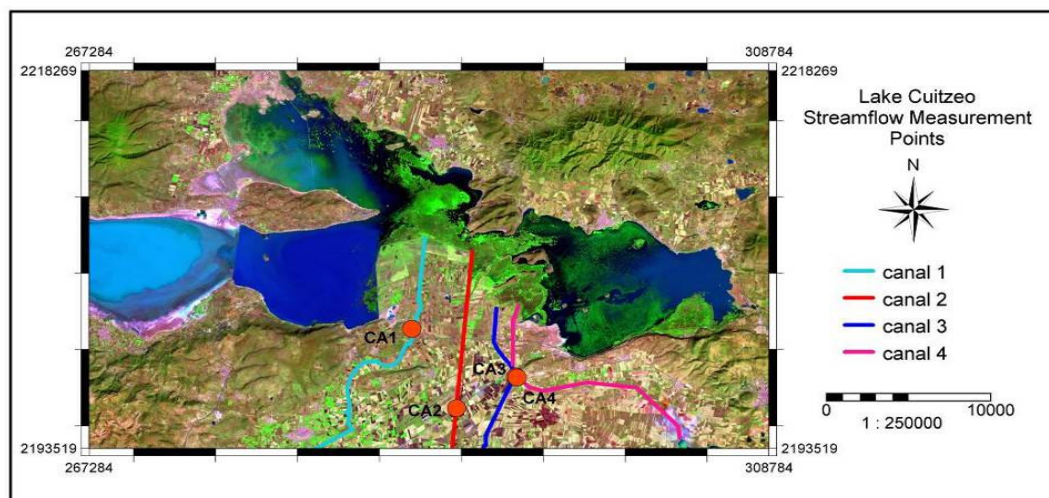


Figure 3-1: Streamflow measurement sites in the Cuitzeo basin

3.1.1. Results of streamflow measurements and discharge calculations

The most accurate method of measuring streamflow is to measure the cross-sectional area of the stream and then, using a current meter, determine the average velocity in the cross-section. Also, a rough estimate of velocity can be made by measuring the time required for a float to travel a fixed distance along the stream (Kuusisto 1996), this method is used in the measurement of streamflow where excessive velocities, depths, floating drift, or any other impediments prohibit the use of a current meter (Parodi 2002).

Streamflow and discharge for canal #1:

The Velocity-Area method was used to determine the streamflow of the first canal. The bridge from where the measurements were done divided the main canal into three sub-sections, all of them were measured.

There were 12 verticals measured for determining the cross section. The total area of the three sub-sections was 27.43 m², the average velocity for all three was 0.25 m s⁻¹, and the calculated total discharge was equal to 7.4 m³ s⁻¹ (see Appendix A for cross section and calculation details).

For canal #1 the floater method was also used to calculate discharge, and compare the differences between methods. The total discharge was equal to 7.9 m³ s⁻¹; which represents an over estimation of 7% (see Appendix A for calculation details). A quite small difference, therefore the floater method could be used for the other measurements.

Streamflow and discharge for canal #2:

Here the Floater Method was used, since the current meter couldn't be placed in the appropriate position.

There were 11 verticals measured for determining the cross section. The area of the canal was 31.65 m², the average velocity was 0.92 m s⁻¹ and the calculated total discharge was equal to 29.1 m³ s⁻¹ (see Appendix A for cross section and calculation details).

Streamflow and discharge for canal #3:

The floater method was repeated for this canal too. There were 9 verticals measured for determining the cross section. The area of the canal was 10.1 m², the average velocity was 0.37 m s⁻¹, and the calculated total discharge was equal to 3.8 m³ s⁻¹ (see Appendix A for cross section and calculation details).

Streamflow and discharge for canal #4:

The floater method was applied for discharge measurement on the last canal as well. There were 11 verticals measured for determining the cross section. The area of the canal was 18.2 m², the average velocity was 0.65 m s⁻¹, and the calculated total discharge was equal to 12 m³ s⁻¹ (see Appendix A for cross section and calculation details).

3.1.2. Comparison of obtained discharge to historical values

There are eighteen gauging stations in the Cuitzeo basin, one of them, El Plan station, is located directly upstream from where the measurement for canal #2 was taken. Figure 3-1 shows average measurements for the month of September for the last twenty three years (1980-2003). The last measurement shown in the figure, 2004, was taken and calculated during fieldwork, and is included in this chart for comparison of values, in other words, to assess how the current amount of water flowing into the lake, compared to historical values. The missing values in the figure are due to lack of data for those years.

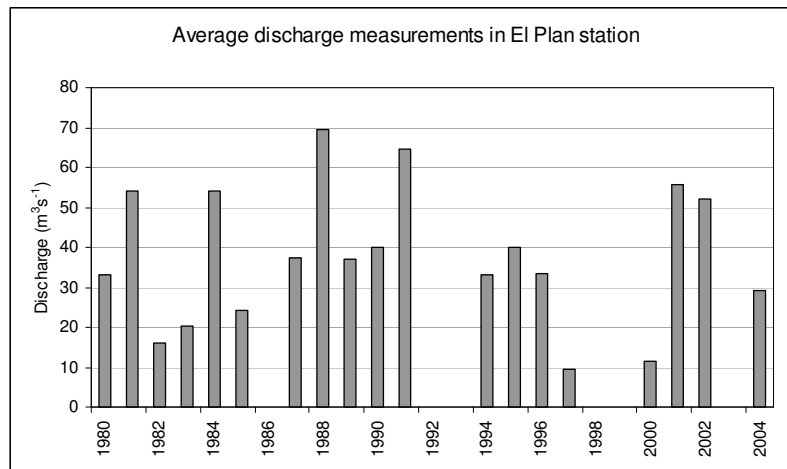


Figure 3-2: Historical discharge values

The discharge for 2004 is $29.1\text{m}^3\text{s}^{-1}$, the historical mean is $39.1\text{m}^3\text{s}^{-1}$, the discharge for 2004 is $10\text{m}^3\text{s}^{-1}$ below the historical mean. However it was observed during fieldwork that discharge for all canals diminished considerably while heading downstream, mainly because of infiltration to groundwater, vegetation developing in the canals, and other obstructions. Since the measurement for canal #2 was taken further downstream than the one taken at El Plan, the value for 2004 should be considered as equal or slightly above the historical mean.

Other than this, in a satellite image obtained in October 2004, the area covered with lake water is much higher than the ones seen in previous years. This suggests that inflow to the lake during 2004 must have been higher than usual.

3.2. Lake cuitzeo water quality issues

The Ramsar Convention on wetlands states that water quality analysis and monitoring are considered part of the basic performance indicators when designing a wetland management plan (Ramsar 2002). The aim of a wetland management plan is the effective conservation of the wetland; and for this purpose the U.S. Environmental Protection Agency specifies that as the effort to protect and enhance wetland resources grows, it is necessary to ensure that the standards for water quality applied to other surface waters are also applied to wetlands (USEPA 1990). Therefore, the water quality analysis

performed for this project aims to follow the Ramsar convention and USEPA suggestions to provide information that helps in the development of a monitoring plan for Lake Cuitzeo.

The first issue to focus on is that during the past forty years Lake Cuitzeo has experienced two steady cycles. The first cycle is an annual one in which the lakes water coverage grows during wet seasons and diminished during dry seasons. The second cycle is a more extreme one. Every five to ten years, the lake loses water to the point where the northern and western parts of the lake become dry. In the opposite peak of the cycle the lake floods again submerging soils that have had deposition of sediments with chemical components attached to it.

The second issue to focus on is that at the same time these cycles takes place; the lake has experienced a growth in vegetation during the last decades, especially in the passageway between the central and eastern parts, where irrigation canals drain after traversing the agriculture fields.

Finally, the thermal springs that have developed mostly around the eastern and western ends of the lake and the ones suspected to have developed inside the lake, alter the status of the water quality in the lake.

3.3. Sampling Lake Cuitzeo

In order to perform a physical analysis of water quality, the following parameters were measured: coordinates X, Y (*m*), depth at sampling point (*m*), temperature ($^{\circ}\text{C}$) and Secchi depth or transparency (*cm*).

The basic chemical parameters analyzed were: Electrical Conductivity ($\mu\text{S cm}^{-1}$), pH, alkalinity ($\text{mg l}^{-1} \text{HCO}_3^{-2}$), total hardness ($\text{mg l}^{-1} \text{CaCO}_3$), Chloride (mg l^{-1}) Bicarbonate (mg l^{-1}), Magnesium (mg l^{-1}), Calcium (mg l^{-1}), Sodium (mg l^{-1}) and Potassium (mg l^{-1}).

The following parameters were analyzed to determine the nutrient load: Nitrate (mg l^{-1}), Phosphate (mg l^{-1}) and Nitrite (mg l^{-1}). Also Sulphate (mg l^{-1}) was analyzed to assess the influence of the thermal springs.

3.3.1. Zonation of the lake

Satellite images reveal boundaries within the lake, some natural some artificial. Within these boundaries differences in reflectance values are observed. One of the causes for this is attributed to the visible color of the water, which is the result of the different wavelengths not absorbed by the water itself, as the result of dissolved and particulate substances present. It can be also an indicator of the depth to which light is transmitted. This, in turn, controls the amount of primary productivity that is possible within the lake by controlling the rate of photosynthesis of the algae present (Chapman 1992), resulting in alteration of the water quality in the lake.

The zonation allows us to study each part of the lake as an individual water body, permitting us to understand the behavior in each before trying to understand the lake as a whole. The zonation was based on the boundaries observed within the lake. For example, the western and central parts of the

lake are divided by a highway, and there is only one point in which water from the central part of the lake can flow to the western part of the lake. Then, the central, northern and eastern part of the lake are essentially three different water bodies that are connected by a “passageway”, however this passageway is the main contributor of water for all three parts, but once it gets to one of these it mixes with other inflows. Figure 3-3 shows the zonation of the lake: in red the central part of the lake, in yellow the passageway part, in orange the east part and in blue the west part. The northern part was not delineated in this zonation since no samples were taken there.

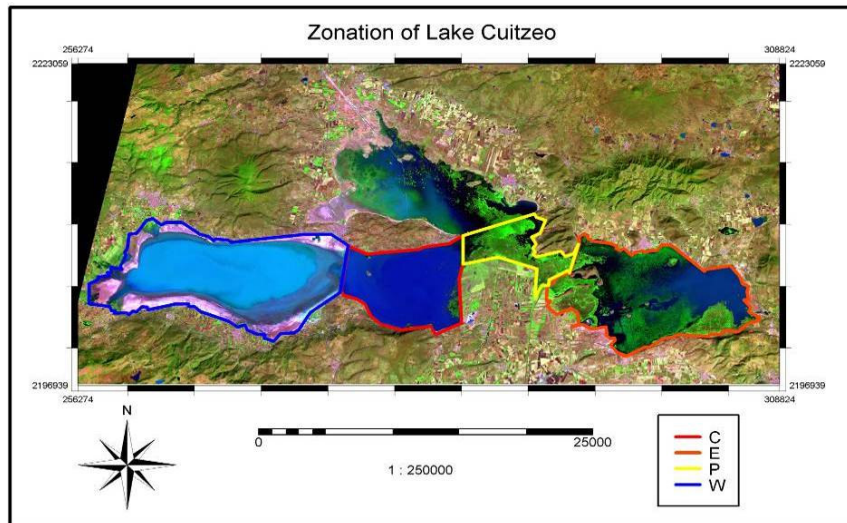


Figure 3-3: Zonation of Lake Cuitzeo

3.3.2. Sampling sites

A sampling strategy was developed after visual interpretation of acquired satellite images. In those acquired during wet seasons, a pattern was observed on the central part of the lake; therefore a stratified random method was used for this part. Special attention was placed on this site when developing the sampling strategy, basically because most of the fishing occurs in this area, and because it is a part of the lake that remains submerged under water all the time, also there is less submerged vegetation than in the eastern part of the lake, which makes it easier for the boats to navigate. A random, less detailed, method was used for the rest of the areas.

During fieldwork, a preliminary interpolation of EC values confirmed that there is a relationship between the pattern observed in the images of the water body taken in the wet seasons of previous years, and the values obtained in field; therefore, the sampling strategy was modified in the attempt to capture and represent the spatial variability of water quality optimally.

The final number of samples obtained during fieldwork was 109. 61 samples in the central part, 25 in the eastern part, 9 in the passage way between the central and eastern parts and 7 in the western part, the northern part of the lake couldn't be sampled due to weather complications. Additionally, 2 samples were collected at pumping stations, 4 on inflowing canals and 1 in a thermal spring. Figure 3-4 depicts the sampling sites inside Lake Cuitzeo, the sample points are depicted in different colors in response to the part of the lake in which they were taken. To the South of the lake the location of

the thermal spring is depicted in cyan, the pumping stations are depicted in black and the canals are depicted in magenta.

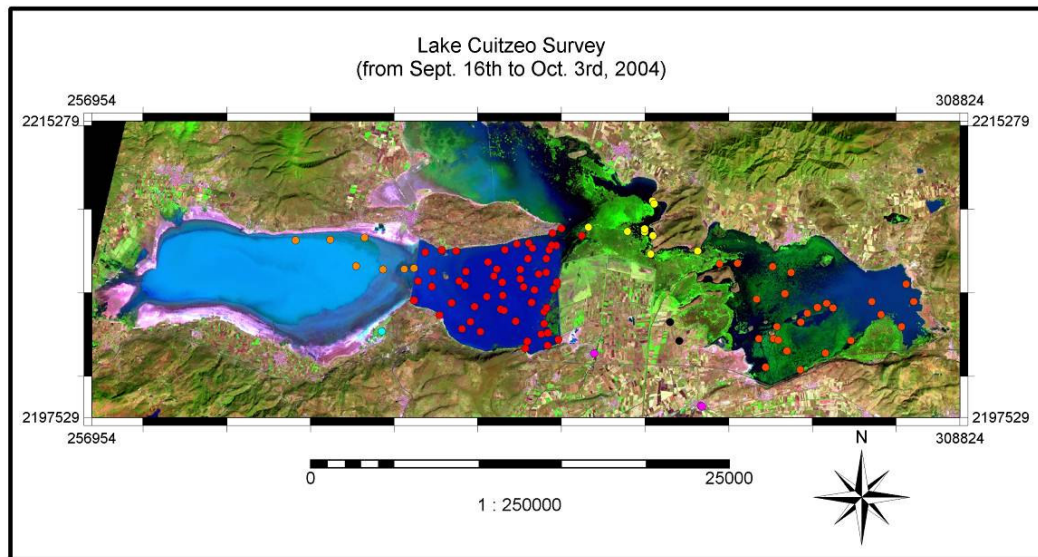


Figure 3-4: Sampling sites for Lake Cuitzeo

3.4. Water quality survey

The first step in sample collection was recording the date and time for each sample, as well as its position with a portable Garmin Etrex GPS (Global Positioning System). Each sample point was assigned a specific code in relation to its location and sample number (see Appendix B: Chemical analysis for a description of the codes).

Before sampling took place, a description of the surrounding area was recorded, it included: water color, types of emergent, submersed or floating vegetation in the area, and any other features present in the water like foam or bubbles.

3.4.1. Chemical analysis of the water samples

The analyses done in situ were: EC, pH, Temp, Alkalinity and Transparency, Total Hardness and Chloride (refer to Appendix B for the list of analysis equipment used).

Then, each sample was filtered with a 0.22 μm filter and with a 0.45 μm filter; as they were filtered they were injected into different vacutainers⁴ and kept refrigerated. These would later be taken to the laboratory in UNAM's Institute of Geography for further analyses in Mexico City, where each sample was tested for basic anions and basic cations.

⁴ A vacutainer is a vacuum sealed test tube with negative pressure on the inside that allowed easy transfer of the sample from the syringe (with the 0.22 μm or 0.45 μm filter) to the tube; also due to the lack of Oxygen and the stable environment inside the tube no acidification was necessary to maintain the samples.

Finally 7% of the samples were filtered with 0.45 µm filters, into 100 ml bottles, acidified with Nitric Acid to a pH of 2.0, refrigerated and brought back to the ITC laboratory for comparison with the values obtained in the UNAM laboratory.

In the UNAM lab in Mexico City, each sample was tested for basic anions, basic cations and Sulphate. For most of the samples a dilution of 1:8 was needed when analyzing anions, for some of the C samples a dilution of 1:4 was needed. For Calcium and Sodium a dilution of 1:10 was needed, and for Magnesium and Sodium a 1:100 dilution was needed (refer to Appendix B for the list of analysis equipment used).

Refer to Appendix B: Chemical analysis, for a detailed table showing the water quality analysis results obtained for the lake, as well as for the canals, pumping stations and thermal spring.

3.4.2. Reliability check

The reliability check lists the major ways to identify apparent inconsistencies in an analysis. It cannot be overemphasized that an inconsistency only indicates that an analysis is unusual, not necessarily wrong (Hounslow 1995).

3.4.2.1. Duplicate comparison

It is generally recommended that duplicate analyses be run for 10% of the samples. Only 7% of the samples taken in Cuitzeo could be brought back to the ITC lab. These samples were taken on different dates, from different parts of the lake, and surrounding areas. They were analyzed for basic cations through Inductivity Coupled Plasma – Atomic Emission Spectroscopy (ICP-AES). Tables 3-4 and 3-5 describe the correlation and standard error calculations found between values obtained in UNAM’s lab in Mexico and the ITC lab (see Appendix B for complete table of values):

Table 3-1: Sample correlations

	<i>Mg</i> (UNAM)	<i>Ca</i> (UNAM)	<i>Na</i> (UNAM)	<i>K</i> (UNAM)
Mg(ITC)	0.94			
Ca(ITC)		1.00		
Na(ITC)			0.98	
K(ITC)				0.98

Table 3-2: Standard error percentage

	<i>Mg</i> (UNAM)	<i>Ca</i> (UNAM)	<i>Na</i> (UNAM)	<i>K</i> (UNAM)
Mg(ITC)	1.8			
Ca(ITC)		0.6		
Na(ITC)			42.7	
K(ITC)				2.6

A correlation of 1.0 would indicate a very strong linear relationship between the two sample sets. Taking into account that the analysis in ITC was done almost one month after the samples were taken, then the values obtained (0.94 – 1.00) are very good. Standard error is the measure of the deviation of a statistic from the data. For standard error calculations the maximum error value is 100%, again the values obtained for Mg, Ca and K (0.6 – 2.6%) seem to be acceptable, however there is an inconsistency in the value obtained for Na, this might be related to the very high levels of Na in the lake, to the time elapsed between the collection of the sample and the analysis in the ITC laboratory,

or many other factor. Nonetheless the Na values obtained at the UNAM laboratory will be used for the rest of the analysis.

3.4.2.2. Anion-cation balance

The analysis accuracy of many water samples may be checked by measuring how electrically neutral the solution is. The charge balance is usually expressed as a percentage:

$$\text{Balance} = \frac{(\sum C - \sum A)}{(\sum C + \sum A)} * 100$$

Where:
 $\sum C$ is the sum of cations
 $\sum A$ is the sum of anions

If the balance is $\pm 10\%$ the analysis is assumed to be good.

If the balance is exactly 0% it is likely that the Na or Na+K were determined by difference.

If the balance is much greater than $\pm 10\%$ then:

- The analysis is poor (inaccurate)
- Other constituents are present that were not used to calculate the balance
- The water is very acid and the H⁺ ions were not included, or
- Organic ions are present in significant quantities (often indicated by colored water).

Out of the 61 samples in the central part of the lake 82% of the samples passed the anion-cation balance. Out of the eleven samples that did not pass, two were very close to the $\pm 10\%$ limit. Six have very high values for the anions, while the cations were detected but in lower values, however they are all located relatively close to each other near the passageway, indicating similarities in the water in that area, and also probably other unexpected cations around the inflows coming from the agricultural area. In two of the samples.

Out of the 25 samples in the Eastern part of the lake 56% of the samples passed the anion-cation balance. Eleven samples did not pass, five of which are close to the $\pm 10\%$ limit. In this part of the lake, also 56% of the samples have Na values which are above normal; this affects the anion-cation balance.

Out of the 9 samples in the passageway between the Central and the Eastern part of the lake 44% of the samples passed the balance test. The five samples that did not pass the test are located on a fine strip of water, between floating vegetation (water hyacinths) and the Northern shore. Assuming that the analysis done in the lab was correct, then there might be other constituents present in the water that were not taken into account when calculating the balance.

Out of the 7 samples in the Western part of the lake 71% of the samples passed the balance test. Out of the two samples that did not pass, one has a very high Na value, as do 85% of the samples in this area; and the second one has a very high Bicarbonate value.

It is important to state that the anion-cation balance had a more significant output in the central part of the lake, where the highest amounts of samples were taken. For parts such as the passageway and the western part only 9 and 7 samples were taken respectively. However is important to state that the probable cause of most of the failing balances has to do with the high amounts of Na in the water.

3.4.3. Interpretation of the samples

Water quality data may be interpreted on the basis of both individual analyses and sets of analyses from one sampling site or different sampling sites in an area or aquifer being examined. They can be compared and interpreted using graphical methods and statistical analyses (Hounslow 1995). Each analysis method offers a different outlook for the same set of samples; therefore it is important to analyze all their different outputs.

3.4.3.1. General lake chemistry analysis

In the absence of any living organisms, a lake contains a wide array of molecules and ions from the weathering of soils in the watershed, and the lake bottom. Therefore, the chemical composition of a lake is fundamentally a function of its climate (which affects its hydrology) and its basin geology. Each lake has an ion balance of the three major anions and four major cations (Horne and Goldman 1994). Table 3-6 describes the typical ion balance for a fresh water lake.

Table 3-3: Typical Ion balance for a fresh water lake

Anions	Percent	Cation	Percent
HCO ₃ ⁻	73%	Ca ²⁺	63%
SO ₄ ²⁻	16%	Mg ²⁺	17%
Cl ⁻	10%	Na ⁺	15%
		K ⁺	4%

The anion-cation balance performed for each part of the lake can be compared to these values to estimate how the anion-cation concentrations in Lake Cuitzeo diverge from those of a typical lake. Figure 3-5 depicts in black the appropriate percentage of the ions in a typical lake, and the variations per ion from that appropriate percentage (from table 3-6), for the different parts of the lake.

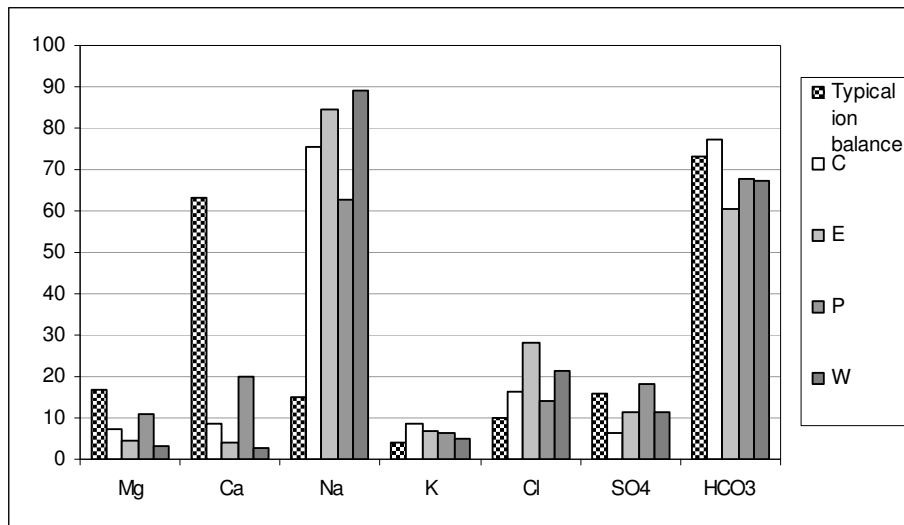


Figure 3-5: Ion balance in typical lakes vs. ion balance in Lake Cuitzeo

This analysis reveals that the percentage of Magnesium is lower than the typical value, in all parts of the lake, as well as Calcium percentage is considerably lower, in all parts of the lake. Sodium percentages are extremely high in all parts of the lake. Potassium and Chloride are also higher than the typical values, in all parts of the lake. Sulphate values are lower, in all parts of the lake, except for the passageway, and Bicarbonate values are lower than the typical values, in all parts of the lake, except for the central part of the lake.

3.4.3.2. Statistical data analysis

This data set contains a number of quantitative variables, whose distribution was analyzed as a first step to understand what the numbers are telling us. The five-number summary offers a reasonably complete description of the spread of the data. It consists of the smaller observation, the first quartile (Q_1), which is larger than 25% of the observations, the mean and median which are two different measures of the center of a distribution, the third quartile (Q_3) is larger than 75% of the observations, and the largest observation. However the five-number summary is not the most common numerical description of a distribution; it is the combination of the mean and the standard deviation, which measures spread by looking at how far the observations are from their mean (Moore 1999).

Figures 3-6 to 3-13 compare the five number summaries for pH, EC, and the major ions from which different water types are determined in the different parts of the lake (refer to Appendix B: chemical analysis for the tables containing the numerical results for the five-number summaries and standard deviations).

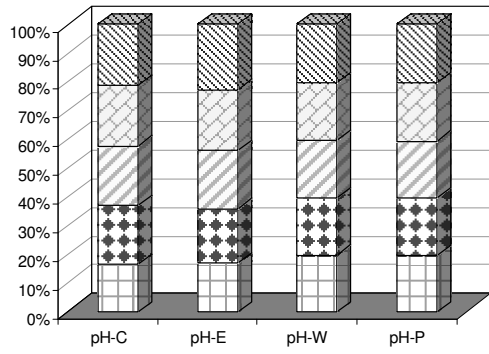


Figure 3-6: Five-number summary comparison for pH in the different parts of the lake

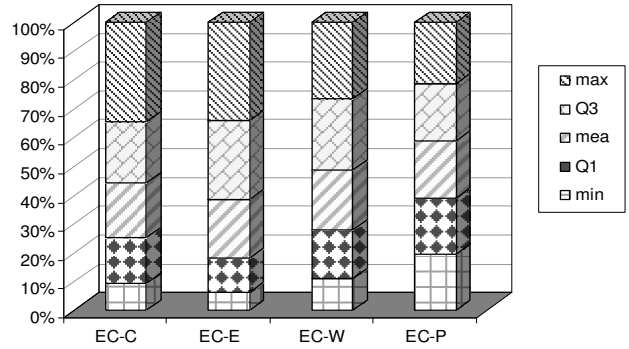


Figure 3-7: Five-number summary comparison for EC in the different parts of the lake

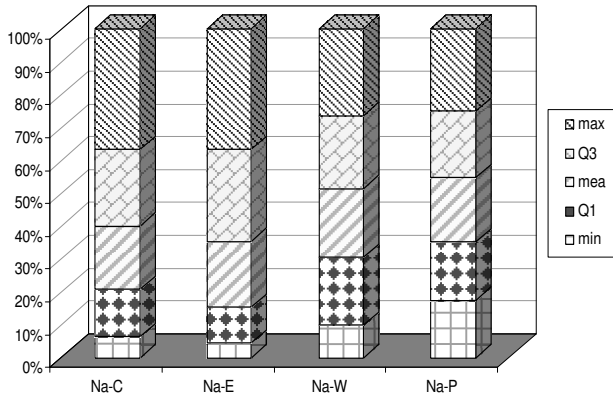


Figure 3-8: Five-number summary comparison for Na in the different parts of the lake

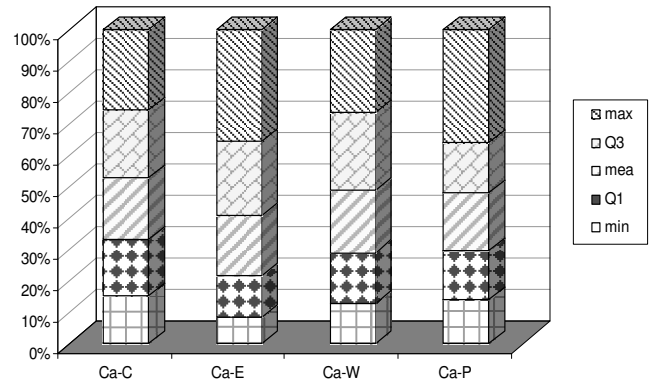


Figure 3-9: Five-number summary comparison for Ca in the different parts of the lake

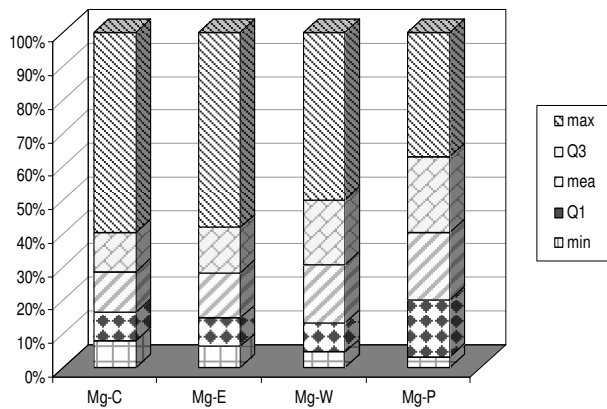


Figure 3-10: Five-number summary comparison for Mg in the different parts of the lake

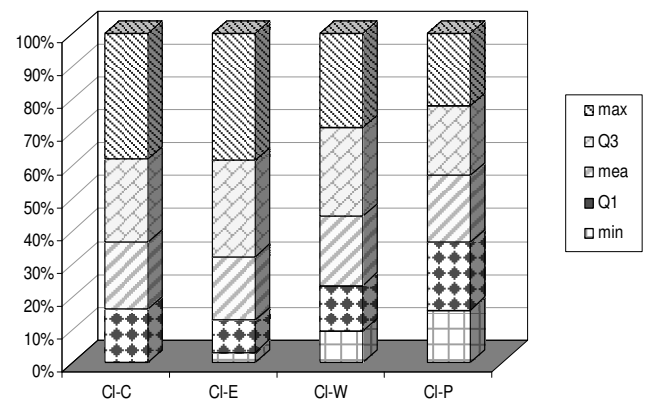


Figure 3-11: Five-number summary comparison for Cl in the different parts of the lake

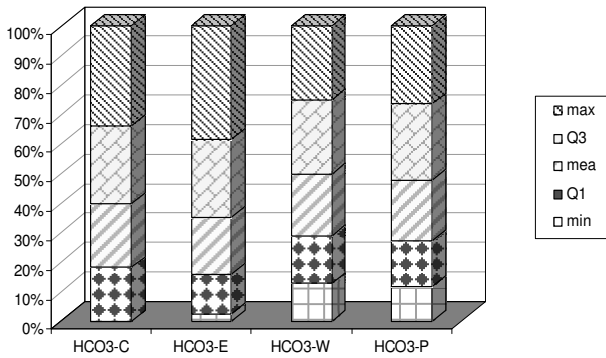


Figure 3-12: Five-number summary comparison for HCO3 in the different parts of the lake

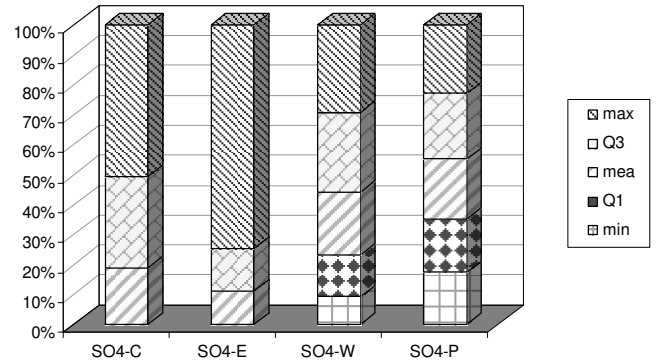


Figure 3-13: Five-number summary comparison for SO4 in the different parts of the lake

Figures 3-14 to 3-16 are a graphical comparison of standard deviation values, the variations of the analyzed variables in the different parts of the lake are easily observed.

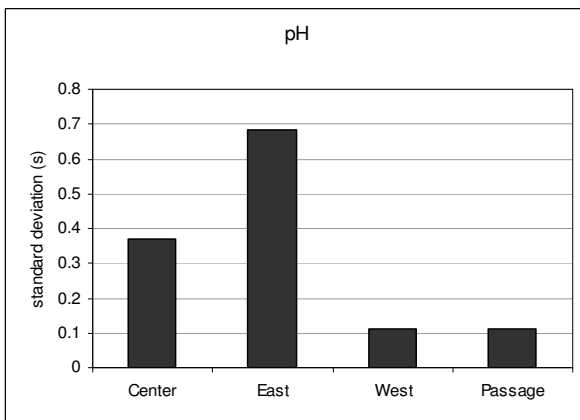


Figure 3-14: Comparison of standard deviation values (pH)

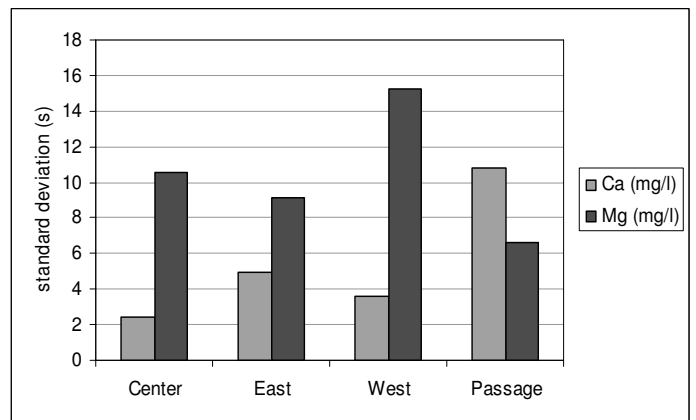


Figure 3-15: Comparison of standard deviation values (Ca and Mg)

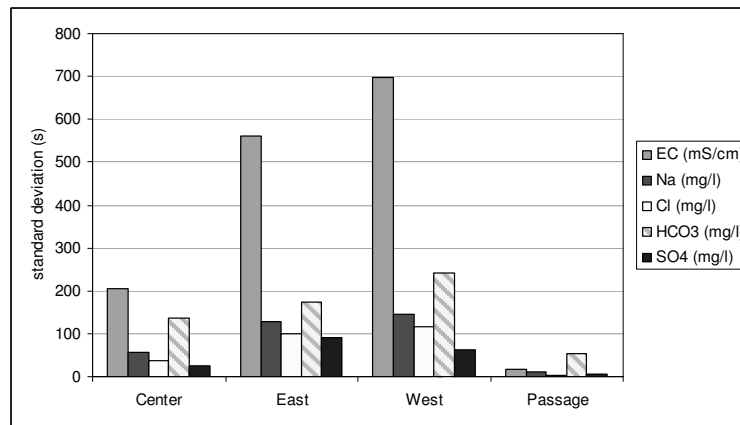


Figure 3-16: Comparison of standard deviation values (EC, Na, Cl, HCO₃ and SO₄)

These graphs are the first indicator of water quality diversity in different parts of the lake. For instance we observe that the passageway, where currents form and flow into the central and eastern parts of the lake, has low standard deviations for all the variables. The eastern part of the lake has higher standard deviations than the central part, for most of the variables except Magnesium. The western part of the lake has the highest standard deviations for most of the variables (Magnesium, EC, Sodium, Chloride and Bicarbonate, 63% of the statistically analyzed variables).

3.4.3.3. Water types

Water type calculations are based on the major ions present in every sample. First all concentrations in the samples are converted to meq/L, all values are then transformed from meq/L to meq%, all parameters which are below a certain limit (10% by default) are removed. Finally the remaining ions are considered major ions. These ions are ordered according to their percentage, cations are ordered first, followed by the anions.

Tables 3-4 to 3-7, and figures 3-17 to 3-20 give an idea of the different water types found in each part of the lake, and the percentage of analysed samples that fall under each category, deciding not only the main water type, but also how many different categories are found in each part of the lake.

Table 3-4: Water types in the Central part of the lake

WATER TYPE	%	Number of samples
Na-HCO ₃ -Cl	84	51
Na-Mg-HCO ₃ -Cl	5	3
Na-HCO ₃	9	5
Na-Mg-Cl	2	2

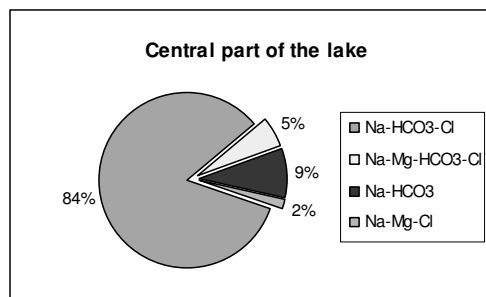


Figure 3-17: Water types in the Central part of the lake

Table 3-5: Water types in the Eastern part of the lake

WATER TYPE	%	Number of samples
Na-HCO ₃ -Cl	76	19
Na-HCO ₃ -SO ₄ -Cl	8	2
Na-Mg-HCO ₃ -Cl	4	1
Na-Ca-Mg-HCO ₃ -SO ₄	4	1
Na-Cl	4	1
Na-Cl-SO ₄	4	1

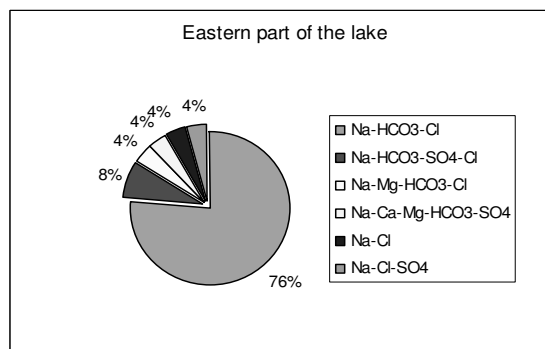


Figure 3-18: Water types in the Eastern part of the lake

Table 3-6: Water types in the Passageway between C and E parts of the lake

WATER TYPE	%	Number of samples
Na-HCO ₃	11	1
Na-Mg-HCO ₃	11	1
Na-Mg-HCO ₃ -SO ₄	22	2
Na-HCO ₃	11	1
Na-Ca-HCO ₃ -SO ₄ -Cl	11	1
Na-Mg-Ca-HCO ₃	11	1
Na-Mg-Ca-HCO ₃ -Cl	11	1
Na-Mg-Ca-HCO ₃ -SO ₄ -Cl	11	1

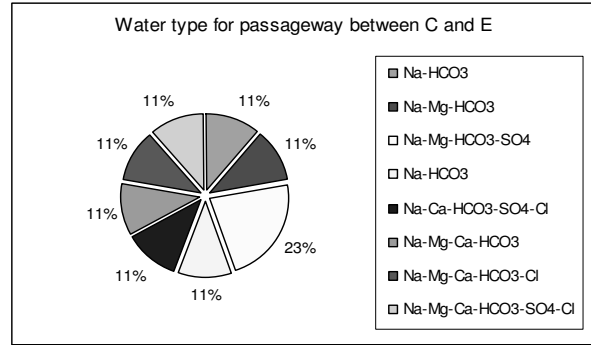


Figure 3-19: Water types in the Passageway between C and E parts of the lake

Table 3-7: Water types in the Western part of the lake

WATER TYPE	%	Number of samples
Na-HCO ₃ -Cl	83	6
Na-Cl	17	1

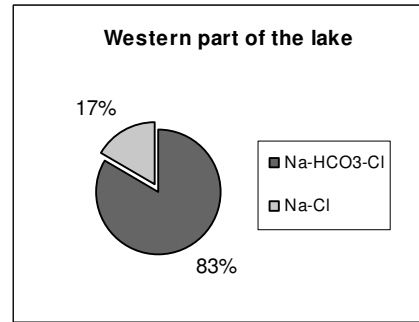


Figure 3-20: Water types in the Western part of the lake

The water type classification for each part of the lake indicates that water type Na-HCO₃-Cl is the main water type for three of the four parts of the lake that were analyzed, but also Na and HCO₃ is present in most of the water types. The Na must be washed out from the agricultural area in to the lake. And nearly two thirds of the carbon (HCO₃⁻) in river water is derived from the atmosphere either directly as gaseous CO₂²⁻ or via photosynthesis followed by plant decay; the remaining HCO₃⁻ is derived largely from weathering of carbonates (O'Sullivan and Reynolds 2003).

The classification also shows that the western part of the lake has the least amount of water types with only two types, and the passageway section has the most types with eight different types. The central part has four types and the eastern part has six types. This analysis is the second indicator of water quality differences in each part of the lake.

Like in the anion-cation balance, the most significant results are those for the central part of the lake, because of the sampling density. However the analysis is applied to all sampled parts to have an idea of differences within them.

Figure 3-21 is a visual interpretation of the water types through the use of Thiessen Polygons, nonetheless because of the differences in sampling, the size of the polygons does not depict the area each water types covers.

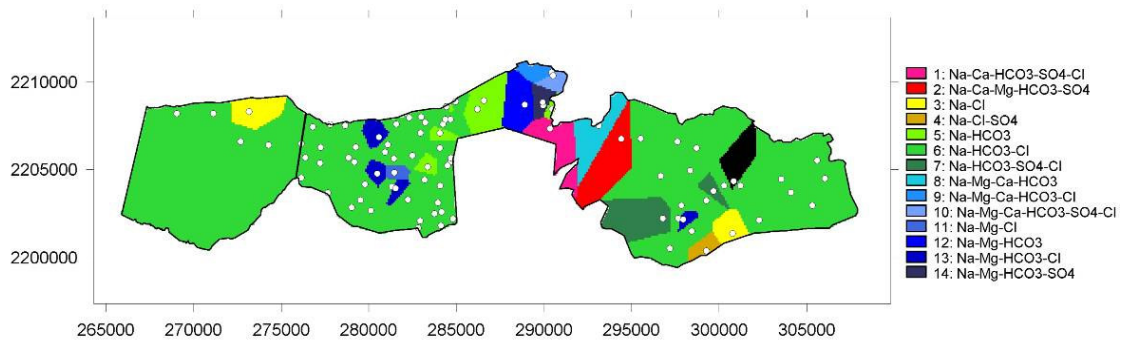


Figure 3-21: Thiessen polygons representing water types in the lake.

3.4.3.4. Graphical analysis

Graphical methods of illustrating water analyses have two objectives. The first is to be able to plot analyses on a map, and the second is to detect chemical trends (Hounslow 1995).

Piper Diagrams:

In 1944 Piper divided the waters into four basic types sowed in a diagram conformed by anion and cation triangles. A diamond shape between them is used to re-plot the analyses. The water type is determined according to their position related to the four corners of the diamond. Samples that plot on the top corner of the diamond are indicative of permanent hardness. Samples that plot near the left corner are in a region of temporary hardness. Samples plotted at the bottom corner are primarily alkali carbonated. Finally, samples near the right corner of the diamond may be considered saline (see Appendix B; figure B 2 for interpretation diagram).

Figures 3-14 to 3-17 depict the results of the Piper diagrams for the different parts of the lake.

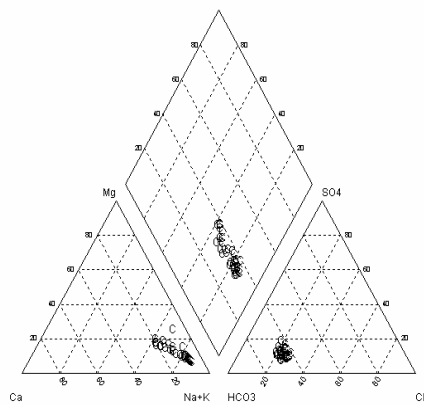


Figure 3-22: Piper plot for the Central part of the lake

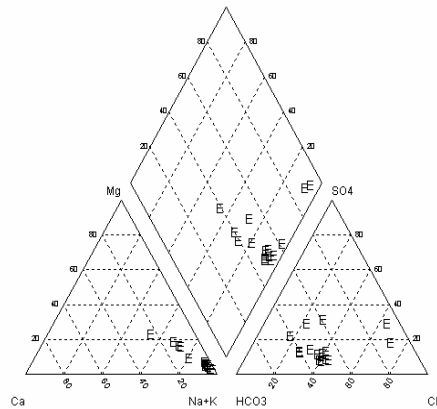


Figure 3-23: Piper plot for the Eastern part of the lake

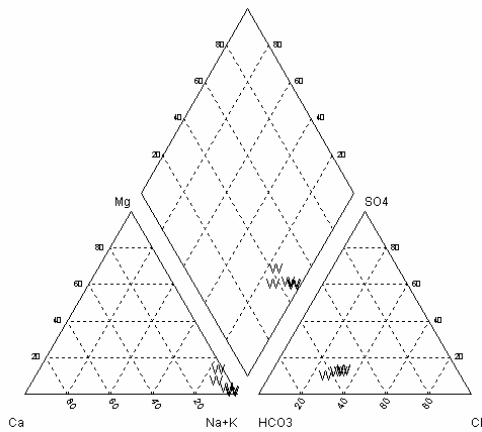


Figure 3-24: Piper plot for the Western part of the lake

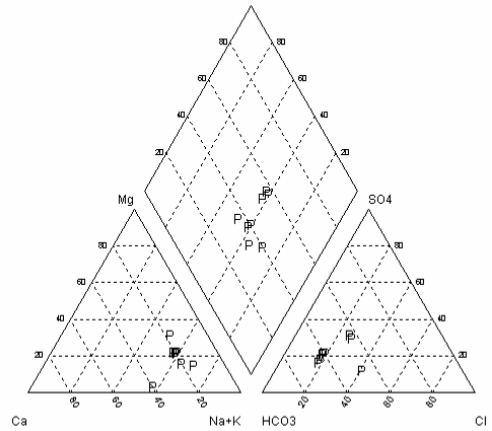


Figure 3-25: Piper plot for the Passageway between the C and E parts of the lake

The plot for the central part of the lake shows all the samples lying on a straight line that extends from above the Alkali Carbonate range towards the Temporary Hardness diamond, very close to the Saline water boundary.

The plot for the Eastern part of the lake shows 88% of the samples lying on the Saline water diamond. The remaining 12% are lying in between the saline and Temporary Hardness diamonds.

The plot for the Western part of the lake shows 85% of the samples lying in the Saline water diamond, and 15% lying close to the Alkali Carbonate triangle.

Finally, the plot for the Passageway shows 11% of the samples lying in the Temporary Hardness diamond, 55% lying between the Temporary Hardness and Saline diamonds, and 33% lying in the Saline water diamond.

Stiff Diagrams:

These diagrams have four parallel, horizontal axes extending on each side of a vertical, zero axes. Four cations and four anions can be plotted on the left and right of the vertical axis, respectively. In this case the cations plotted on the left are Sodium, Calcium and Magnesium, and the anions plotted on the right are Chloride, Bicarbonate and Sulphate. Figure 3-18 shows the ions represented on a Stiff plot. Figures 3-19 and 3-20 depict the results of the stiff diagram for every sample in the different parts of Lake Cuitzeo.

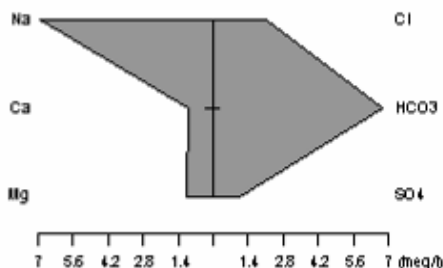


Figure 3-26: Main ions represented on the Stiff diagrams

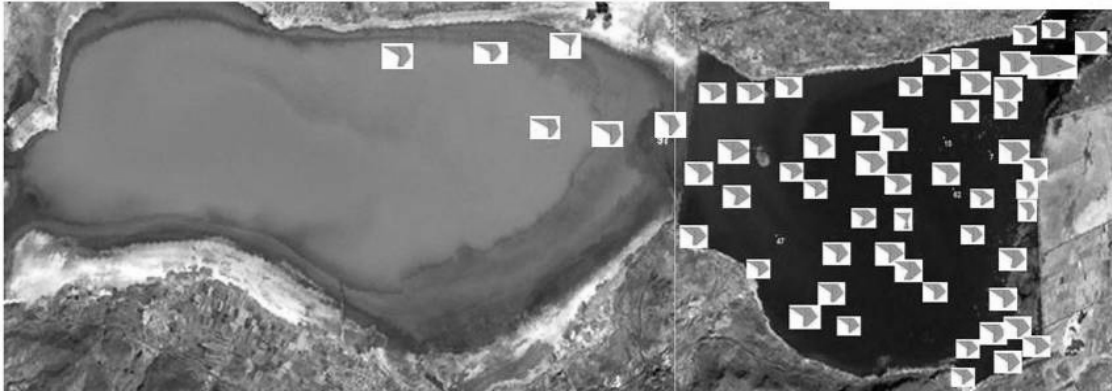


Figure 3-27: Stiff diagrams for the western and central part of the lake.

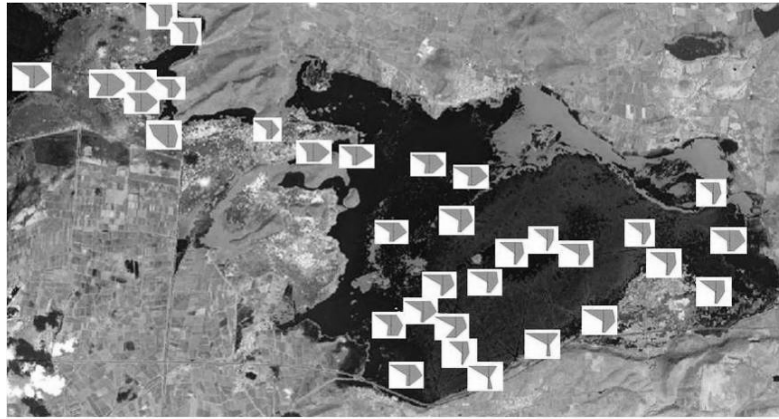


Figure 3-28: Stiff diagrams for the passageway and eastern parts of the lake.

All the stiff plots for different parts of the lake indicate a high presence of Bicarbonate and Sodium in all the samples taken. The variation of the shape of the diagram by influence of Magnesium, Calcium, Chloride and Sulphate is minimal.

3.5. Location of thermal springs in the lake

As mentioned in the description of the study area, the Lake Cuitzeo basin is located on Mexico's Transversal Volcanic Axis, which has faults in the NE-SW and E-W directions, and has experienced recent volcanism. As a result of this, thermal springs have developed on the areas surrounding the lake, and it is suspected that they exist inside the lake as well.

In an attempt to locate possible thermal springs inside the lake, a correlation analysis was performed on the sample obtained from the thermal spring, outside the west part of the lake, vs. all other samples collected during fieldwork. The water quality variables of the sample points plotted in figure 3-29 correlate by 90% or more to the water quality from the thermal spring sample. However it is important to state that one thermal spring sample is not representative of all thermal waters. Further sampling on other thermal springs would be needed to come up with final locations for thermal springs inside the lake.



Figure 3-29: Location of potential thermal waters inside the lake

3.6. Eutrophic state of the lake

Eutrophication is defined as the enrichment of water with plant nutrients, primarily Phosphorous and Nitrogen. This leads to enhanced plant growth, development of microbes and acceleration of decomposition. On decaying, this plant material causes depletion of oxygen, leading to an array of secondary problems such as fish mortality, liberation of corrosive gases, and other undesirable toxic substances (Vollenweider 1989). Each of the above seriously jeopardizes almost every kind of water use.

The *Handbuch der Technischen Gewasseraufsicht* (handbook for the technical supervision of water resources) offers chemical standards used in the lake investigation program in the province of Bavaria, Germany. In other words, it expresses water quality parameters and regulation limits that are continuously monitored in lakes. It states that pH values should range from 7.5 – 9.0., Sulphate values should be below 1 mg/l, Phosphate values should be below 0.005 mg/l, Nitrate values should be below 0.02 mg/l, Chloride values should be below 5 mg/l, Calcium should be below 2 mg/l and Magnesium should be below 1 mg/l (Bayern 2002).

Tables 3-8 to 3-11 show the compliance of the values (for certain parameters) in Lake Cuitzeo, with some of the parameters mentioned in the Bavarian monitoring plan for eutrophication control.

Table 3-8: Eutrophication analysis for the Central part of the lake

Parameters	Samples that meet the limits	Samples that do not
pH	90%	10%
SO ₄	38%	62%
PO ₄	82%	18%
NO ₃	69%	31%
Cl	7%	93%
Ca	0%	100%
Mg	0%	100%

Table 3-9: Eutrophication analysis for the Eastern part of the lake

Parameters	Samples that meet the limits	Samples that do not
pH	18%	82%
SO ₄	36%	64%
PO ₄	100%	0%
NO ₃	48%	32%
Cl	0%	100%
Ca	0%	100%
Mg	0%	100%

Table 3-10: Eutrophication analysis for the Western part of the lake

Parameters	Samples that meet the limits	Samples that do not
pH	29%	71%
SO ₄	14%	86%
PO ₄	86%	14%
NO ₃	29%	71%
Cl	14%	86%
Ca	0%	100%
Mg	0%	100%

Table 3-11: Eutrophication analysis for the Passageway part of the lake

Parameters	Samples that meet the limits	Samples that do not
pH	22%	78%
SO ₄	11%	89%
PO ₄	78%	22%
NO ₃	67%	33%
Cl	11%	89%
Ca	0%	100%
Mg	0%	100%

The handbook includes many more parameters to be monitored; unfortunately not all these parameters could be analyzed for Lake Cuitzeo.

It is a fact that for most inland water, total Phosphorus are the limiting nutrient determining productivity, and in some estuaries total Nitrogen appears to be more limiting to algal growth than phosphates (O'Sullivan and Reynolds 2003). Since the water in most parts of Lake Cuitzeo can be considered between brackish, and in some cases saline, Nitrate could be considered as an indicator of the levels of total Nitrogen present in the lake. Once compared to the handbook values, it is seen that the number of samples that comply with the established values for NO₃ are greater than those that do not. The PO₄ values are also mostly within the limits.

Another eutrophic state indicator is macrophyte development. The macrophytes stabilize the clear water state by competing with algae for nutrients in the water. It has been settled that the full spectrum of macrophyte life-forms (hyperhydrites, ephydrites and hyphydrites) may be encountered in clear oligotrophic lakes, in which the sunlight generates more photosynthetic processes, and dense

carpets of isoetids⁵ are able to develop; this is the case of the northern area of the central part of the lake, most of the passageway and most of the eastern parts of the lake.

On the other hand, algae render the water turbid and cause the disappearance of submersed vegetation. In humic brown-water lakes the sub-zones are compressed and displaced upwards. With increased turbidity, including that attributable to the abundance of phytoplankton, first the isotetids and then the elotetids, are excluded. At the same time, the biomass and density of emergent and floating-leaved plants usually increases, this is the case of most of the central part of the lake and the southeast area in the eastern part of the lake.

In figures 3-22 and 3-23, false color composites (made up of bands 4, 3 and 2) of the central and eastern parts of Lake Cuitzeo, from a SPOT 4 image taken in October 2004, show the water in red and black tones. During fieldwork the water that appears black on the image was observed to be clear water, with deeper transparency; it was also noticed that all types of macrophytes were found here. On the other hand, the reddish water was observed to be turbid water, where only emergent macrophytes were observed.

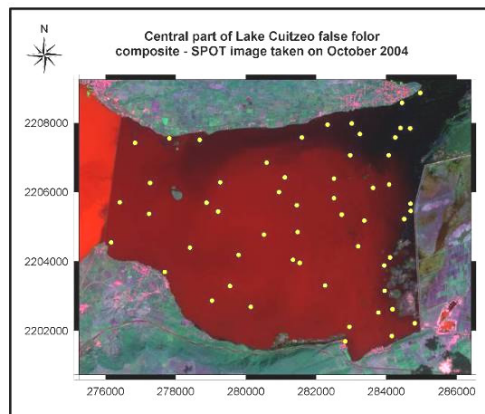


Figure 3-30: Remote sensing applied to eutrophication detection in the Central part of the lake

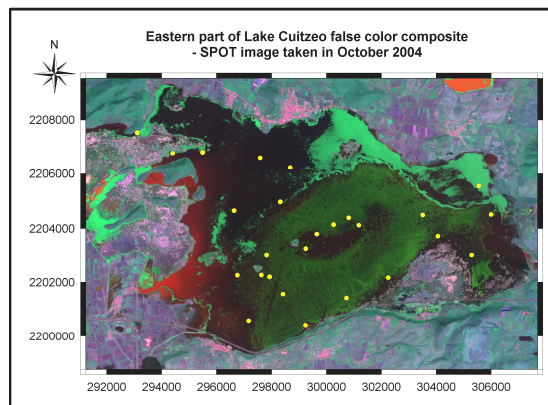


Figure 3-31: Remote sensing applied to eutrophication detection in the Eastern part of the lake

⁵ “Isoetid” is a generic term used to encompass aquatic macrophytes with a small, stiff rosette of leaves, with air spaces linking roots and shoots, including *Isoetes* spp (fern allies and one of our few remaining lycopods).

Note that the bright green vegetation observed on the images, in the lake, are ephydates or floating vegetation, the dark green vegetation are hyphydates or submersed vegetation, and the greyish vegetation are hyperhydrites or emergent vegetation.

It is believed that the results obtained in this analysis might shed some light on the trophic state of the lake; however for a quantitative eutrophication study, analysis of parameters such as Chlorophyll-a, Ammonia, and Dissolved Oxygen are needed.

3.7. Suitable areas for wetland vegetation

In an experiment conducted for the restoration of an agricultural landscape, the combination of water purification and peat land restoration was tested by (Wild, Kamp et al. 2001), in a degraded area. *Typha* was cultivated in constructed wetlands, and the wetlands were provided with drainage water from an agricultural watershed. First, a water regime typical of fenland was re-established and second, the *Typha* showed a high phytomass production. In the first year the plants reached a mean height of 1.4 m, and after a year and a half they reached a mean height of 2.1 m.

This experiment confirms the theory that the water reaching the lake through the drainage canals provides it with much needed elements to preserve the wetland vegetation cycle, and explains the increase of vegetation in the passageway area between the central and eastern parts of Lake Cuitzeo. Since the water from this area moves into other parts of the lake, it transports those elements which stimulate the growth of wetland vegetation in those parts; specially the eastern area of the central part, and the eastern part of the lake.

Of course other local factors play significant roles in preserving wetland vegetation. According to De Steven and Toner, hydrologic regime has the strongest correlation to vegetation type; also depression size interacts with hydrogeology to favour open-water pond vegetation (De Steven and Toner 2004), like Water Hyacinth (*Eichhornia crassipes*) present mostly in the passageway and eastern parts of Lake Cuitzeo.

Finally after visual analysis of satellite images, fieldwork and chemical analysis of water samples, it can be concluded that the least fitting area for wetland vegetation growth in the lake is the west part of the lake. The highest salinity levels were reached in this part, and the least vegetation was observed. The highest vegetation variety was observed in the eastern and passageway parts of the lake, they also seemed to be oligotrophic.

4. Spatial variability of water quality

In this chapter, we seek answers to research question number three: “What is the spatial structure of the water quality parameters? How precisely can they be modelled?” The research methods used to answer the questions include non-spatial analysis of the samples, variogram analysis and model fitting for the variables with good spatial structure, also use of trend surface fitting interpolation techniques for those variables where an experimental variogram could not be computed.

The geostatistical analysis done in this chapter was only applied to the samples taken on the Central part of the lake, since the most intensive sampling took place there.

4.1. Geostatistical analysis of the parameters

As mentioned in subsection 3.3.2., a sampling strategy was developed after visual interpretation of acquired satellite images. In those acquired during wet seasons, a pattern was observed on the Central part of the lake; hence special attention was paid to this site, in the attempt to capture the variability of the different water quality parameters, after assuming that there is some connection between water color and water quality.

4.1.1. Non-spatial analysis of variables

Non-spatial analyses like histogram analysis and box plots were performed on the different variables to understand their distribution. In case of coming across a not normal distribution, a logarithmic transformation was applied to the variable. Variogram cloud and experimental variogram analyses were carried out for the normally distributed variables.

Figures 4-1 to 4-4 are examples of variables with normal distributions represented through histograms and box plots. For EC and Chloride a log transformation was necessary to obtain a normal distribution; for Hardness and Bicarbonate the original values provided normal distributions.

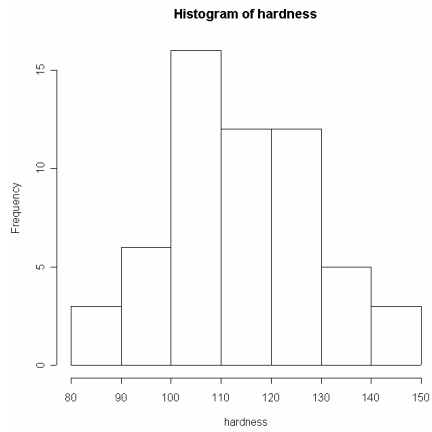


Figure 4-1: Histogram of Hardness

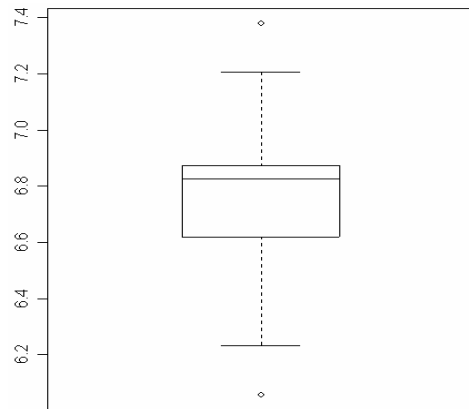


Figure 4-2: Box plot for the log of EC

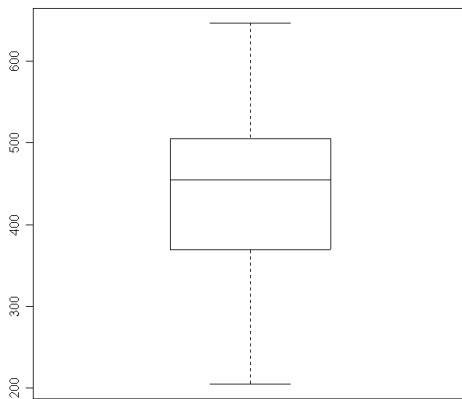


Figure 4-3: Box plot for HCO₃

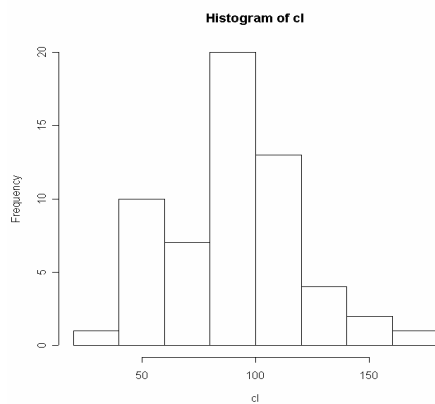


Figure 4-4: Histogram of the log of Cl

Figures 4-5 & 4-6 are examples of not normal distribution, which could not be normalized even after a log transformation.

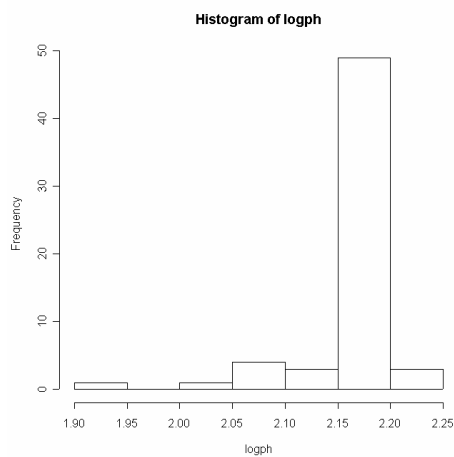


Figure 4-5: Histogram of the log of pH

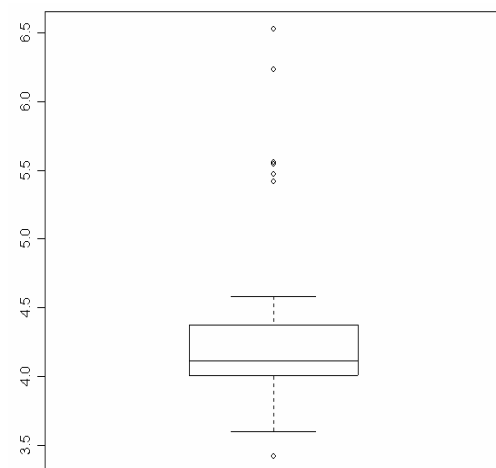


Figure 4-6: Box plot for the log of Alkalinity

4.1.2. Variograms and models used for the analysis

Variogram selection is an iterative process that usually starts with the examination of the experimental variogram. Scattered data create the need for a type of distance tolerance in experimental variogram analysis. Because all data pairs are separated by different distances, all data within a specified distance interval or “lag distance” are treated together. Lag distances that are too large mask the spatial structure, whereas small lag distances may not capture enough samples. The sensitivity of the lag distance is tested by making it larger or smaller (Muñoz 2002). After the appropriate lag distance is chosen, a variogram model is fitted to the experimental variogram by adjusting the model parameters until it reproduces the experimental variogram as closely as possible.

Out of all the variables analyzed in Lake Cuitzeo, the following four showed the most expressed spatial structures, therefore models could be properly fitted to their experimental variograms, so kriging was the most reasonable interpolation method to be applied. Table 4-1 describes the parameters used in the experimental variograms and the models fitted to them.

Table 4-1: Variogram model, Sill, Nugget, Range and Lag for EC, Cl, Hardness and Bicarbonate

Parameter	log transformed	Model	Partial Sill	Nugget	Range	Lag Distance
EC	yes	Gaussian	0.072	0.0118	3500.0	600
Cl	yes	Gaussian	0.130	0.0180	3500.0	600
Hardness	no	Exponential	201.9	48.3	2988.1	750
HCO ₃	yes, log10	Exponential	0.018	0.0076	11520	1250

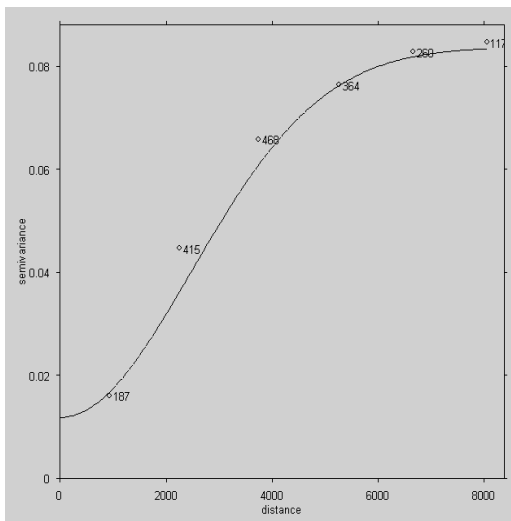


Figure 4-7: Variogram model for log of EC

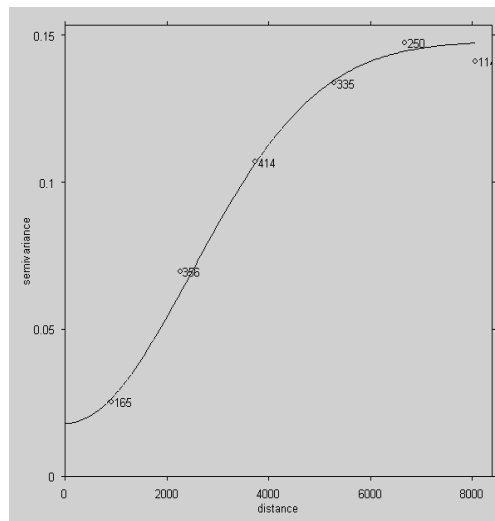


Figure 4-8: Variogram model for log of Cl

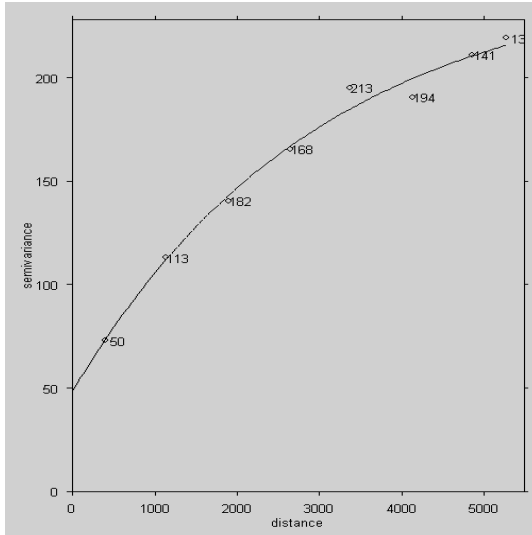


Figure 4-9: Variogram model for Hardness

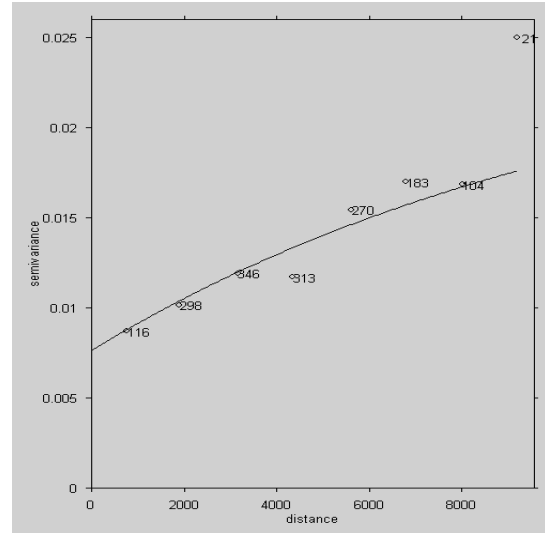


Figure 4-10: Variogram model for log of Bicarbonate

For EC and Chloride, Gaussian models were chosen. Any other model would have had a nugget below zero. The Gaussian model has a parabolic behaviour at its origin, indicating that it represents a regionalized variable that is smooth enough to be differentiable (*i.e.*, the slope between two points tends to a well-defined limit as the distance between the points vanishes). For Hardness and Bicarbonate, Exponential models were chosen. This model is popular particularly in hydrologic applications, because it depicts better the smoother changes (Kitanidis 1997).

4.1.3. Kriging predictions

Kriging is probably the most realistic approach for the estimation of local values; given that a model is correctly fitted on the variogram, kriging always produces the Best Linear Unbiased Estimation (Clark 1979).

The Ordinary Kriging results explain the distribution of the water quality parameters over the Central part of the lake, which are related to the movement of the main current in this part of the lake. The main irrigation canals deposit water into the passageway between the northern, central and eastern parts of the lake. This water movement generates currents that flow into all the three parts. In the central part, the main current follows the northern coast line of the central part, and turns onto the mid part, where it mixes with a lesser current generated by a pumping station that deposits water onto the west coast of the central part. Figures 4-11 and 4-12 depict the results for EC and Chloride. They show why the Gaussian model was appropriate for this variable. The parabolic behaviour at the beginning of the model suggests that there are similar values to each point pair until about 1000 m, and after that distance the variability increases. In this case, the current generated at the passageway in the upper right corner plays an important role; it seems to be the most important factor in the dispersion or spatial variation of these variables.

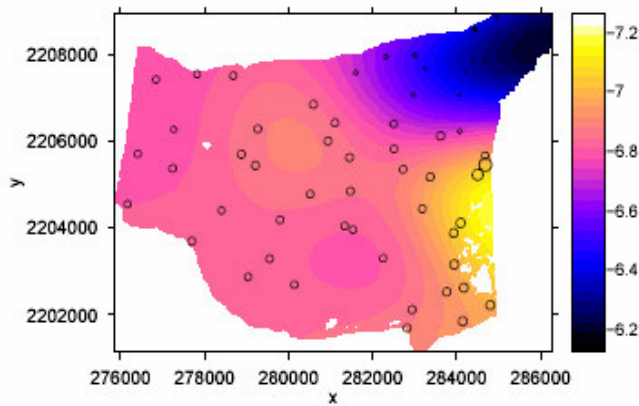


Figure 4-11: Ordinary kriging results for the log of EC

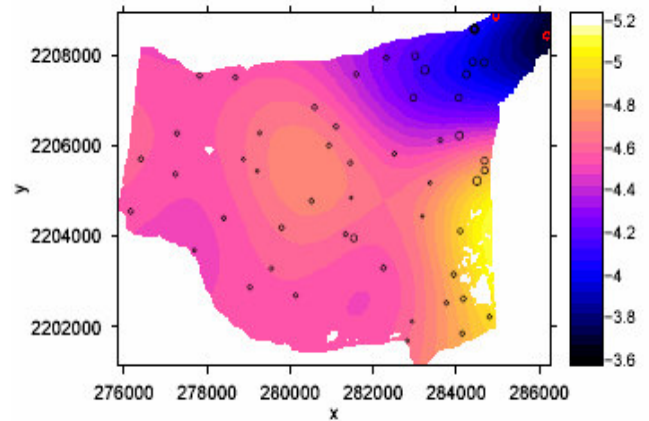


Figure 4-12: Ordinary kriging results for the log of Cl

Besides understanding the dispersion of variables, these results also help understand the water movement inside this part of the lake. However the satellite images were already suggesting the flow direction in this section of the lake. Observe the similar patterns in figure 4-13, band 1 of a SPOT 4 satellite image, and in figure 4-14, result of the Ordinary Kriging for Chloride.

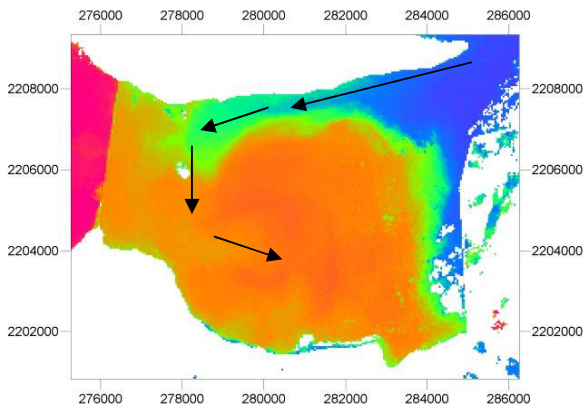


Figure 4-13: Current observed in band 1 of SPOT 4 image

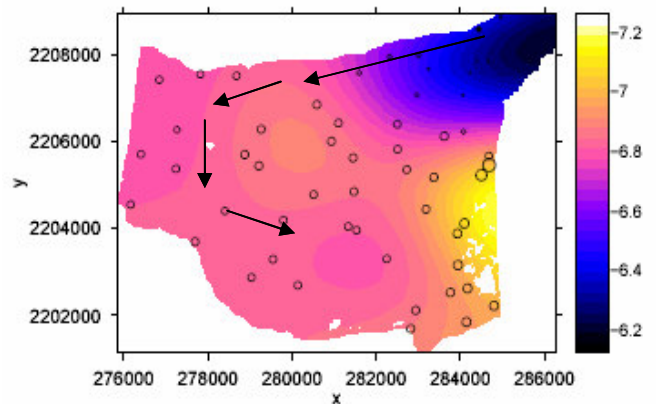


Figure 4-14: Current revealed in interpolation result

In the case of Hardness and Bicarbonate, Ordinary Kriging indicates that these variables are more affected by dilution of values in certain points. Also in the case of Bicarbonate, the water coming from the pumping station located in the East bank seems to be affecting its spatial variability. There is higher variation between most point pairs regardless of how close or far apart, than in the previous examples, this is the reason why the Exponential model fits the experimental variograms for Hardness and Bicarbonate better.

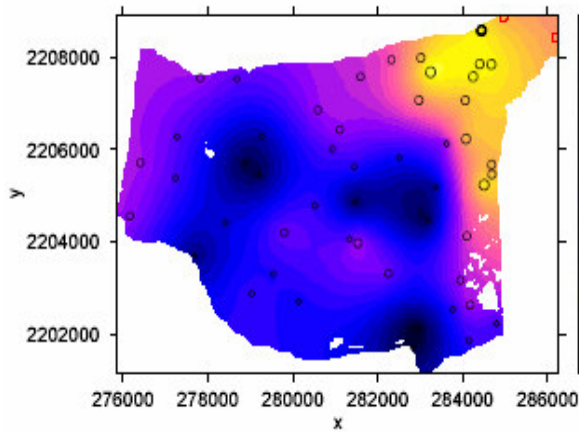


Figure 4-15: Ordinary kriging results for Hardness

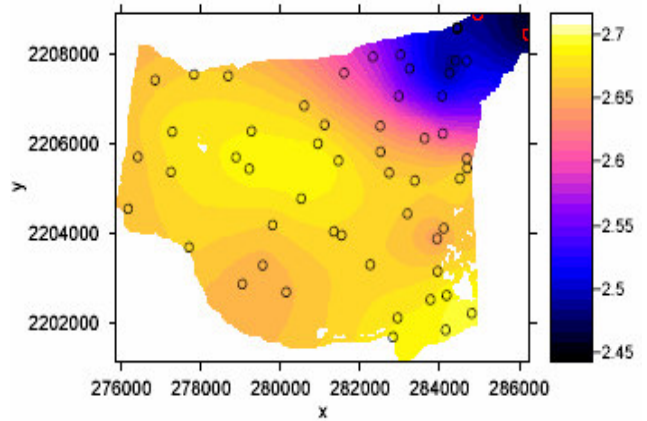


Figure 4-16: Ordinary kriging results for log₁₀ of Bicarbonate

On trying to determine how precisely could Kriging model the spatial structure of the water quality parameters that were interpolated using this method, tables 4-2 to 4-5 show the five-number summary for the values to which Ordinary Kriging was applied and the five-number summary for the predictions made by Ordinary Kriging.

Table 4-2: Predictions and prediction variances for Ordinary Kriging on the log of EC

	Minimum	1 st Qu	Mean	3 rd Qu	Maximum
log EC	6.057	6.617	6.746	6.874	7.379
OK Predictions	6.234	6.793	6.794	6.860	7.168
Variances	0.01282	0.01364	0.01485	0.01527	0.04966

Table 4-3: Predictions and prediction variances for Ordinary Kriging on the log of Cl

	Minimum	1 st Qu	Mean	3 rd Qu	Maximum
log Cl	3.497	4.256	4.483	4.644	5.136
OK Predictions	3.671	4.528	4.536	4.639	5.132
Variances	0.01600	0.01790	0.01981	0.02021	0.04595

Table 4-4: Predictions and prediction variances for Ordinary Kriging on Hardness

	Minimum	1 st Qu	Mean	3 rd Qu	Maximum
Hardness	85.1	100.1	110.5	120.1	140.1
OK Predictions	91.47	100.70	106.30	109.00	129.70
Variances	56.38	91.15	101.50	107.00	183.70

Table 4-5: Predictions and prediction variances for Ordinary Kriging on Bicarbonate

	Minimum	1 st Qu	Mean	3 rd Qu	Maximum
log 10 HCO₃	2.312	2.569	2.626	2.701	2.811
OK Predictions	2.459	2.654	2.647	2.675	2.700
Variances	0.008566	0.009418	0.009766	0.010010	0.012000

When observing the Ordinary Kriging predictions and the prediction variances, the Ordinary Kriging predictions for EC, chloride and Bicarbonate are very close to the original data values. dness predictions are not as close because in this case the interpolation was performed using the original values and not log transformed ones, allowing more room for variances. However, the overall results indicate that there is accuracy in modelling the spatial structure of EC, Chloride, Hardness and Bicarbonate, using Ordinary Kriging (refer to Appendix C for computation methods in the statistical programm “R”).

Finally with the intention of comparing results for various kriging methods, Universal Kriging was applied to the log of EC values. First a trend surface was fitted, and then the residuals were calculated. An experimental variogram was computed for the residuals, and a Spherical model was fitted to it (Partial Sill: 0.029, Nugget: 0.006, and Range: 3000). Finally Universal Kriging was applied using the trend and the model fitted on the variogram of the residuals. After kriging, the variance to the mean was calculated for both the Ordinary and Universal Kriging results; the variances were 0.015 for Ordinary Kriging, and 0.017 for Universal Kriging. Very similar values, but lower for Ordinary Kriging. Also Universal Kriging results defined a pronounced anisotropy in the data. In effect, there seems to be some anisotropy in the data, but the interpolation results using Universal Kriging made it seem as if there was a substantial inflow in the South-East corner of the central part, but this is not the case.

4.1.4. Other interpolation methods and results

There are cases in which the data does not seem to present strong spatial structure, figure 4-17 is an example or erratic behaviour for one of the variables. The experimental variogram was computed several times, with different lag spacing, and different cut-offs, and in none of the cases an acceptable variogram model could be fitted to it.

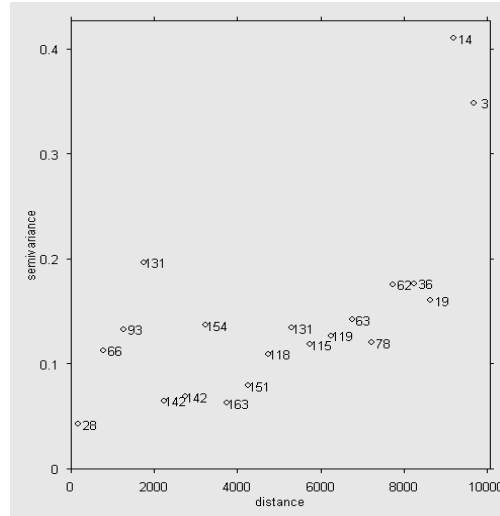


Figure 4-17: Experimental variogram for pH

For cases like these, other interpolation methods were used for determining the spatial variability of the water quality variables. So, for the remaining variables the interpolations were done through trend surface fitting. The interpolated values are calculated here by fitting a surface through all point values in the map, and surface fitting is done by the Least Squares Fit method (Nijmeijer, de Haas et al. 2001).

The order of the polynomial used for the final trend surface interpolation was chosen after analyzing the results of several interpolations. First, the calculated values at the actual sampling points are correlated with the observed values, then the residuals are calculated for each interpolation attempt, and a sum of the residuals is calculated. Finally, a visual analysis is performed on the interpolation attempts to make sure the results look reasonable. The polynomial with the highest correlation to the original values and with the minor residual sum were the ones chosen for the interpolation.

Table 4-6 shows the polynomial orders chosen for the interpolation of different water quality variables, their correlation to the original data, and the sum of the residuals.

Table 4-6: Properties of Trend Surface interpolation results

Variable	Polynomial Order	Correlation to original values	Sum of the residuals
pH	5 th degree	0.9	0.2
Na	5 th degree	0.9	3.4
Depth	5 th degree	0.9	0.1
Mg	6 th degree	0.6	2.0
Transparency	3 rd degree	0.3	25.1
Ca	5 th degree	0.9	0.0

Figures 4-18 to 4-23 show the interpolation results for the mentioned water quality parameters, with their respective polynomial orders stated in table 4-6.

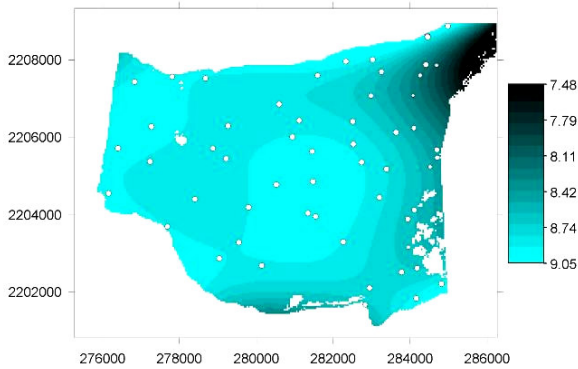


Figure 4-18: Interpolation results for pH values

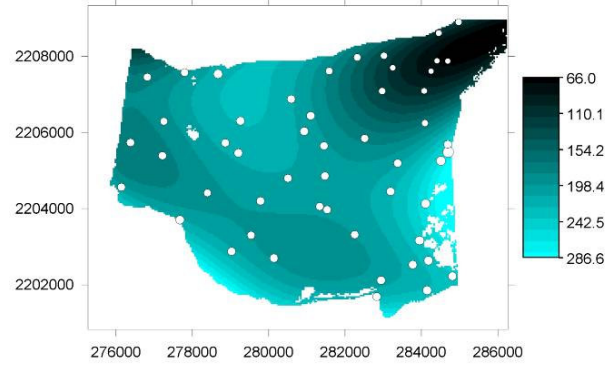


Figure 4-19: Interpolation results for Na

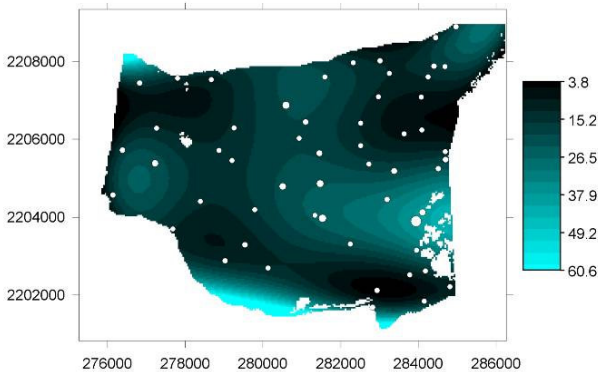


Figure 4-20: Interpolation results for Mg

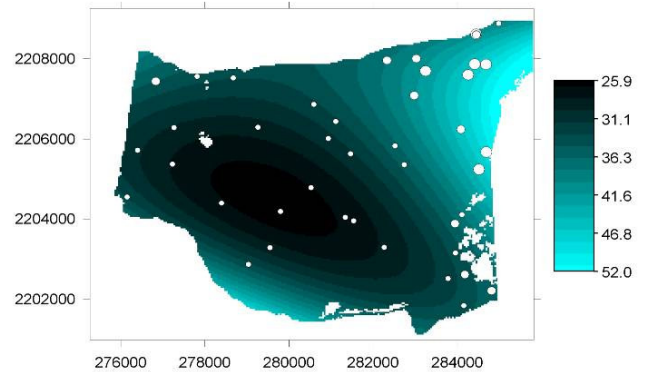


Figure 4-21: Interpolation results for Transparency

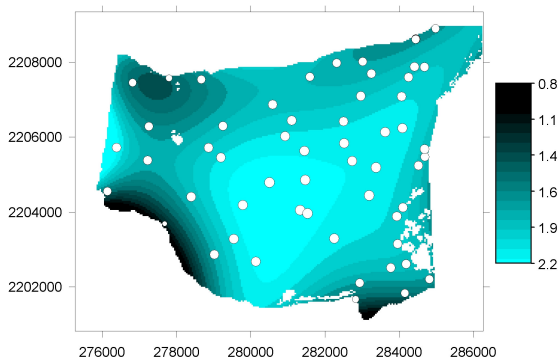


Figure 4-22: Interpolation result for depth

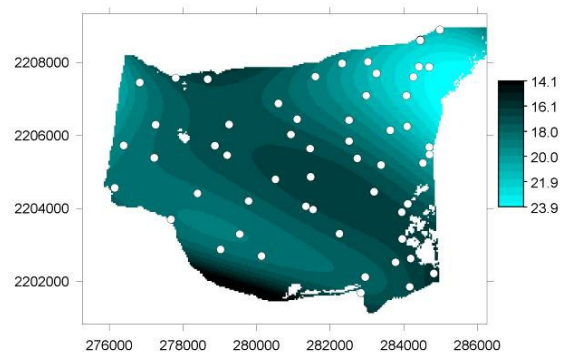


Figure 4-23: Interpolation result for Ca

This test shows that higher degree polynomial orders tend to fit this data set better than lower ones, except for Transparency and this is because Transparency has less measurement points than the other variables. Also, since the residuals are very low, the original values could be used for the interpolation.

5. Remote sensing and water quality

It is known that various conditions of water bodies manifest themselves primarily in the visible wavelengths. Clear water absorbs very little energy, however as the turbidity of the water changes transmittance and therefore reflectance-changes dramatically. For example, water containing large quantities of suspended sediments normally have much higher visible reflectance than clear water; likewise, the reflectance of water changes when chlorophyll concentration is involved (Lillesand, Kiefer et al. 2004).

In this chapter we seek an answer to the following question: “What is the relationship, if any, between reflectance values of optical multi-spectral sensors and water quality?”

It must be stated that the objectives of the exercises performed to answer this question are not to quantify water quality values through the use of remote sensing. The objectives are to try to identify patterns in the water that have a relationship with some water quality variables. If a significant relationship is found, the methods applied to unveil it can be used in a monitoring plan. As part of the monitoring plan, these patterns could be observed over time, and then it could be determined if they could be used as an indicator of water quality. If this is determined, the patterns can also be used to identify sampling sites of interest before going to the field.

The methods used in this chapter include Principal Component Analysis (PCA) of the lake water in the most recently acquired satellite image. Also a correlation analysis was performed between water quality variables, and values of the principal components at the sampling sites. Then, values obtained through the PCA were used in CoKriging transparency values. And finally the relationship between transparency and certain ions was discussed.

5.1. Principal component analysis of remotely sensed data

Images generated by digital data from various wavelength bands, often appear similar (highly correlated) and convey essentially the same information. Principal component transformation is a technique designed to reduce such redundancies in multi-spectral data. The purpose of the procedure is to compress all the information contained in an original n -band data set into fewer than n “new bands”. Then the new bands are used in the further analysis, instead of the original data (Lillesand, Kiefer et al. 2004). The new bands are ordered in terms of the amount of variance explained by each. The first two or three components will carry most of the real information of the original data set, while the rest explain only the minor variations (Nijmeijer, de Haas et al. 2001).

The first step before performing the Principal Component Analysis (PCA) is to execute atmospheric corrections to the image. The ERDAS add-on ATCOR was used for this task. The image used for

this exercise is a SPOT 4 image taken on the 18th of October 2004; the image was taken one week after the fieldwork was completed (see Appendix D for image specifications).

After the atmospheric corrections were done, all further analysis was done using ILWIS 3.2 Academic. First by digitizing the shape of the lake, it was extracted from the rest of the image in each band, and the first PCA is performed on the entire lake. This analysis reveals that Principal Component 1 (PC1) clearly captures the differences between water and vegetation. Then, using PC1, a threshold representation was created, which was later used to perform a conditional operation that eliminated the vegetation on each of the bands and shows only the water in the lake. A second PCA was performed on the bands containing only the water; results are shown in tables 5-1 and 5-2.

Table 5-1: Variance percentages per band

Band 1	Band 2	Band 3	Band 4
77.29	15.85	6.20	0.66

Table 5-2: PCA coefficients calculated for the SPOT image of the water body of the Cuitzeo Lake

	Band 1	Band 2	Band 3	Band 4
PC 1	-0.621	-0.763	-0.138	0.110
PC 2	0.097	0.081	-0.984	-0.124
PC 3	-0.079	0.224	-0.111	0.965
PC 4	-0.773	0.601	-0.001	-0.203

Figures 5-1 to 5-4 show the results for the PCA performed on the water, PC1, composed mostly of bands 1 and 2 seems to explain most of the variations in the water, while PC2, composed mostly of band 3, identifies areas where patches of submersed vegetation are located, PC3 and PC4 show some similarities with PC1, but mostly minor variations.

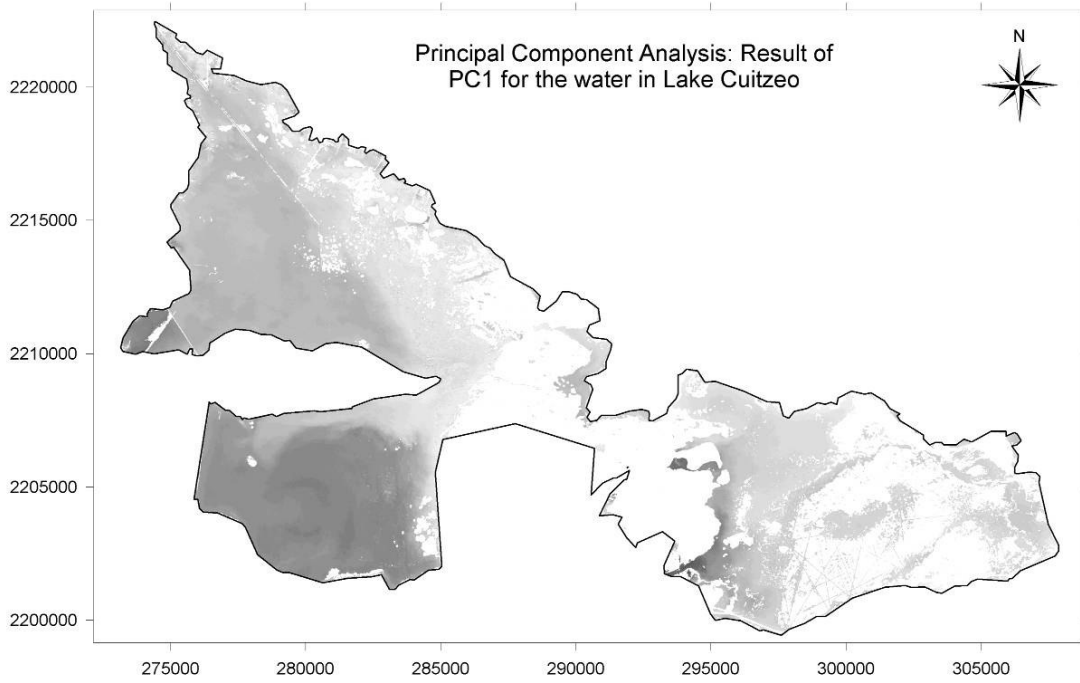


Figure 5-1: Differences in the water captured by PCA-PC1

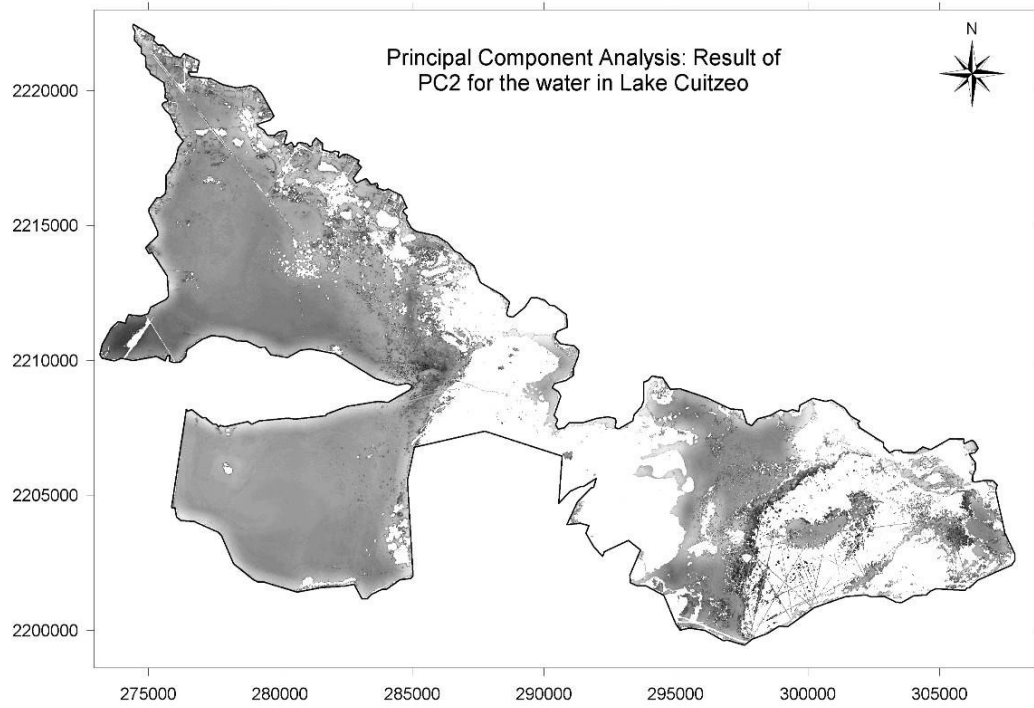


Figure 5-2: Differences in the water captured by PCA-PC2

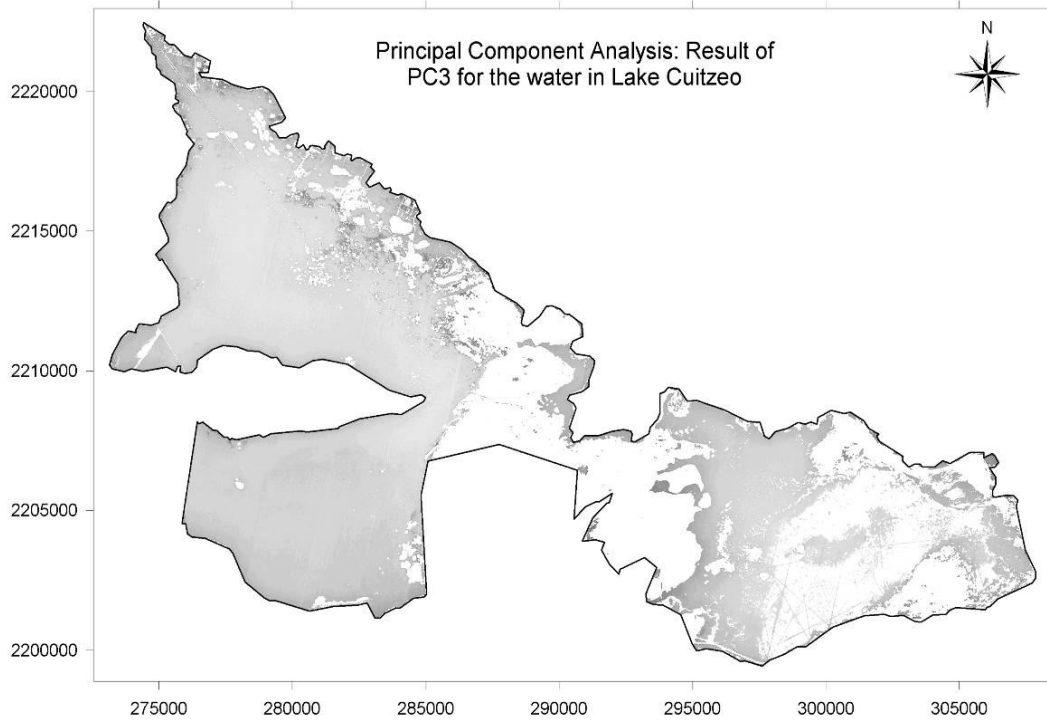


Figure 5-3: Differences in the water captured by PCA-PC3

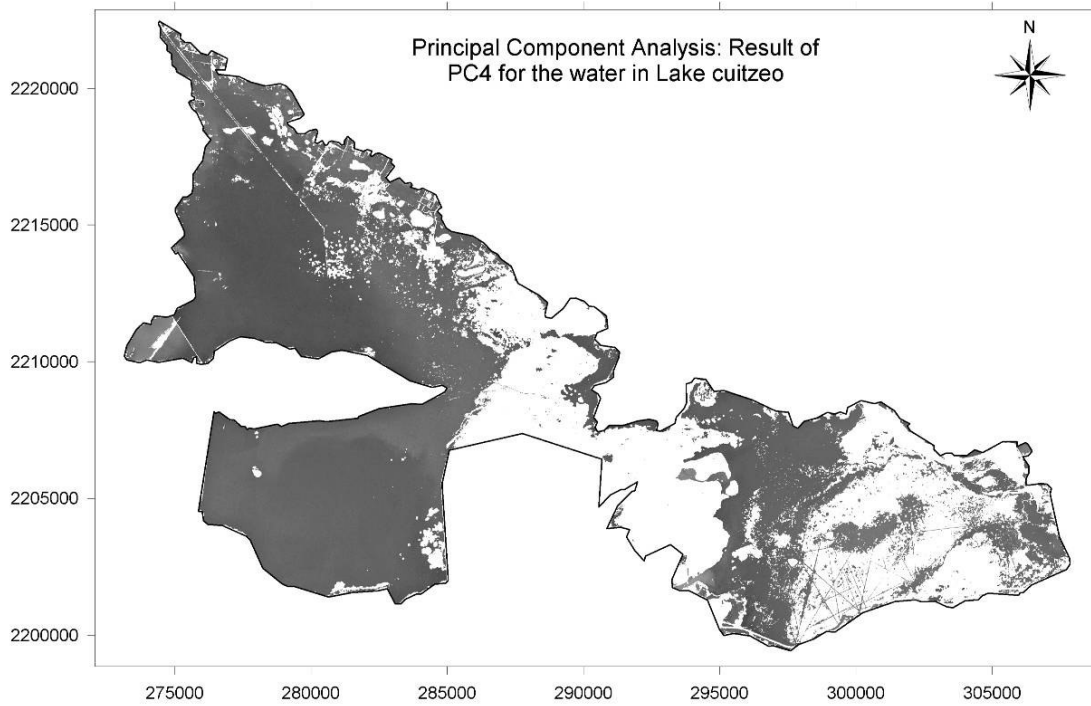


Figure 5-4: Differences in the water captured by PCA-PC4

5.2. Correlation analysis of remotely sensed data and water quality

Many important water characteristics such as dissolved oxygen concentration, pH, and salt concentration, cannot be observed directly through changes in water reflectance. However, such parameters sometimes correlate with observed reflectance (Lillesand, Kiefer et al. 2004).

Using the coordinates for all the samples, and the results from the PCA performed on the water, the value of each PC at the exact point where a sample was taken was extracted. These values were then used in the correlation analysis between actual water quality values for different variables, and values for PC's.

Tables 5-3 and 5-4 show the results of the correlation analyses performed individually on the samples taken in the Central, and Eastern parts of the lake. It was not performed on the samples taken in the Western part of the lake, because the image does not include this part of the lake. The Passageway was also excluded because of the little amount of water that can be seen in the image; most of the area is covered by vegetation.

Table 5-3: Correlation coefficients for the PC values and the samples in the Central part of the lake

	Depth	EC	pH	Temperature	Alkalinity	Transparency	Hardness	Cl	Mg	Ca	Na	K	SO ₄	HCO ₃	NO ₃	PO ₄
Water PC1	-0.37	0.51	-0.36	-0.07	0.20	0.82	0.73	-0.30	-0.11	0.68	-0.58	-0.25	0.40	-0.53	0.00	0.29
Water PC2	-0.49	0.01	0.40	-0.10	-0.07	0.07	0.23	0.04	-0.16	0.09	0.01	0.13	0.12	0.11	-0.16	0.00
Water PC3	-0.39	0.43	0.32	0.08	-0.19	-0.55	-0.56	0.35	-0.10	-0.61	0.52	0.41	-0.16	0.46	0.03	0.44
Water PC4	0.17	-0.19	-0.22	0.01	0.11	0.13	0.18	-0.08	-0.08	0.44	-0.22	-0.30	-0.05	-0.19	0.07	0.36

Table 5-4: Correlation coefficients for the PC values and the samples in the Eastern part of the lake

	Depth	EC	pH	Temperature	Alkalinity	Transparency	Hardness	Cl	Mg	Ca	Na	K	SO ₄	HCO ₃	NO ₃	PO ₄
Water PC1	-0.04	0.22	0.03	0.48	-0.03	-0.22	-0.28	0.25	0.01	-0.26	0.25	0.25	0.04	0.53	0.26	NA
Water PC2	0.27	-0.05	-0.20	0.68	0.05	0.09	-0.06	-0.07	-0.16	0.05	-0.05	-0.08	0.16	0.33	0.10	NA
Water PC3	-0.16	-0.16	-0.69	0.06	0.03	0.05	-0.02	-0.11	0.03	0.25	-0.15	-0.18	-0.11	-0.13	0.02	NA
Water PC4	-0.33	0.70	0.74	-0.25	0.43	-0.43	-0.52	0.70	-0.29	-0.73	0.71	0.74	0.46	0.49	0.34	NA

Correlation results reveal that there are several water quality variables and PC's with correlations between 50 and 97%.

For the Central part of the lake, transparency, hardness, Calcium, Sodium, Bicarbonate and EC show correlations to PC1; also Calcium, hardness, transparency and Sodium show correlations with PC3. And for the Eastern part of the lake, Bicarbonate shows correlation with PC1, temperature shows correlation with PC2, pH shows correlation with PC3, and pH, Potassium, Calcium, Sodium, EC, Chloride and hardness show correlations with PC4.

After examining figures 5-1, 2, 3 & 4, we see that the pattern in the Central part of the lake becomes noticeable in PC1, and somewhat in PC3 and PC4, but we also see patterns in the Northern and Eastern parts of the lake. Notice that the water in the Eastern area of the Northern part, as well as in the Eastern part of the lake has similar characteristics to the water entering the Central part of the lake. These three bands seem to be good for looking at the water itself, while PC2 is more effective in distinguishing between areas that have patches of submersed vegetation and those that don't.

Correlations of the PC's with transparency might seem obvious. It is often said that when remotely sensed images are used for looking at water in shallow lakes, what is observed is the lake bottom rather than the water itself. However the highest correlation with transparency was observed in PC1 in the central part of the lake, the average transparency here was 36 cm while the average depth was 1.9 m. Therefore it is established that in this part of the lake, what is seen is not the lake bottom but the suspended matter in the water, i.e. this is optically deep water.

In the Eastern part of the lake, the water transparency is superior, but there is a great deal of submersed vegetation. In the areas where the submersed vegetation was thicker it created mats on the water surface which were removed when the water was extracted from the lake image. However there are areas in which vegetation wasn't removed but the transparency of the lake is such, that what is observed in the images is the submersed vegetation and not suspended matter in the water. In these areas, the submersed vegetation alters the reflectance values, and what is seen in the image is not the suspended matter in the water but a combination of water and submersed vegetation.

5.3. Remote Sensing applied to CoKriging of water quality parameters

CoKriging is an estimation method where if the correlation between two variables is high (either positive or negative), then it might be possible to use the information about the spatial variation of a well-sampled variable (the co-variable) to help interpolate a sparsely sampled variable (the predictand).

For Lake Cuitzeo the sparsely sampled variable or predictand was transparency. Lack of appropriate equipment during the first days of fieldwork hindered the measurements of transparency; therefore it has fifteen samples less than the other variables, plus the measurements are not precise.

First an experimental variogram is computed for the transparency values and a model is fitted to it. Table 5-5 describes the experimental variogram and model used for the original transparency values.

Table 5-5: Variogram model, Sill, Nugget, Range and Lag for Transparency

Parameter	Log transformed	Model	Partial Sill	Nugget	Range	Lag Distance
Transparency	no	Spherical	70	19	10000	1000

Then Ordinary Kriging is applied using the variogram model mentioned in table 5-5. Table 5-6 shows the five-number summary for the prediction variances obtained through Ordinary Kriging, when applied to transparency.

Table 5-6: Predictions and prediction variances for Transparency using Ordinary Kriging

	Minimum	1 st Qu	Mean	3 rd Qu	Maximum
OK Predictions	29.47	29.84	33.57	35.42	47.93
OK Variances	22.04	28.88	31.30	32.28	50.80

Using the values obtained in PC1 as reference for the missing transparency measurements, CoKriging was applied in the attempt to reduce the predicting variances obtained through Ordinary Kriging.

The first step in CoKriging is computing the cross-variogram. It calculates experimental semi-variogram values for the two input variables and cross-variogram values for the combination of both variables. After computing the cross-variogram, the fitted model for the target value is overlaid with all three variograms, and then it is fitted to each individually. Table 5-7 describes the results of the cross-variogram function and the fitted variogram models on each variogram, and figure 5-5 depicts the results of the cross variogram function and the fitted variogram models.

Table 5-7: Fitted variogram model, Sill, Nugget, and Range for Transparency, PC1 and Transp.PC1 cross-variogram

Parameter	Model	Partial Sill	Nugget	Range
Transparency	Spherical	68.59	20.86	10000
PC1	Spherical	30.46	4.61	10000
Transp.PC1	Spherical	42.76	9.81	10000

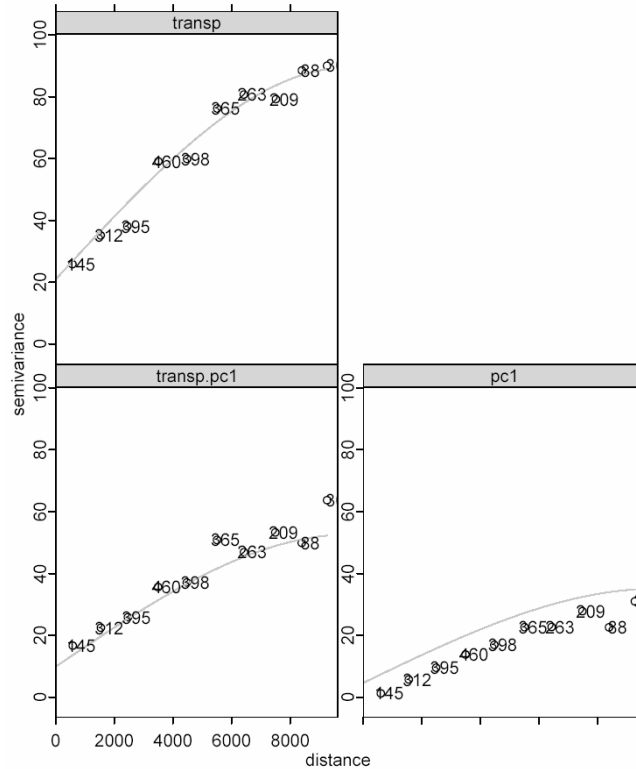


Figure 5-5: Cross-variogram for Transparency and PC1

CoKriging is applied using the model applied to the cross-variogram. Table 5-8 shows the predictions and prediction variances obtained with CoKriging, and table 5-9 shows the differences in variance between Ordinary Kriging and CoKriging.

Table 5-8: Prediction variances for CoKriging

	Minimum	1 st Qu	Mean	3 rd Qu	Maximum
CK Predictions	28.28	29.87	33.45	35.41	47.54
CK Variances	23.55	29.09	31.14	32.10	46.26

Table 5-9: Differences between Ordinary Kriging and CoKriging prediction variances

	Minimum	1 st Qu	Mean	3 rd Qu	Maximum
OK Variances	22.04	28.88	31.30	32.28	50.80
CK Variances	23.55	29.09	31.14	32.10	46.26
Difference	-1.51	-0.21	0.16	0.18	4.54

As observed, when compared to Ordinary Kriging, the CoKriging operation yields better prediction variances for the Mean, 3rd Quartile and Maximum values than for the Minimum and 1st Quartiles. A reason for this could be that the PC1 model has a good shape but has systematically high nugget and sill; this increases the prediction variance but does not change the predictions. Besides this, the

CoKriging map clearly shows the influence of the co-variable, and has greater detail than the Ordinary Kriging map, representing much better the observations done during fieldwork. Figures 5-6 to 5-9 depict the predictions made by Ordinary Kriging and CoKriging for Transparency as well as the prediction variances in both cases. Figure 5-10 shows the difference between CoKriging and Ordinary Kriging; the darker spots are places where Ordinary Kriging has higher prediction values, and the light spots are places where CoKriging has higher prediction values.

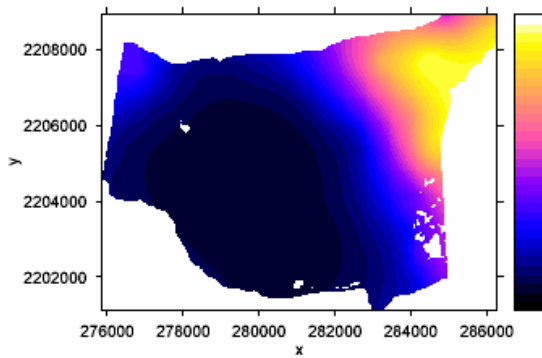


Figure 5-6: Transparency predictions using Ordinary Kriging

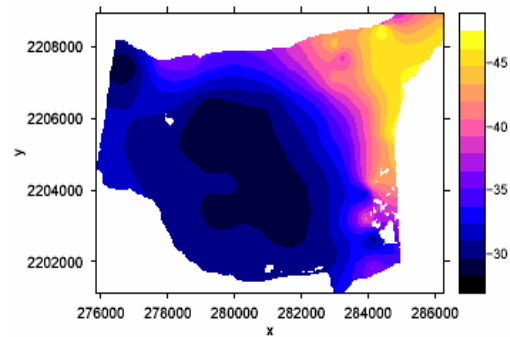


Figure 5-7: Transparency predictions using Universal Kriging

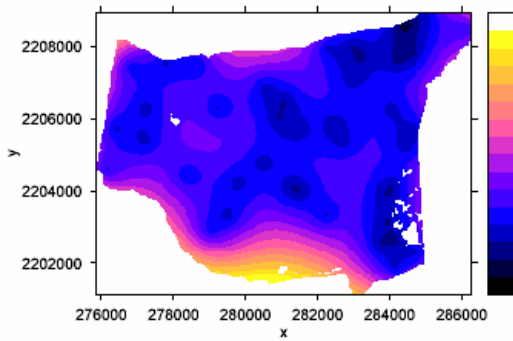


Figure 5-8: Transparency prediction variances for Ordinary Kriging

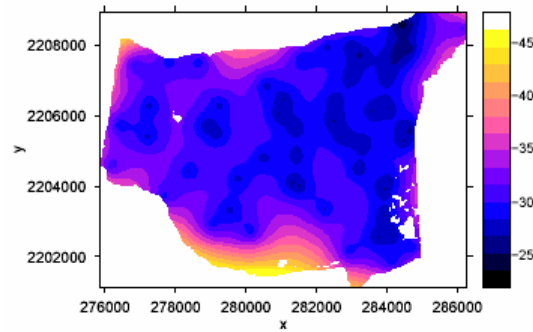


Figure 5-9: Transparency prediction variances for CoKriging

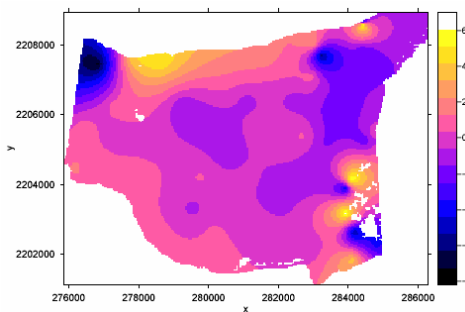


Figure 5-10: Difference between CoKriging and Ordinary Kriging predictions

In figure 5-10, there are two spots in the Northwest area where Ordinary Kriging and CoKriging manifest differences. In the first case the PC value gives more weight to the actual transparency measurement in that point, and assigns a lesser transparency value for CoKriging than for Ordinary Kriging. To the right of that spot there is an area where CoKriging gives higher transparency than Ordinary Kriging; here the PC value manifests itself strongly and gives a slightly higher transparency value than the recorded one. On the South east area the differences are in places where transparency measurements were not done (refer to Appendix E for computation method in “R”).

5.4. Remote sensing applied to water quality monitoring in Lake Cuitzeo

The examination of several images of the lake starting from 1979 to 2004, generated by different sensors (MSS, ETM, and SPOT), revealed that the same pattern is observed in the central part of the lake in the images acquired during wet seasons. Presumably, it is caused by the intensive inflow to this part of the lake through the passageway, which generates one main current that follows the northern coast of the central part, which then mixes with more turbid water. During the dry periods this pattern disappears, indicating that because of the decrease in inflow the current is not generated, and the water mixes more evenly across this part of the lake.

The water coming in from the passageway contains less suspended sediments, therefore it is clearer water than the one on the rest of the central part, and thus the current is visible from the satellite images. Also, because of the high correlation between transparency and PC1, it is known that the pattern observed in the image, is related to transparency.

As mentioned in the beginning of this chapter, the objective of the exercise was to identify patterns in the water, try to determine if they can be associated to water quality, and if they can be used for monitoring water quality. Since the patterns have been identified, the correlation with transparency is proved, further water quality parameters are to be discussed.

For this purpose, a correlation analysis was performed between transparency and those ions identified as the primordial ones in determining the water types in the lake, which were Sodium, Bicarbonate and Chloride. Figures 5-11 to 5-13 depict scatter plots of transparency vs. Sodium, Bicarbonate, and Chloride. In addition a trend line was added to each graph showing not their fit to a linear relationship, but the main trend of the data.

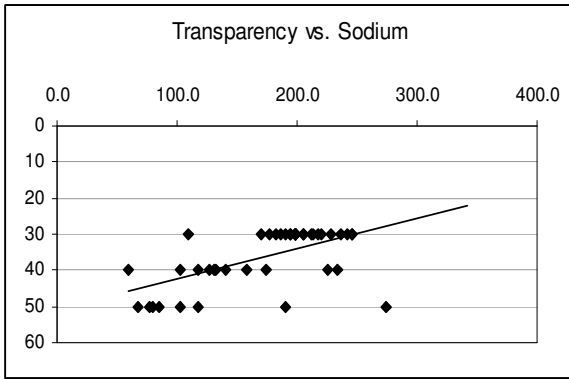


Figure 5-11: Relationship between Transparency and Sodium

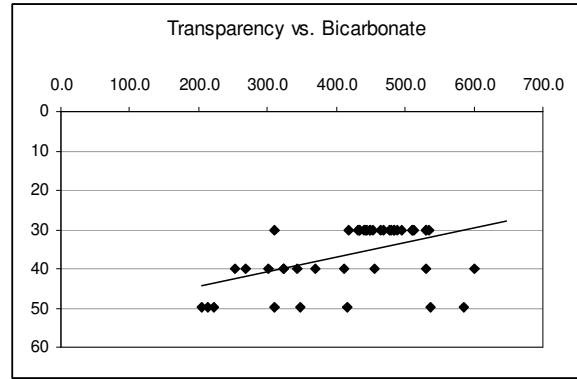


Figure 5-12: Relationship between Transparency and Bicarbonate

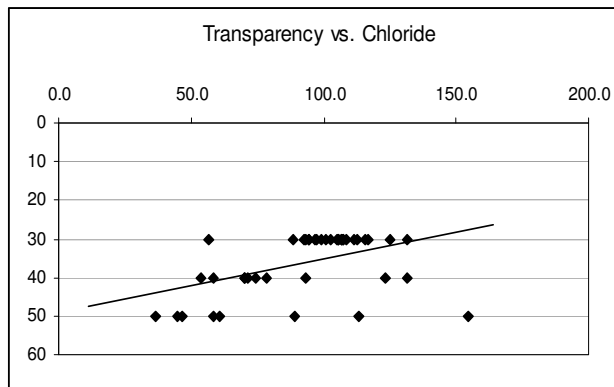


Figure 5-13: Relationship between Transparency and Chloride

In all three cases, the ions have very similar relationships with transparency. The first tendency is shown by the trend lines in the plots; overall the values of the ions decrease as transparency increases. The second trend observed is that the ions have very similar values in the shallowest transparency, but as it increases the spread of the values also increases.

The relationship between these ions and transparency has to be studied over time, to determine how they behave during dry periods when transparency seems to decrease in the central part of the lake. To do so, Sodium, Bicarbonate and Chloride should be sampled during dry periods, in those areas where the transparency is greater during wet periods. If the relationship is true, then in the dry periods the ions should have very similar values, and not as spread out as in the higher transparencies.

6. Conclusions and recommendations

“Every lake is a mirror of its environment. Although the primary influence of human beings is on terrestrial systems, because of the interdependence of terrestrial and aquatic ecosystems, human impact on nature finds its most sensitive response in inland waters, especially in lakes (O'Sullivan and Reynolds 2003).”

This final chapter will express the conclusions obtained through the results of the diverse analyses performed in this research, and their given interpretations.

6.1. Conclusions

Representative sample points obtained throughout Lake Cuitzeo portray a picture of the water quality inside the lake for this period in time. The values of the main ions, Mg^{2+} , Ca^{2+} , Na^+ , K^+ , Cl^- , SO_4^{2-} , and HCO_3^- , obtained in Lake Cuitzeo during the wet season of 2004, were compared to values of the same ions found in typical lakes. The results show that Magnesium is lower than usual in Lake Cuitzeo, Calcium is extremely low, Sodium is extremely high, Potassium is fairly high, Chloride values are higher than normal, and Sulphate values are normal as well as Bicarbonate values.

The water type analysis revealed that there are fourteen different water types identified in Lake Cuitzeo. Out of the fourteen, Na- HCO_3 -Cl is the dominant type in the central, eastern and western parts of the lake. However in the passageway, where the main source of water reaches the lake, each sample represents a different water type. The statistical analysis performed on the data revealed that this part of the lake has the least spread of values when compared to other parts of the lake, except for Calcium. The reason why Calcium is not part of the main water type is because other ions have similar spread of values that are higher than the spread of Calcium. This similar spread of values gives equal weight to those ions, thus they all play a similar role when determining the water types.

As mentioned before, Sodium values are extremely high, also Chloride values are high. The water type analysis identifies Na- HCO_3 -Cl as the main water type in most of the lake, and Electrical Conductivity values are high in most of the lake as well. All this coincides with the results of the Piper analysis, which reveals that a great portion of the water samples can be considered brackish and others even saline.

About the location of thermal springs inside the lake, it is important to state that one thermal spring sample is not representative of all thermal waters. Further sampling on other thermal springs would be needed to come up with final locations for thermal springs inside the lake.

The second subject addressed was the relationship between water quality, eutrophic levels and wetlands vegetation. As explained in Chapter 3, the relationship is the following; eutrophication is

the enrichment of water with decaying plant nutrients which cause oxygen depletion, this process alters water quality and causes a wide array of problems. Also the decomposing algae turn the water turbid, and cause the disappearance of submersed vegetation, but increase emergent and floating vegetation. The clear parts are stabilized by macrophytes that compete with the algae for the nutrients.

When this relationship is applied to Lake Cuitzeo, it is determined that the passageway and eastern parts of the lake, which have clear water and all types of macrophytes, comply with the signs of oligotrophic lakes; and the central and western parts of the lake; which are turbid and show only emergent vegetation, seem to have higher eutrophic levels. However for a quantitative study of eutrophication levels, further parameters such as Dissolved Oxygen, Ammonia, and Chlorophyll a must be analyzed.

Following this relationship, the eastern and passageway parts of the lake seem to be the most suitable ones for the further development of wetlands vegetation, while the central and western parts seem to be more unsuitable.

The spatial analysis for the central part of the lake has shown that during wet seasons the distribution of some water quality variables is affected by the main current that is generated at the Northeast corner of the lake, circulates along the northern coast and towards the middle. The distribution of other parameters is more affected by their dilution throughout the lake.

Some variables have a strong special structure, and can be modelled using Ordinary Kriging. Those that could not be modelled using Kriging were modelled by fitting a trend surface to the sample points. To determine how precisely the parameters were modelled, the variances produced by Ordinary Kriging, and the residuals produced by trend surface fitting were analyzed. The prediction variances produced by Ordinary Kriging are minimal (refer to tables 4-2 to 4-5), also the sum of the residuals produced by trend surface fitting are very small for most of the parameters (refer to table 4-6); in the case of transparency the residuals are higher because there are less number of measurements for this parameter, therefore increasing the errors produced by the interpolation method. Overall the spatial distribution of the water quality parameters was precisely modelled.

To determine the relationship between the information provided by optical multi-spectral sensors and water quality, first principal component analysis was performed on a SPOT 4 image taken one week after the fieldwork period. This analysis revealed that PC1 was the most successful in describing differences within the water itself, and PC2 described the difference between water and vegetation. Then, the PC values at the exact sampling locations were correlated to the different water quality variables. The most significant correlation was found between PC1 and the transparency values.

Two more analyses were performed based on this correlation. The first one was the use of the PC1 values, at the sampling locations, as a co-variable in the CoKriging interpolation method, for improving the predictions made by Ordinary Kriging of the transparency values. The results show that in this case, CoKriging has less prediction variances in the mean and over the mean values and slightly higher prediction variance in the lower values, but the overall CoKriging has improved the prediction of transparency values, since the output map resembles more the reality observed in the

lake during fieldwork. Also, since the transparency values are rough estimates of transparency, it is believed that if they could have been measured in a more exact manner, then this analysis would yield much better results. These results prove that PC values can be useful as co-variables in interpolation attempts.

The second and final analysis based on the correlation between PC1 and transparency was the determination of a relationship between transparency and water quality. For this analysis a correlation was sought out between transparency and the ions playing the major role on determining the main water type in the lake, these ions were Sodium, Bicarbonate and Chloride. The results of this analysis showed that all three ions have similar behaviours when correlated to the transparency values. The main trend, discovered in the correlation analysis, was that the lesser the transparency the more similar the values for the ions, and as transparency increased the overall values of the ions decreased, but the outliers have a wider spread, and tend to have higher values.

The relationship between these ions and transparency has to be studied repeatedly over time, first to determine if the similarities in behaviour have anything to do with the lack of precision in the transparency values. Also to analyse and understand its behaviour during dry periods, and again during wet periods; to determine if there is a cycle as the seasons change. If there is a repetitive cycle, and it can be detected through satellite images, then the correlation between transparency and PC1 can prove useful for monitoring changes in the lake, and identifying specific sampling locations where change has been detected. The new samples will then reveal if there are also modifications in water quality as the seasons change.

6.2. Recommendations and future research

Some recommendations offered to the local government or other students who would like to carry on with this topic are the following:

- Repeat the transparency measurements with a more accurate Secchi Disk. These measurements will confirm if the correlation between them and the information from an optical multi spectral sensor is greater than the one obtained in this study. Further studies will prove if they can be used in monitoring changes in the lake.
- Perform Turbidity and Total Suspended Sediments measurements; since they are also visible parameters, they could probably also be used in a monitoring plan to detect changes over time. The same exercises performed on transparency can be performed on these variables.
- A monitoring plan for the lake should be developed; the following considerations should be taken into account (Ramsar 2002):
 1. An overall agreement of the wise use of the resources by people is essential between the various managers, owners, occupiers and other stakeholders.
 2. The management plan should be a technical document; it should be supported by legislation and in some circumstances to be adopted as a legal document.

3. The plan should be kept under review and adjusted to take into account the monitoring process, changing priorities, and emerging issues.
 4. An authority should be appointed to implement the management planning process, and this authority should be clearly identified to all stakeholders.
 5. A management plan, and the management planning process, should only be as large or complex as the site requires. The production of a large, elaborate and expensive plan will not be possible, and certainly not justifiable, for many sites. However, for large or zoned sites, it may be appropriate to develop separate detailed plans for different sections of the site, within an overall statement of objectives for the whole site.
 6. Management planning should not be restricted to the defined site boundary; it should also take into account the wider context of planning and management, notably in the basin.
 7. It is important to ensure that the site planning takes into account the external natural and human-induced factors and their influence on the site (for a list of the most important functions of a wetland management planning process and a management plan go to Appendix E: Wetlands management plan).
- Perform a detailed eutrophication study taking into consideration parameters such as Chlorophyll - a, Ammonia, Dissolved Oxygen, total Phosphorous, total Nitrogen, and any others necessary.
 - Perform sampling and monitoring during dry periods. Evaluate water quality, vegetation, fish, and other typical components of wetlands, both in wet and dry periods. In time this will help understand the behaviour of the wetland.
 - Perform further analysis of the rest of the lake, specially the northern and eastern part of the lake, and the sites that could not be visited during field work. Also on other thermal springs around the lake, their analysis will provide further reference of their chemical composition, and aid in locating actual thermal springs inside the lake.

References

- Alfaro, R., V. Martinez, et al. (2001). "Radon behavior in springs and wells around Cuitzeo Lake, Lerma river basin, Mexico." Geofisica Internacional **41**(4): 439-445.
- Bayern, P. v. (2002). Handbuch der Technischen Gewässeraufsicht, Bayerisches Landesamt für Wasserwirtschaft.
- Chapman, D. (1992). Selection of Water Quality Variables. Water Quality Assessments - A Guide to Use of Biota, Sediments and Water in Environmental Monitoring.
- Clark, I. (1979). Practical Geostatistics. London, Applied Science Publishers LTD.
- De Steven, D. and M. Toner (2004). "Vegetation of upper coastal plain depression wetlands: environmental templates and wetland dynamics within a landscape framework." Wetlands **24**(1): 23-42.
- Horne, A. J. and C. R. Goldman (1994). Lake ecology overview. Limnology. New York, USA, McGraw Hill.
- Hounslow, A. (1995). Water Quality Data. Oklahoma, Lewis Publishers.
- Kitanidis, P. K. (1997). Introduction to Geostatistics: Applications in Hydrogeology. Palo Alto, California.
- Kuusisto, E. (1996). Hydrological Measurements. Water Quality Monitoring - A Practical Guide to the Design and Implementation of Freshwater Quality Studies and Monitoring Programmes. UNEP/WHO.
- Lillesand, T. M., R. W. Kiefer, et al. (2004). Remote sensing and image interpretation. Madison, John Wiley & Sons, Inc.
- Moore, D. S. (1999). The basic practice of statistics. New York, W.H. Freeman and Company.
- Muñoz, L. E. (2002). Spatial Water Quality Monitoring and Assessment in Malewa River and Lake Naivasha, Kenya [MSc thesis]. WREM.2. Enschede, International Institute for Geo-Information Science and Earth Observation (ITC): 111.
- Nijmeijer, R., A. de Haas, et al. (2001). ILWIS 3.0 Users Guide. ITC, Enschede, The Netherlands.

- O'Sullivan, P. and C. Reynolds (2003). The lakes handbook: Limnology and limnetic ecology, Blackwell Publishing.
- Parodi, G. (2002). Methods for discharge measurements in open channels. Enschede, WRES ITC.
- Ramsar (2002). National Reports prepared for the 8th Meeting of the Conference of the Contracting Parties to the Convention on Wetlands, The Ramsar Convention on Wetlands.
- Ramsar (2002). New Guidelines for management planning for Ramsar sites and other wetlands, The Ramsar Convention on Wetlands.
- Rojas, J. and A. Novelo (1995). Flora y Vegetacion Acuaticas del Lago de Cuitzeo, Michoacan, Mexico. Acta Botanica Mexicana. I. d. E. A.C.
- Rossiter, D. G. (2004). Spatial analysis-geostatistics lecture: An introduction to applied geostatistics. Part 2 -Theory of random functions; Modelling the variogram. ITC, The Netherlands.
- Small, H. (1998). Ion Chromatography. New York, Plenum Press.
- Stein, A. (2004). Spatial analysis-geostatistics lecture. Introduction to Ordinary Kriging. ITC, The Netherlands.
- USEPA (1990). National Guidance Water Quality Standards for Wetlands, U.S. Environmental Protection Agency.
- USEPA (2004). Benefits of Restoration, Environmental Protection Agency.
- Vollenweider, R. A. (1989). "Global problems of eutrophication and its control" in: O'Sullivan and Reynolds The lakes handbook.
- Wild, U., T. Kamp, et al. (2001). "Cultivation of Typha spp. in constructed wetlands for peatland restoration." Ecological Engineering **17**: 49-54.

Appendix A: Hydrologic analysis

Procedure for measuring discharge by Velocity-Area method (Kuusisto 1996):

1. All measurements of distance should be made to the nearest centimetre.
2. Measure the horizontal distance b_1 ; from reference point 0 on shore to the point where the water meets the shore, point 1 (Figure A 1).
3. Measure the horizontal distance b_2 from reference point 0 to vertical line 2.
4. Measure the channel depth d_2 at vertical line 2.
5. With the current meter make the measurements necessary to determine the mean velocity v_2 at vertical line 2.
6. Repeat steps 3, 4 and 5 at all the vertical lines across the width of the stream.

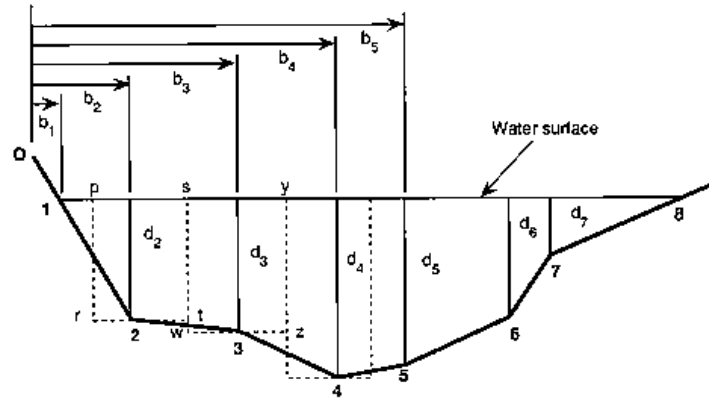


Figure A-1: Cross-section of a stream divided into vertical sections for measurement of discharge

The computation for discharge is based on the assumption that the average velocity measured at a vertical line is valid for a rectangle that extends half of the distance to the verticals on each side of it, as well as throughout the depth at the vertical. Thus, in Figure 12.2, the mean velocity \bar{v}_2 would apply to a rectangle bounded by the dashed line p, r, s, t. The area of this rectangle is:

$$a_2 = \frac{b_3 - b_1}{2} * d_2$$

And the discharge through it will be:

$$Q_2 = a_2 * \bar{v}$$

Similarly, the velocity \bar{v}_3 applies to the rectangle s, w, z, y and the discharge through it will be:

$$Q_3 = \frac{b_4 - b_2}{2} * d_3 * \bar{v}_3$$

The discharge across the whole cross-section will be:

$$Q_T = Q_1 + Q_2 + Q_3 \dots Q_{(n-r)} + Q_n$$

In the example of Figure A.1, $n = 8$. The discharges in the small triangles at each end of the cross-section, Q_1 and Q_n , will be zero since the depths at points 1 and 8 are zero.

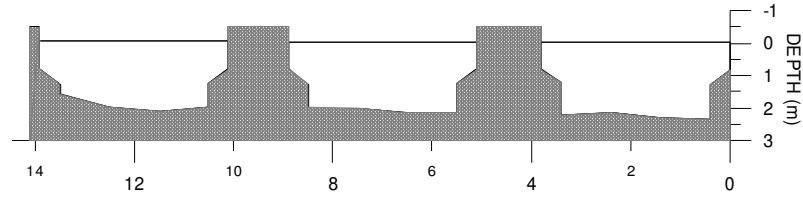


Figure A 1: Cross section of canal #1

Table A 1: Current meter discharge calculations for canal #1

Verticals	Distance from initial point (m)	Depth (m)	Meter depth	Revs	Revs/sec	T (s)	A (m ²)	v (ms ⁻¹)	Mean v (ms ⁻¹)	Q (m ³ s ⁻¹)
1	0.4	2.34	0.6	39.0	0	0		0	0	0
2	1.4	2.30	0.6	67.3	0.65	60	2.3	0.16	0.16	0.15
	1.4		1.1	36.6	1.12	60		0.27	0.24	0.56
	1.4		1.8	74.0	0.61	60		0.15		
3	2.4	2.12	0.6	73.3	1.23	60	2.12	0.32		
	2.4		1.1	71.0	1.22	60		0.31	0.28	0.59
	2.4		1.6	54.0	1.18	60		0.30		
4	3.4	2.20	0.6	101.6	0.90	60	4.51	0.22		
5	5.5	2.14	0.6	111.6	1.69	60	3.317	0.43	0.43	0.95
6	6.5	2.13	0.6	108.6	1.86	60	2.13	0.47	0.47	0.40
	6.5		1.1	82.3	1.81	60		0.46	0.40	0.85
	6.5		1.6	92.3	1.37	60		0.35		
7	7.5	2.02	0.6	111.6	1.54	60	2.02	0.39		
	7.5		1.1	97.6	1.86	60		0.47	0.38	0.77
	7.5		1.6	66.0	1.63	60		0.41		
8	8.5	2.00	0.6	114.6	1.10	60	4	0.26		
9	10.5	1.98	0.6	99.0	1.91	60	2.97	0.48	0.48	0.97
10	11.5	2.08	0.6	94.6	1.65	60	2.08	0.42	0.42	0.33
	11.5		1.1	95.0	1.58	60		0.40	0.38	0.79
	11.5		1.6	79.3	1.58	60		0.40		
11	12.5	1.98	0.6	95.6	1.32	60	1.98	0.34		
	12.5		1.1	84.6	1.59	60		0.41	0.34	0.67
	12.5		1.6	61.3	1.41	60		0.36		
12	13.5	1.57	0.6	53.3	1.02	60		0.24		

Q_T (m³/s) 7.4
 Q_T (l/s) 7366

The following relationship was used to calculate the velocity of the water:

$$n \leq 0.75$$

$$v = 0.2256 * n + 0.029$$

$$0.75 \leq n \leq 10.12$$

$$v = 0.2456 * n + 0.014$$

v = Velocity in m/s

n = number of revolutions in 1/s

Procedure for measuring discharge by Floater method:

The method consists essentially of observing the time required for a float to traverse a course of known length and noting its position in the channel so that:

$$v = \frac{L}{t}$$

Where v is the float velocity ($m\ s^{-1}$), L is the distance traveled (m), and t is the time of travel over distance L (m) (Parodi 2002).

For canals #2, 3 and 4 the procedure followed is as described:

1. The cross section was measured from a bridge, like in the previous method.
2. The width of the bridge was recorded.
3. A float was dropped into the water, and the time it took for it to cross the width of the bridge was recorded.
4. Step 3 was repeated two more times, and the average time was computed.

Table A 2: Floater discharge calculations for canal #1

	Distance (m)	Average T (s)	Velocity (ms^{-1})	A (m^2)	Q (m^3s^{-1})	Error
1st opening	5.45	15.7	0.35	7.6	2.6	7%
2nd opening	5.45	12.7	0.43	7.0	3.0	
3rd opening	5.45	15.3	0.36	6.4	2.3	
				$Q_T =$	7.9	

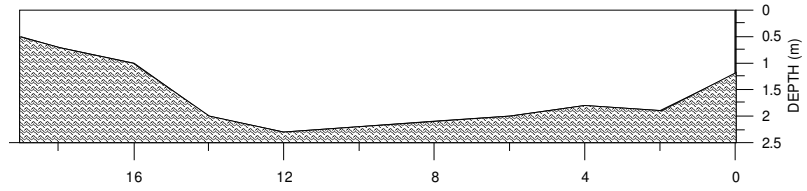


Figure A 2: Cross section of canal #2

Table A 3: Floater discharge calculations for canal #2

Dist (m)	Depth (m)	Width (m)	Average T (s)	Velocity (ms ⁻¹)	A (m ²)	Q (m ³ s ⁻¹)
0	1.2	15	16.3	0.92	31.65	29.1
2	1.9					
4	1.8					
6	2.0					
8	2.1					
10	2.2					
12	2.3					
14	2.0					
16	1.0					
18	0.7					
19	0.5					

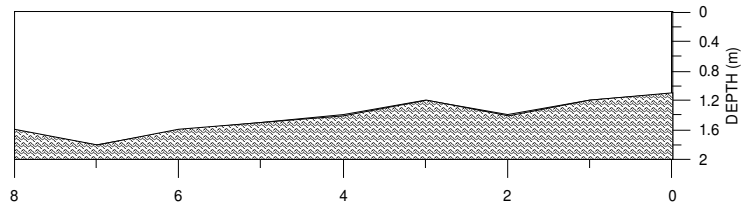


Figure A 3: Cross section of canal #3

Table A 4: Floater discharge calculations for canal #3

Dist (m)	Depth (m)	Width (m)	Average T (s)	Velocity (ms ⁻¹)	A (m ²)	Q (m ³ s ⁻¹)
0	1.1	13	35	0.371429	10.1	3.8
1	1.2					
2	1.4					
3	1.2					
4	1.4					
5	1.5					
6	1.6					
7	1.8					
8	1.6					

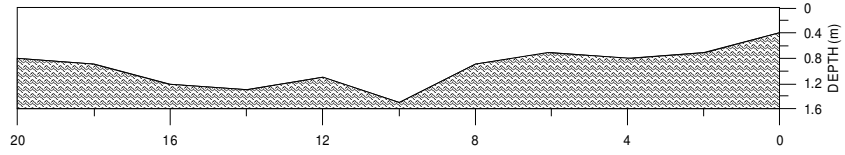


Figure A 4: Cross section of canal #4

Table A 5: Floater discharge calculations for canal #4

Dist (m)	Depth (m)	Width (m)	Average T (s)	Velocity (ms ⁻¹)	A (m ²)	Q (m ³ s ⁻¹)
0	0.4	12	18.3	0.65	18.2	12
2	0.7					
4	0.8					
6	0.7					
8	0.9					
10	1.5					
12	1.1					
14	1.3					
16	1.2					
18	0.9					
20	0.8					

Appendix B: Chemical analysis

Codes used when sampling in different parts of the lake and study area

Table B 1: Description of the codes given to each sample

Location of the sample	Code
Central part	C
Passageway between Central and Eastern parts	P
Eastern part	E
Western part	W
Canals	CA
Pumping Stations	PS
Thermal Spring	TS

Equipment used for Chemical analysis

Table B 2: Parameters analyzed in the field and analysis method

Parameter analyzed	Analysis method
EC	LF 340/SET: Conductivity Hand Held Meter
pH	pH 340/SET: pH Combined Electrode with Integrated Temperature Probe
Temperature	pH 340/SET: pH Combined Electrode with Integrated Temperature Probe
Alkalinity	Aquamerck Alkalinity Test Kit
Transparency	Secchi Disk
Total Hardness	Aquamerck total Hardness Test Kit
Chloride	Aquamerck Chloride Test Kit

Table B 3: Parameters analyzed in the lab and analysis method

Parameter analyzed	Analysis method
SO ₄ ²⁻ , HCO ₃ ²⁻ , NO ₃ ⁻ , PO ₄ ²⁻ , Cl ⁻	Waters IC-PAK Chromatogram (see Appendix B for details)
Mg ²⁺ , Ca ²⁺ , Na ⁺ , K ⁺	Atomic Absorption (see Appendix B for details)

Chromatograph analysis:

Principle:

A small volume of the sample, typically less than 0.5 ml, is introduced into the injection system of an ion chromatograph. The sample is mixed with an eluent and pumped through a guard column, a separation column, a suppressor device and a detector, normally a conductivity cell.

The separation column is an ion exchange column which has the ability to separate the ions of interest. The separation column is often preceded by a shorter guard column of the same substrate as in the separation column to protect the separation column from overloading and particles. Different types of separation columns, eluents and suppression devices have to be used for anions and cations respectively. Each ion is identified by its retention time within the separation column. The sample ions are detected in the detection cell, and the signals produced (chromatograms) displayed on a strip chart recorder or a PC equipped with the necessary software for measurement of peak height or area.

The ion chromatograph is calibrated with standard solutions containing known concentrations of the ions of interest. Calibration curves are constructed from which the concentration of each ion in the unknown sample is determined (Small 1998).

Atomic Absorption analysis:

Principle:

The technique of flame atomic absorption spectroscopy (FAAS) requires a liquid sample to be aspirated, aerosolized, and mixed with combustible gases, such as acetylene and air or acetylene and nitrous oxide. The mixture is ignited in a flame whose temperature ranges from 2100 to 2800 °C.

During combustion, atoms of the element of interest in the sample are reduced to free, unexcited ground state atoms, which absorb light at characteristic wavelengths, as shown in Figure B-1.

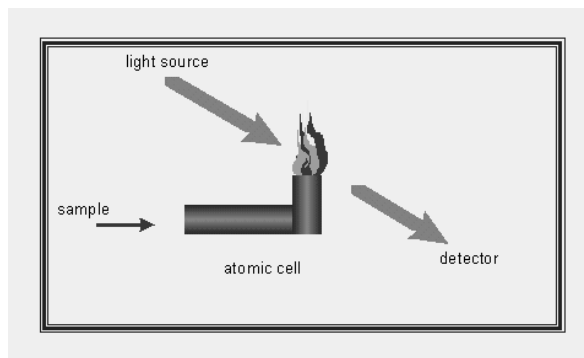


Figure B-1: Operation principle of an atomic absorption spectrometer

The characteristic wavelengths are element specific and accurate to 0.01-0.1nm. To provide element specific wavelengths, a light beam from a lamp whose cathode is made of the element being determined is passed through the flame. A device such as photon multiplier can detect the amount of reduction of the light intensity due to absorption by the analyte, and this can be directly related to the amount of the element in the sample.

Table B 4: Field and laboratory results for the samples taken in the Central part of the lake

Date	Time	Code	X m	Y m	Depth m	EC mS/cm	pH	Temp C	Alkalinity mg/l HCO ₃ ⁻	Transp cm	Total Hardness mg/l CaCO ₃	SO ₄ ²⁻ mg/l	HCO ₃ ²⁻ mg/l	NO ₃ ⁻ mg/l	PO ₄ ²⁻ mg/l	Cl ⁻ mg/l	Mg ²⁺ mg/l	Ca ²⁺ mg/l	Na ⁺ mg/l	K ⁺ mg/l
16-9-04		C-1	284688	2205466	1.8	1602	8.5	24.1	36.6		120.1	0.0	646.4	0.0	0.0	164.0	16.8	19.8	341.4	21.9
16-9-04		C-2	281472	2204856	2.2	953	8.9	25.7	54.9		85.1	61.0	0.0	0.0	0.0	0.0	32.6	16.1	210.0	18.7
16-9-04		C-3	278877	2205708	2.0	967	8.7	27.0	61.0		90.1	0.0	469.8	0.0	0.0	105.8	12.6	18.6	198.0	19.0
16-9-04		C-4	281594	2207589	1.8	771	8.7	26.8	48.8		110.1	49.6	374.1	0.0	0.0	74.7	11.6	18.8	156.8	15.6
18-9-04	9:01	CT-5	284437	2208603	1.7	638	9.0	22.1	36.6		120.1	49.6	334.3	0.0	0.0	63.7	12.6	19.9	126.9	12.9
18-9-04	9:27	C-6	284061	2207072	2.0	539	7.7	22.2	259.3		120.1	50.0	269.7	0.0	0.6	47.1	12.6	23.5	93.0	10.4
18-9-04	9:49	C-7	283620	2206130	2.1	1013	8.9	23.1	54.9		100.1	0.0	534.1	1.9	0.8	122.7	12.6	21.2		
18-9-04	10:08	C-8	283373	2205185	2.2	987	8.9	23.0	54.9		90.1	0.0	511.6	0.0	0.0	11.2	20.0	18.1	213.9	19.5
18-9-04	10:26	C-9	283187	2204449	2.2	965	9.0	23.4	61.0		85.1	57.3	477.8	2.8	0.0	99.9	14.7	17.7	213.9	19.2
18-9-04	10:52	C-10	282940	2202124	1.8	977	8.9	23.5	42.7		85.1	0.0	492.5	0.0	0.0	106.4	13.7	17.7	210.0	20.7
18-9-04	11:10	C-11	282823	2201698	1.4	979	8.6	24.4	36.6		90.1	0.0	505.1	0.0	0.0	109.4	13.7	17.8	213.9	20.7
18-9-04	11:50	C-12	280139	2202700	2.1	928	8.9	24.8	61.0		100.1	0.0	437.1	0.0	0.0	94.7	10.5	17.2	202.0	19.7
18-9-04	12:22	C-13	277696	2203701	0.8	960	8.8	25.8	61.0		90.1	0.0	487.9	2.6	0.0	108.9	12.6	18.1	225.9	19.2
18-9-04	12:49	C-14	279211	2205449	2.0	991	8.9	26.4	54.9		90.1	0.0	536.4	0.8	0.7	115.8	10.5	15.5	213.9	20.2
18-9-04	13:21	C-15	282504	2206406	2.0	918	8.8	27.2	58.0			0.0	491.6	0.0	0.0	100.9	10.5	17.2		
19-9-04	8:43	CT-16	284443	2208586	1.7	664	9.1	22.4	48.8	40	120.1	37.8	301.4	0.0	0.0	53.7	13.7	22.6	126.9	13.4
19-9-04	9:07	C-17	284963	2208870	1.7	605	9.0	21.8	36.6	30	120.1	50.0	310.0	0.0	0.0	56.9	15.8	22.7	109.0	11.9
19-9-04	13:41	C-25	286194	2208444	1.8	427	7.0	25.8	225.7	50	120.1	48.7	204.9	3.0	0.0	36.6	10.5	21.1	67.1	16.3
20-9-04	8:43	CT-26	284441	2208600	1.7	648	9.1	23.1	54.9	50	120.1	47.8	346.9	0.0	0.0	58.6	16.8	22.4	116.9	28.5
20-9-04	9:03	C-27	283013	2207995	1.8	728	8.9	22.7	51.9	40	120.1	55.7	369.1	0.0	0.7	70.1	16.8	21.2	130.9	31.9
20-9-04	9:20	C-28	282320	2207953	1.8	749	8.9	22.8	54.9	40	110.1	52.3	412.2	0.0	0.0	74.4	12.6	20.3	158.7	38.7
20-9-04	9:42	C-29	278682	2207521	1.7	914	9.0	24.1	73.2	30	105.1	61.4	477.9	0.0	0.0	93.0	12.6	16.8	245.8	30.0
20-9-04	10:00	C-30	277821	2207556	1.3	900	8.8	24.5	67.1	30	110.1	0.0	468.4	0.0	0.0	96.6	12.6	16.1	182.1	22.1
20-9-04	10:18	C-31	276844	2207431	1.6	898	9.0	23.8	79.3	40	60.1	0.0	455.2	0.0	0.0	93.4	15.8	19.7	174.7	42.6
20-9-04	10:37	C-32	276408	2205715	1.9	899	8.9	22.2	73.2	30	110.1	0.0	432.5	0.0	0.0	107.2	15.8	18.4	186.1	18.2
20-9-04	10:52	C-33	276165	2204558	1.7	901	9.0	22.9	61.0	30	110.1	57.9	445.1	0.0	0.0	92.6	13.7	18.2	190.0	23.1
20-9-04	11:06	C-34	277242	2205380	1.9	924	9.0	23.5	73.2	30	105.1	0.0	479.9	0.0	0.0	99.2	27.4	19.7	198.0	24.1
20-9-04	11:29	C-35	280515	2204786	2.2	925	8.9	24.0	85.4	30	105.1	0.0	509.9	0.0	0.0	105.5	29.5	18.6	198.0	24.1
20-9-04	11:45	C-36	281337	2204053	2.2	922	8.9	24.0	70.2	30	100.1	0.0	495.3	0.0	0.0	94.4	10.5	16.6	194.0	23.6

WATER QUALITY AND ITS SPATIAL VARIABILITY IN LAKE QUITZEO, MEXICO

Date	Time	Code	X m	Y m	Depth m	EC mS/cm	pH	Temp C	Alkalinity mg/l HCO ₃ ⁻	Transp cm	Total Hardness mg/l CaCO ₃	SO ₄ ²⁻ mg/l	HCO ₃ ²⁻ mg/l	NO ₃ ⁻ mg/l	PO ₄ ²⁻ mg/l	Cl ⁻ mg/l	Mg ²⁺ mg/l	Ca ²⁺ mg/l	Na ⁺ mg/l	K ⁺ mg/l
20-9-04	12:02	C-37	282251	2203310	2.1	915	8.9	25.1	67.1	30	110.1	45.2	448.1	0.0	0.0	97.2	11.6	18.3	194.0	23.6
20-9-04	12:33	C-38	284803	2202227	1.7	1073	9.0	26.7	97.6	40	100.1	56.4	600.1	0.0	0.0	123.6	12.6	16.3	225.9	27.5
20-9-04	13:00	C-39	283933	2203892	2.0	1058	8.8	26.8	73.2	40		0.0	252.6	0.0	0.0	0.0	80.0	14.7		
21-9-04	8:35	CT-40	284444	2208586	1.7	586	8.99	22.3	61.0	40	135.1	0.0	0.0	0.0	0.0	1.6	15.8	23.4	116.9	28.5
21-9-04	8:54	C-41	284675	2207853	1.9	513	7.81	21.9	256.2	50	130.1	46.0	538.1	0.2	0.5	113.2	11.6	21.9	80.1	19.5
21-9-04	9:26	C-42	281453	2205632	2.1	962	8.81	21.3	82.4	30	105.1	0.0	530.4	0.0	0.6	105.5	23.2	17.7	198.0	24.1
21-9-04	9:38	C-43	280937	2206013	2.0	967	8.96	21.3	85.4	30	105.1	54.7	535.6	0.0	0.0	116.8	12.6	17.2	227.9	27.8
21-9-04	9:51	C-44	280591	2206858	1.9	975	8.99	22.2	91.5	30	110.1	0.0	487.9	24.5	0.0	102.6	36.8	18.1	213.9	26.0
21-9-04	10:11	C-45	279266	2206291	1.9	962	8.96	22.0	91.5	30	95.1	0.0	484.2	0.0	0.0	88.3	10.5	17.3	217.9	26.5
21-9-04	10:25	C-46	277275	2206279	1.8	848	8.89	22.9	61.0	30	105.1	0.0	531.1	0.0	0.0	105.3	10.5	16.9	170.7	17.8
21-9-04	10:54	C-47	278405	2204409	2.1	882	8.92	23.0	73.2	30	100.1	0.0	0.0	0.8	0.0	0.0	11.6	18.4	176.7	17.8
21-9-04	11:08	C-48	279037	2202879	2.0	913	8.93	24.1	79.3	30	105.1	51.0	433.3	0.0	0.0	106.9	13.7	19.5	206.0	18.2
21-9-04	11:17	C-49	279548	2203297	2.1	936	8.93	24.0	79.3	30	100.1	49.5	418.9	0.0	0.0	108.7	13.7	18.4	198.0	19.2
21-9-04	11:38	C-50	283766	2202532	1.9	1010	8.94	24.3	88.5	30	100.1	50.9	453.1	0.4	0.0	111.3	12.6	16.3	219.9	20.4
23-9-04	8:37	CT-51	284441	2208591	1.7	650	9.12	23	70.15	40	130.1	55.5	322.8	0.0	0.7	71.4	11.6	17.9	59.2	12.9
23-9-04	9:01	C-52	284246	2207587	1.9	509	8.13	22.2	237.9	50	130.1	46.8	212.7	9.9	1.4	45.0	12.6	23.4	77.1	10.0
23-9-04	9:18	C-53	284077	2206234	2.1	748	8.53	22.2	36.6	40	130.1	47.5	344.2	1.1	0.0	78.4	12.6	22.1	132.9	13.9
23-9-04	9:36	C-54	284098	2204123	2	1116	8.75	22.3	67.1	30	115.1	65.3	511.4	2.3	0.0	131.8	26.3	18.3	241.8	21.4
23-9-04	9:55	C-55	283944	2203163	1.9	1101	8.06	22.5	509.35	30	110.1	53.0	513.5	0.0	0.0	124.9	10.5	15.8	245.8	22.9
23-9-04	10:14	C-56	284172	2202627	1.9	1072	8.8	22.5	54.9	40	115.1	60.6	530.6	0.0	0.0	131.3	10.5	17.4	233.9	22.6
23-9-04	10:29	C-57	284147	2201856	1.6	1075	8.87	22.7	54.9	30	105.1	51.4	483.6	9.6	0.0	115.4	10.5	16.4	235.8	22.6
23-9-04	10:52	C-58	281534	2203968	2.2	914	8.97	22.6	82.35	30	120.1	53.3	443.3	2.1	0.0	107.4	42.1	18.5	198.0	19.7
23-9-04	11:13	C-59	279796	2204196	2.1	929	8.96	23.6	61	30	110.1	47.4	433.3	0.0	0.0	101.0	10.5	15.5	211.9	19.7
23-9-04	11:36	C-60	281105	2206433	2	944	8.9	25	67.1	30	110.1	55.0	448.8	0.7	0.6	107.0	13.7	18.0	206.0	19.7
23-9-04	11:53	C-61	282510	2205830	2.1	936	8.9	25.4	61	30	100.1	60.6	439.9	0.0	0.0	94.6	10.5	15.7	198.0	19.7
23-9-04	12:14	C-62	282728	2205361	2.1	928	8.92	25.8	73.2	30		57.2	464.6	0.0	0.0	112.5	10.5	16.4		
23-9-04	12:33	C-63	282968	2207074	2	693	8.56	25.8	30.5	40	120.1	57.0	479.9	0.0	0.0	70.3	11.6	20.6	140.8	14.8
23-9-04	12:49	C-64	283244	2207682	1.9	564	8.81	26.2	42.7	50	140.1	46.3	322.8	0.1	0.0	60.8	12.6	22.0	103.0	11.9
23-9-04	13:03	C-65	284399	2207861	1.9	513	8.75	26.4	36.6	50	125.1	47.9	309.3	0.0	0.0	46.8	13.7	24.7	85.1	10.0
24-9-04	8:38	CT-66	284439	2208583	1.7	602	8.9	22.0	61.0	40	140.1	50.3	222.8	2.0	0.7	58.3	16.8	22.3	103.0	11.9
24-9-04	13:04	C-69	284503	2205236	1.9	1347	8.1	26.4	683.2	50	140.1	90.1	268.0	0.9	0.0	154.6	16.8	20.4	273.7	18.7

Date	Time	Code	X m	Y m	Depth m	EC µS/cm	pH	Temp C	Alkalinity mg/l HCO ₃ ⁻	Transp cm	Total Hardness mg/l CaCO ₃	SO ₄ ²⁻ mg/l	HCO ₃ ²⁻ mg/l	NO ₃ ⁻ mg/l	PO ₄ ²⁻ mg/l	Cl ⁻ mg/l	Mg ²⁺ mg/l	Ca ²⁺ mg/l	Na ⁺ mg/l	K ⁺ mg/l
24-9-04	13:51	C-70	284680	2205676	2.0	901	8.7	27.7	61.0	50	120.1	61.8	584.9	0.7	0.8	89.1	12.6	21.1	190.0	16.5

Table B 5: Field and laboratory results for the samples taken in the Eastern part of the lake

Date	Time	Code	X m	Y m	Depth m	EC µS/cm	pH	Temp C	Alkalinity mg/l HCO ₃ ⁻	Transp cm	Total Hardness mg/l CaCO ₃	SO ₄ ²⁻ mg/l	HCO ₃ ²⁻ mg/l	NO ₃ ⁻ mg/l	PO ₄ ²⁻ mg/l	Cl ⁻ mg/l	Mg ²⁺ mg/l	Ca ²⁺ mg/l	Na ⁺ mg/l	K ⁺ mg/l
27-Sep-04	10:03	E-71	297175	2200572	2.1	806	9.0	21.8	73.2	60	130.1	0.0	276.2	0.0	0.0	63.3	12.6	20.5	149.8	15.1
27-Sep-04	10:20	E-72	297643	2202265	2.3	860	9.6	21.4	79.3	60	105.1	0.0	333.3	0.9	0.0	98.9	12.6	14.4	164.7	15.8
27-Sep-04	10:37	E-73	297940	2202192	2.3	1010	10.4	24.5	183	50	60.1	0.0	304.1	1.4	0.0	115.5	53.7	8.4	206.0	14.8
27-Sep-04	10:58	E-74	297830	2202991	2.4	787	9.6	23.2	109.8	50	90.1	0.0	246.5	1.5	0.0	93.7	9.5	11.4	152.8	13.6
27-Sep-04	11:13	E-75	299254	2203262	2.4	2000	10.0	24.5	286.7	40	60.1	136.7	616.4	0.0	0.0	314.1	6.4	5.2	386.9	30.4
27-Sep-04	11:30	E-76	299659	2203792	2.4	2000	10.0	23.9	292.8	40	60.1	435.3	684.9	6.3	0.0	309.9	5.7	5.0	441.7	32.9
27-Sep-04	11:49	E-77	301192	2204117	2.3	1946	10.1	25.5	280.6	40	60.1	118.5	616.1	0.0	0.0	285.2	6.7	6.0	421.8	30.9
27-Sep-04	12:18	E-78	300270	2204130	2.3	1615	10.7	27.4	274.5	100	75.1	54.3	484.5	4.4	0.0	222.2	10.5	7.8	313.5	24.1
27-Sep-04	12:59	E-79	298328	2204961	2.5	766	9.5	27.6	91.5	40	100.1	0.0	261.2	0.0	0.0	86.6	12.6	14.4	164.7	15.3
27-Sep-04	13:15	E-80	298693	2206236	2.5	710	9.0	27.5	73.2	30	110.1	51.5	316.1	0.0	0.0	81.9	15.8	18.3	130.9	12.6
27-Sep-04	13:40	E-81	297595	2206592	2.5	613	8.9	25.8	61.0	50	120.1	40.8	240.4	0.2	0.0	61.7	15.8	19.1	107.0	10.2
27-Sep-04	14:00	E-82	295502	2206791	2.6	464	8.5	26.5	30.5	50	100.1	0.0	219.2	0.0	0.0	40.3	10.5	18.4	75.1	7.8
27-Sep-04	14:12	E-83	294411	2206769	2.5	363	7.9	24.8	164.7	50	105.1	45.7	161.7	0.0	0.0	26.7	12.6	21.4	53.2	6.0
27-Sep-04	12:41	E-84	296765	2202255	2.2	607	9.6	24.7	91.5	50	100.1	82.1	177.5	1.3	0.0	48.2	11.6	14.4	94.0	9.7
28-Sep-04	9:21	E-85	298431	2201550	2.3	1254	9.9	19.3	158.6	50	70.1	0.0	341.7	2.8	0.0	154.0	11.6	10.3	261.7	19.5
28-Sep-04	9:52	E-86	299252	2200416	1.8	1786	9.7	21.2	201.3	30	80.1	146.6	44.6	2.8	0.0	244.5	7.2	8.0	389.4	26.8
28-Sep-04	10:12	E-87	300735	2201418	1.8	2000	9.7	20.8	259.25	30	70.1	108.2	80.8	2.5	0.0	324.0	13.7	8.0	434.2	31.4
28-Sep-04	11:20	E-88	302259	2202168	1.8	1778	9.3	23.2	152.5	40	80.1	76.6	633.0	7.7	0.0	278.9	12.6	8.6	391.9	29.2
28-Sep-04	11:40	E-89	304072	2203719	1.8	1520	9.3	23.6	137.25	40	70.1	62.2	460.1	0.0	0.0	233.6	13.7	10.4	337.4	27.5
28-Sep-04	12:03	E-90	305299	2202996	2.0	1430	9.2	24.8	73.2	40	75.1	58.1	463.7	0.0	0.0	253.6	10.5	10.2	313.5	26.0
29-Sep-04	11:25	E-91	306009	2204500	2.0	463	8.6	23.1	79.3	20	65.1	48.2	233.4	0.0	0.0	80.8	5.9	10.8	93.0	12.1
29-Sep-04	12:26	E-92	305555	2205544	1.7	1299	8.9	24.5	183	40	65.1	78.0	466.4	1.1	0.0	195.2	7.8	9.3	277.7	24.3

29-Sep-04	13:35	E-93	303516	2204481	2.3	1531	10.2	26.8	109.8	50	65.1	88.8	465.9	2.0	0.0	218.7	7.2	7.3	309.5	25.1
29-Sep-04	14:21	E-94	300820	2204381	1.4	1506	10.7	27.0	286.7	70	90.1	0.0	341.4	0.6	0.0	206.3	11.6	6.7	289.6	22.4
29-Sep-04	15:30	E-95	298648	2204645	2.5	519	9.1	27.2	292.8	40	100.1	0.0	180.5	0.0	0.0	39.4	10.5	15.6	89.0	8.5

Table B 6: Field and laboratory results for the samples taken in the Passageway between the Central and Eastern parts of the lake

Date	Time	Code	X m	Y m	Depth m	EC µS/cm	pH	Tem p C	Alkalinity mg/l HCO ₃ ⁻	Transp cm	Total Hardness mg/l CaCO ₃	SO ₄ ²⁻ mg/l	HCO ₃ ²⁻ mg/l	NO ₃ ⁻ mg/l	PO ₄ ²⁻ mg/l	Cl ⁻ mg/l	Mg ²⁺ mg/l	Ca ²⁺ mg/l	Na ⁺ mg/l	K ⁺ mg/l
19-Sep-04	9:30	P-18	286582	2208931	1.9	461	7.1	20.9	225.7	85	135.1	43.6	223.9	0.0	0.0	36.2	10.5	21.8	75.1	9.0
19-Sep-04	9:53	P-19	288913	2208692	1.9	446	7.2	22.2	207.4	40	105.1	48.5	224.5	1.2	0.0	37.7	24.2	22.0	71.1	7.5
19-Sep-04	10:47	P-20	289951	2208656	1.8	463	7.2	22.5	207.4	50	110.1	55.9	212.1	0.0	0.0	36.5	14.7	22.3	71.1	7.5
19-Sep-04	11:09	P-21	290443	2208445	1.6	478	7.3	22.6	213.5	45	110.1	43.6	158.6	0.0	0.0	28.2	11.6	19.6	102.0	9.0
19-Sep-04	11:44	P-22	289931	2208830	1.7	464	7.3	24.6	219.6	54	110.1	57.7	204.7	0.0	0.0	38.8	14.7	21.1	72.1	7.5
19-Sep-04	12:07	P-23	290328	2207347	1.9	467	7.1	22.8	231.8	45	120.1	53.1	99.8	0.0	0.6	37.2	2.0	49.8	77.1	8.0
19-Sep-04	12:31	P-24	293120	2207523	1.9	503	7.4	24.0	244.0	40	115.1	0.0	103.9	1.2	0.0	0.0	13.7	21.7	87.1	7.5
24-Sep-04	9:54	P-67	290423	2210518	1.6	499	7.7	22.6	201.3	50	120.1	15.51	80.0	6.7	0.7	40.4	14.7	23.2	69.1	7.5
24-Sep-04	10:08	P-68	290524	2210336	1.6	479	7.5	22.5	207.4	50	120.1	58.1	102.3	0.0	0.0	35.2	13.7	21.2	69.1	7.3

Table B 7: Field and laboratory results for the samples taken in the Western part of the lake

Date	Time	Code	X m	Y m	Depth m	EC µS/cm	pH	Tem p C	Alkalinity mg/l HCO ₃ ⁻	Transp cm	Total Hardness mg/l CaCO ₃	SO ₄ ²⁻ mg/l	HCO ₃ ²⁻ mg/l	NO ₃ ⁻ mg/l	PO ₄ ²⁻ mg/l	Cl ⁻ mg/l	Mg ²⁺ mg/l	Ca ²⁺ mg/l	Na ⁺ mg/l	K ⁺ mg/l
3-Oct-04	9:45	W-96	276158	2206492	1.5	1176	9.0	20.1	54.9	20	90.1	43.6	223.9	0.0	0.0	36.2	10.5	21.8	75.1	9.0
3-Oct-04	10:00	W-97	275584	2206441	1.5	1172	9.0	20.3	61.0	20	105.1	48.5	224.5	1.2	0.0	37.7	24.2	22.0	71.1	7.5
3-Oct-04	10:18	W-98	274317	2206424	1.5	2640	9.3	19.6	164.7	10	40.0	55.9	212.1	0.0	0.0	36.5	14.7	22.3	71.1	7.5
3-Oct-04	10:37	W-99	272716	2206607	1.5	2780	9.2	20.1	183.0	10	35.0	43.6	158.6	0.0	0.0	28.2	11.6	19.6	102.0	9.0
3-Oct-04	11:05	W-100	273216	2208307	1.4	2620	9.2	20.2	170.8	10	40.0	57.7	204.7	0.0	0.0	38.8	14.7	21.1	72.1	7.5
3-Oct-04	11:33	W-101	271160	2208193	1.5	2520	9.2	20.6	164.7	10	45.0	53.1	99.8	0.0	0.6	37.2	2.0	49.8	77.1	8.0
3-Oct-04	11:57	W-102	269098	2208175	1.5	2330	9.1	20.3	146.4	10	40.0	0.0	103.9	1.2	0.0	0.0	13.7	21.7	87.1	7.5

Table B 8: Field and laboratory results for the samples taken outside the lake

Date	Time	Code	X m	Y m	Depth m	EC µS/cm	pH	Temp C	Alkalinity mg/l HCO ₃ ⁻	Transp cm	Total Hardness mg/l CaCO ₃	SO ₄ ²⁻ mg/l	HCO ₃ ²⁻ mg/l	NO ₃ ⁻ mg/l	PO ₄ ²⁻ mg/l	Cl ⁻ mg/l	Mg ²⁺ mg/l	Ca ²⁺ mg/l	Na ⁺ mg/l	K ⁺ mg/l
26-9-04	11:45	CA1	286941	2201385	2.1	190	7.2	18.5	79.3	10	105.1	18.6	118.9	0.0	0.0	4.7	24.2	16.9	27.0	6.3
26-9-04	13:20	CA2	289670	2196205	1.4	409	7.3	20.2	152.5	10	100.1						6.8	18.6	34.6	5.8
2-10-04	11:10	CA3	293298	2198258	1.5	596	7.4	20.4	183.0	10	190.2	0.0	0.0	0.9	0.0	31.5	16.8	32.8	77.1	5.8
2-10-04	11:40	CA4	293374	2198215	0.7	125	7.4	21.0	61.0	10	55.1	20.1	63.2	0.0	0.0	12.9	4.2	9.2	13.1	3.6
2-10-04	13:23	PS2	291489	2203434		1795	7.6	22.5	427.0		320.3	379.2	0.0	0.0	0.0	179.7	50.5	55.4	289.6	12.1
2-10-04	17:50	PS3	292029	2202213		1790	8.1	23	1012.6		220.2	0.0	464.6	0.0	0.0	177.2	27.4	31.7	229.9	21.2
4-10-04	11:20	TS-1	274078	2202441		2660	7.4	56.4	774.7		30.0	456.1	765.5	0.0	0.0	272.5	4.7	6.2	654.3	34.1

Duplicate Comparison

Table B 9: Cation values obtained in UNAM's lab and cation values obtained in ITC lab

Sample	Mg	Ca	Na	K	Mg(ITC)	Ca(ITC)	Na(ITC)	K(ITC)
MG-E86	7.2	8	389.4	26.8	9.66	8.29	456	32.07
MG-E87	13.7	8	434.2	31.4	12.76	7.7	430	36.44
MG-E88	12.6	8.6	391.9	29.2	14.3	8.98	387	34.36
MG-W96	11.6	16.1	253.8	20.2	10.3	16.39	248	21.67
MG-CA-3	16.8	32.8	77.1	5.8	18.48	37.54	94	9.9
MG-CA-4	4.2	9.2	13.1	3.6	5.47	8.89	32	6
MG-TS	4.7	6.2	654.3	34.1	2.54	6.39	579	46.6

Statistical analysis: Five-number summaries

Table B 10: Five-number summary for the Central part of the lake.

Variable	Minimum	Q ₁	Mean	Q ₃	Maximum	Standard Deviation
pH	7.0	8.8	8.8	9.0	9.1	0.36966
EC (μS/cm)	427	748	876	967	1600	205.639
Na (mg/l)	59.2	133.0	180.0	214.0	341.0	56.4461
Ca (mg/l)	14.7	17.2	18.9	20.6	24.7	2.40817
Mg (mg/l)	10.5	11.6	16.1	15.8	80.0	10.5677
Cl (mg/l)	0.0	70.1	87.5	109.0	164.0	36.1777
HCO ₃ (mg/l)	0.0	344	414	495	646	135.934
SO ₄ (mg/l)	0.0	0.0	33.4	54.7	90.1	27.0371

Table B 11: Five-number summary for the Eastern part of the lake.

Variable	Minimum	Q ₁	Mean	Q ₃	Maximum	Standard Deviation
pH	7.9	9.0	9.5	10.0	10.7	0.6840
EC (μS/cm)	363	710	1190	1620	2000	560.63
Na (mg/l)	53.2	131.0	242.0	337.0	442.0	128.04
Ca (mg/l)	5.0	8.0	11.6	14.4	21.4	4.9632
Mg (mg/l)	5.7	7.8	12.4	12.6	53.7	9.1012
Cl (mg/l)	26.7	80.8	163.0	245.0	324.0	100.16
HCO ₃ (mg/l)	44.6	233.0	346.0	466.0	685.0	174.87
SO ₄ (mg/l)	0.0	0.0	65.3	82.1	435.3	90.007

Table B 12: Five-number summary for the Western part of the lake.

Variable	Minimum	Q ₁	Mean	Q ₃	Maximum	Standard Deviation
pH	9.00	9.05	9.14	9.20	9.30	0.11339
EC (μS/cm)	1170	1750	2180	2630	2780	698.488
Na (mg/l)	254	533	532	575	679	144.135
Ca (mg/l)	8.6	10.9	13.3	16.6	17.8	3.62623
Mg (mg/l)	4.40	8.35	16.90	18.50	48.40	15.2416
Cl (mg/l)	131	188	286	366	391	117.307
HCO ₃ (mg/l)	533	685	879	1050	1060	242.234
SO ₄ (mg/l)	65.6	99.0	150.0	189.0	208.0	62.9126

Table B 13: Five-number summary for the Passageway part of the lake

Variable	Minimum	Q ₁	Mean	Q ₃	Maximum	Standard Deviation
pH	7.10	7.15	7.23	7.30	7.40	0.11127
EC (μS/cm)	466	462	469	473	503	17.7710
Na (mg/l)	71.1	71.6	79.4	82.1	102.0	11.4375
Ca (mg/l)	19.6	21.4	25.5	22.2	49.8	10.7647
Mg (mg/l)	2.0	11.1	13.1	14.7	24.2	6.59415
Cl (mg/l)	28.2	36.3	35.8	37.6	38.8	3.82030
HCO ₃ (mg/l)	99.8	131.0	175.0	218.0	225.0	54.8912
SO ₄ (mg/l)	43.6	44.8	50.4	55.2	57.7	6.11425

Piper plot interpretation diagram

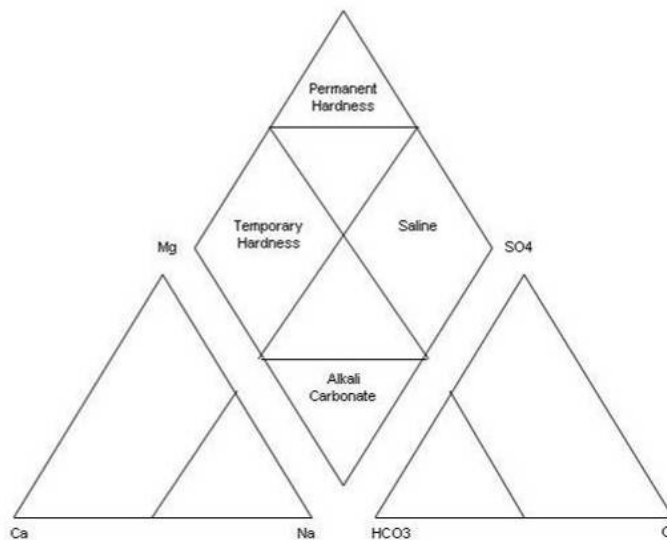


Figure B 2: Different water types in the diamond portion of Piper diagram

Appendix C: Geostatistical analysis

Permitted variogram models

There are several types of permitted functions which are called authorized variogram models; they must be able to model monotonically increasing, constant or asymptotic maximum (sill), non-negative intercept (nugget), and anisotropy. They must obey mathematical constraints, so that the resulting kriging equations are solvable (Rossiter 2004). Some authorized models are Pure Nugget, Linear, Circular, Spherical, Exponential and Gaussian.

1. Pure Nugget (no spatial structure): $\gamma(h) = c_0, \forall h > 0$
2. Linear: $\gamma(h) = \omega h^\alpha, 0 < \alpha < 2$, where $\alpha=1$.

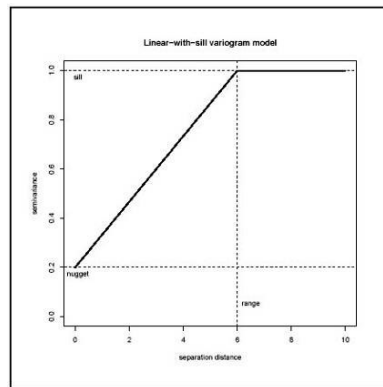


Figure C 1: Linear variogram model

3. Circular, sill c , range a :
$$\gamma(h) = \begin{cases} c \left\{ \frac{3h}{2a} - \frac{1}{2} \left(\frac{h}{a} \right)^3 \right\} & h < a \\ c & h \geq a \end{cases}$$

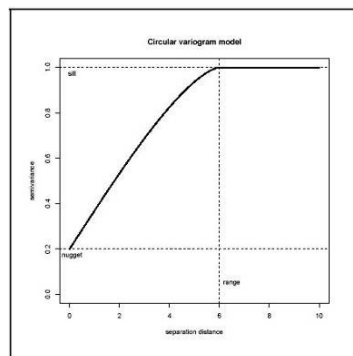


Figure C 2: Circular variogram model

4. Spherical, sill c , range a :
$$\gamma(h) = \begin{cases} c \left\{ \frac{2h}{\pi a} \sqrt{1 - \frac{h^2}{a^2}} + \frac{2}{\pi} \arcsin \frac{h}{a} \right\} & h < a \\ c & h \geq a \end{cases}$$

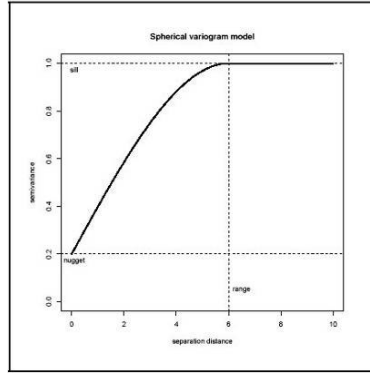


Figure C 3: Spherical variogram model

5. Exponential, sill c , effective range $3a$:
$$\gamma(h) = c \left\{ 1 - e^{-\left(\frac{h}{a}\right)} \right\}$$

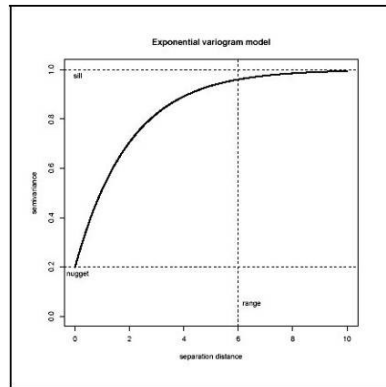


Figure C 4: Exponential variogram model

6. Gaussian, parameters as for exponential, but effective range is $\sqrt{3a}$: $\gamma(h) = c \left\{ 1 - e^{-\left(\frac{h}{a}\right)^2} \right\}$

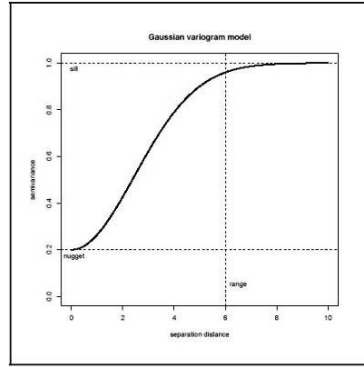


Figure C 5: Gaussian variogram model

Ordinary kriging principle

In the case of the four parameters analyzed in section 4.1.1., the prediction of “spatially dependent” unknowns, based on measured observations, will take place (Stein 2004). For applying Ordinary kriging, first the mean is estimated:

$$\hat{\mu} = (1_n^T C^{-1} 1_n)^{-1} 1_n^T C^{-1} z$$

Where:

1_n is a vector of n elements, all 1.

C is the n by n covariance matrix

z is the vector with the n data

Then the kriging predictor:

$$T = \hat{\mu} + c_0^T C^{-1} (z - \hat{\mu} 1_n)$$

Where:

c_0 contains the covariance function evaluations between $Z(x_0)$ and the observations $Z(x_i)$.

And finally the kriging variance:

$$Var(T - Z(x_0)) = c_{00} - c_0^T C^{-1} c_0 + x_a^2 / V$$

Where:

$$x_a = 1 - c_0^T C^{-1} 1_n$$

$$V = (1_n^T C^{-1} 1_n)$$

Ordinary Kriging in R (gstat) statistical software

Ordinary Kriging of EC values:

```
vlogec<-variogram(logec~1, ~x+y, c1, width=6000, cutoff=8000)
vmlogec<-vgm(0.072, "Gau", 3500, 0.0118)
oklogec<-krige(logec~1, ~x+y, c1, model=vmlogec, grid)
```

Ordinary Kriging of Chloride values:

```
vlogcl<-variogram(logcl~1, ~x+y, c3, width=600, cutoff=8000)
vmlogcl<-vgm(0.13, "Gau", 3500, 0.018)
oklogcl<-krige(logcl~1, ~x+y, c3, model=vmlogcl, grid)
```

Ordinary Kriging of Hardness values:

```
vhardness<-variogram(hardness~1, ~x+y, c4, width=750, cutoff=6000)
vmhardness<-vgm(230, "Exp", 4000, 55)
vmfhardness<-fit.variogram(vhardness, vmhardness)
okhardness<-krige(hardness~1, ~x+y, c4, model=vmfhardness, grid)
```

Ordinary Kriging for Bicarbonate values:

```
vl10hco3<-variogram(110hco3~1, ~x+y, c6, width=1250, cutoff=10000)
vml10hco3<-vgm(0.014, "Exp", 8000, 0.0075)
vmf10hco3<-fit.variogram(vl10hco3, vml10hco3)
okl10hco3<-krige(110hco3~1, ~x+y, c6, model=vmf10hco3, grid)
```

Appendix D: Water quality and Remote Sensing

SPOT 4 specifications

Scene Extract Parameters

Scene ID:	5 584-310 04/10/18 17:28:35 2 J			
K-J identification:	584-310			
Date:	2004-10-18 17:28:35.0			
Instrument:	HRG 2			
Shift Along Track:	0 0			
Pre-processing level:	1B			
Spectral mode:	J			
Number of spectral bands:	4			
Spectral band indicator:	HI1	HI2	HI3	HI4
Gain number:	7	8	5	5
Absolute calibration gains: (W/m ² /sr/μm)	2.139452	3.866820	1.738550	10.694748
Orientation angle:	13.052189 degree			
Incidence angle:	L2.877904 degree			
Sun angles (degree) Azimuth:	152.297236			
Elevation:	56.698056			
Number of lines:	6020			
Number of pixels per line:	5986			

Scene Center Location

Latitude:	N20° 0' 58"
Longitude:	W100° 54' 54"
Pixels number:	2988
Line number:	3011

Corners Location

Corner	Latitude	Longitude	Pixel n°	Line n°
1	N20° 20'31"	W101° 7'42"	1	1
2	N20° 13'11"	W100° 34'14"	5985	1
3	N19° 41'25"	W100° 42'6"	5984	6020
4	N19° 48'44"	W101° 15'28"	1	6020

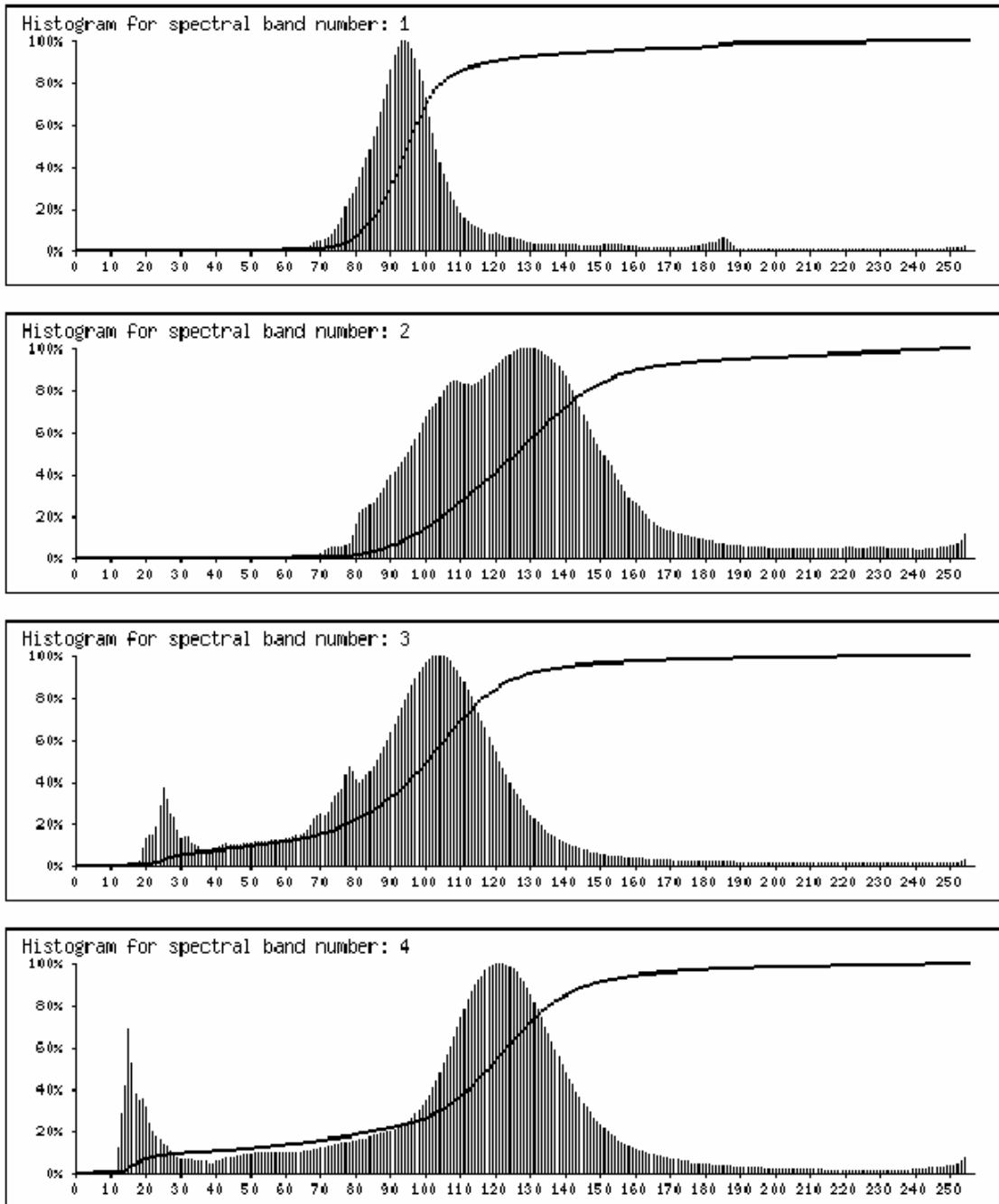


Figure D 1: Histograms for SPOT4 image bands 1-4.

CoKriging in R (gstat) statistical software

```
vtr<-variogram(transp~1, ~x+y, tr, width=1000, cutoff=10000)
vmtr<-vgm(70, "Sph", 10000, 19)

g<-gstat(id="transp", form=transp~1, loc=~x+y, data=tr)
g<-gstat(g, id="pc1", form=pc1~1, loc=~x+y, data=pc)

v.cross<-variogram(g, width=1000, cutoff=10000); str(v.cross); table(v.cross$id)

g<-gstat(g, id="transp", model=vm2tr, fill.all=T)

g<-fit.lmc(v.cross, g)
plot(variogram(g, width=1000, cutoff=10000), model=g$model, pl=T)

ck<-predict.gstat(g, grid)
summary(ck)

summary(oktr$var1.pred)
summary(ck$transp.pred)
summary(ck$transp.pred-oktr$var1.pred)

summary(oktr$var1.var)
summary(ck$transp.var)
summary(ck$transp.var-oktr$var1.var)

frame<-data.frame(x=ck$x, y=ck$y, diff=ck$transp.pred-oktr$var1.pred)

levelplot(diff~x+y, frame, aspect=mapasp(frame), col.regions=bpy.colors(100))
```


Appendix E: Wetlands management plan

The most important functions of a wetland management planning process and a management plan are:

- Function I. To identify the objectives of site management
- Function II. To identify the factors that affect, or may affect, the features
- Function III. To resolve conflicts
- Function IV. To define the monitoring requirements
- Function V. To identify and describe the management required to achieve the objectives
- Function VI. To maintain continuity of effective management
- Function VII. To obtain resources
- Function VIII. To enable communication within and between sites, organizations and stakeholders
- Function IX. To demonstrate that management is effective and efficient
- Function X. To ensure compliance with local, national, and international policies